AN EVALUATION OF THE ABILITY OF GAMMA ALUMINA TO REMOVE SULFUR AND NITROGEN FROM A COAL DERIVED LIQUID BOTH IN THE PRESENCE AND ABSENCE OF HYDROGEN TREAT GAS

By

JAN WILLIAMS WELLS

Bachelor of Science

Oklahoma State University

Stillwater, Oklahoma

May, 1971

Submitted to the Faculty of the Graduate College
of the Oklahoma State University
in partial fulfillment of the requirements
for the Degree of
MASTER OF SCIENCE
May, 1977

AN EVALUATION OF THE ABILITY OF GAMMA ALUMINA TO REMOVE SULFUR AND NITROGEN FROM A COAL DERIVED LIQUID BOTH IN THE PRESENCE AND ABSENCE OF HYDROGEN TREAT GAS

Thesis Approved:

Billy L. Crynes
Thesis Adviser

Robert L. Robinson, Jr.

[signature]

Norman N. Durham
Dean of the Graduate College

PREFACE

The ability of a gamma alumina support to remove nitrogen and sulfur from raw anthracene oil (coal derived liquid) both in the presence and absence of hydrogen treat gas has been measured. This study was conducted in a trickle bed reactor operating at 750°F (399.2°C) and 1500 psig. Data were obtained at three liquid volume hourly space times: 0.46 hrs., 0.92 hrs., and 1.84 hrs. The treat gas flow rate was maintained at 1500 scf/bbl. Three experimental runs were made in this study: two with hydrogen treat gas and one with nitrogen treat gas. Also, the effects of presulfiding of an alumina support were assessed.

I would like to express my gratitude to Professor B. L. Crynes for his aid and guidance. Also, I would like to thank Dr. Steven D. Hottman, Gil Greenwood, Dalip Soni, R. Sivasubramanian, and Mushtaq Ahmed. The discussion with these individuals greatly helped in the preparation of this work. I would also like to thank the members of the undergraduate coal group who helped in both the experimental and analytical phases of this study.

Financial support for this study was gratefully received from the School of Chemical Engineering, and United States Energy Research and Development Administration.

Finally, I must thank the people whose sacrifices and encouragement have made it all possible: Anna Charlene, Janette and Charley.

TABLE OF CONTENTS

LIST OF TABLES

LIST OF FIGURES

CHAPTER I

INTRODUCTION

The United States of America is one of the greatest civilized nations which has ever existed. One reason this country has grown to this high state of development is the ready availability of economical energy. In the 19th century coal was the great source of energy, it fueled the great factories of the east and spurred our economic progress of that era. In the 20th century coal has largely been replaced by petroleum as the major source of energy. During this century, energy utilization technology has developed at an extremely high rate. This has caused an improved standard of living which has encouraged a high per capita consumption of energy. During recent years, this high level of energy usage and an increasing population has resulted in mild energy shortages. These shortages and rising energy prices have made this country realize that petroleum's days as a cheap energy source may be numbered.

As a result of these high prices and shortages, the United States Government has initiated a program to develop alternate sources of energy. The major alternate sources are nuclear, coal, solar, and geothermal energy. The most promising of these sources for the long run is nuclear energy (fission and fusion), but opposition by environmental groups and construction delays have prevented extensive development of nuclear energy. Solar and geothermal energy are still in the

very early development stages and only time will tell what impact these energy sources will have. For these reasons, more and more research is being done on coal as an alternate energy source. Also, the United States has an abundant coal supply. At present, research is concentrating on the conversion of solid coal to liquid and gaseous products, and the removal of nitrogen and sulfur from these products. Part of this research is being conducted at Oklahoma State University. This program is designed to tailor catalyst for the upgrading of coal derived liquids. Specifically, the goal of this program is to develop catalysts for the removal of sulfur and nitrogen from coal derived liquids. This study is part of that program.

The specific goals of this study were:

1. Evaluation of the ability of gamma alumina (no active metals present) to cause hydrodenitrogenation, hydrodesulfurization and hydrogenation in a coal derived liquid.
2. Evaluation of the effect of presulfiding on activity of gamma alumina for hydrodenitrogenation and hydrodesulfurization.
3. Evaluation of the extent to which thermal reactions affect nitrogen and sulfur compounds in a coal derived liquid.

CHAPTER II

BACKGROUND

In this study, the activity of a gamma alumina for hydrogenation, hydrodesulfurization and hydrodenitrogenation of a coal derived liquid has been evaluated. Also the extent of sulfur and nitrogen removal from the same liquid in absence of hydrogen gas was assessed. The principle tools of this study were gamma alumina support and a trickle bed reactor. In order to interpret the result of this study four specific literature areas must be evaluated.

First, the nature of the active sites on gamma-alumina, silica-alumina, porcelain and a $CoO/MoO_3/\gamma Al_2O_3$ catalyst will be considered. The results of this study show that the hydrodesulfurization and hydrodenitrogenation activity and products obtained from gamma alumina differ significantly from those of porcelain and $CoO/MoO_3/\gamma Al_2O_3$ catalyst. These results could be due to the difference in the nature of the active sites on these materials. Next the effect of contacting efficiency, mass transfer and axial dispersion in a trickle bed reactor will be evaluated. Each of these factors can affect reactor efficiency and therefore the results of this study. Also the effects and normal ranges of operating parameters such as temperature, pressure, space time and hydrogen flow rate will be reviewed. An finally the kinetics of hydrodenitrogenation and hydrodesulfurization will be considered. Here the effect of inhibitors and promoters will be discussed and experimentally

observed orders for hydrodesulfurization and hydrodenitrogenation reviewed.

The Nature of Active Sites

An important variable in this study is the nature of the active sites on catalysts, support material and so-called "inert solids". The number, type, and adsorption strength of the active surface structures determine the activity of the catalyst for certain types of reactions and the type of products obtained from these reactions. Also the relative effectiveness of poisons or inhibitors is determined by surface structure, adsorption strength, and number of the active sites. In this study, the hydrodesulfurization and hydrodenitrogenation ability of gamma alumina has been evaluated. As will be seen, the results obtained from the gamma alumina support will be significantly different from those obtained from ceramic beryl saddle (so-called inert solids) and a $CoO/Mo/\gamma Al_2O_3$ catalyst. One possible explanation for these different results might be due to the nature of the active sites on these three materials. In order to compare these results, the nature of the active sites of gamma alumina, $CoO/MoO_3/\gamma Al_2O_3$ and porcelain (ceramic beryl saddle) must be considered.

Gamma Alumina

In recent years, anhydrous alumina (Al_2O_3) has found widespread industrial use as a catalyst and a catalyst support material. Alumina can be obtained in eight phases (19). The most popular for catalytic applications have been the gamma and eta phases. These materials exhibit high surface area and excellent thermal stability. In this

study, the active site on gamma alumina will be considered. Gamma alumina (the support alone) acts as a catalyst for a number of reactions (21). Among these are olefin isomerization, olefin saturation, cyclic paraffin rearrangement, hydrocarbon cracking and polymerization.

Since a large number of reactions occur on gamma alumina, a considerable amount of work has been done to determine the nature of the active sites (11, 17, 21, 22, 34, 65). These studies have found that the activity of gamma alumina is a function of three variables. These are:

1. Reaction temperature (59)
2. Calcining temperature (51, 58)
3. The presence of alkali metals (33, 58).

The effects of reaction temperature on activity of gamma alumina was studied by Tung and McIninch (65). They found that below 752°F (400°C) the activity of high purity alumina for propylene polymerization and cumene cracking was low while above 752°F (400°C) the alumina demonstrated high activity for these reactions. The activity of gamma alumina is also a function of calcining temperature. Haags and Pines (17) stated that the maximum activity for isomerization of cyclohexene occurred when the catalyst was calcined at 1112°F (600°C) to 1292°F (700°C). Hightower (21) found that calcining at 967°F (520°C) resulted in maximum activity for isomerization of D_2 exchange reaction for cyclic and noncyclic olefins. The presence of alkali metals (K and Na) in the alumina also affected catalyst activity. Haag and Pines (17) found that sodium present in concentrations greater than 0.05 wt% significantly decreased alumina's activity for isomerization of cyclohexene and dehydration of 1-butanol. Tung and McIninch (34) confirmed

this.

At present, the surface of active gamma alumina is considered to have four types of active sites. These sites are as follows:

1. An exposed Al^{+3} ion in combination with an O^{-2} ion. This site is caused by a structure defect in the alumina surface. Also it is susceptible to poisoning by hydrogen sulfide, methyl mercaptan, ammonia, and sulfur dioxide. The effectiveness of these poisons depends on the reaction temperature (48).
2. A highly energetic, structurally unique O^{-2} ion present on the surface. This site is poisoned by carbon dioxide (48).
3. Two adsorption sites which strongly adsorb olefins and aromatics at low temperatures. The exact nature of these sites has not been determined (21).
4. A possible "passive" Bronsted acid site active only at higher temperatures (65).

The majority of these studies were performed at relatively low pressures (1 atm) in microreactors.

Silica-Alumina

The silica-alumina catalyst is a very broad class of catalysts. Like alumina it can be used as a support for active metals or as a catalyst by itself. As a catalyst it is extensively used in catalytic cracking, isomerization, reforming, cationic polymerization and alkylation processes (22). The activity of silica-alumina toward different types of reactions varies with the ratio of silica to alumina (23, 24). This makes the silica-alumina catalyst very versatile and widely used by the petroleum and chemical industry. Like alumina, because of its

versatility, it has been widely studied (6, 22, 23, 24, 32, 39, 56). Two major active structures have been found on silica-alumina; a Lewis acid site (electron acceptor) and a Bronsted site (proton donor). Schwartz (56) has proposed the following structures for these sites:

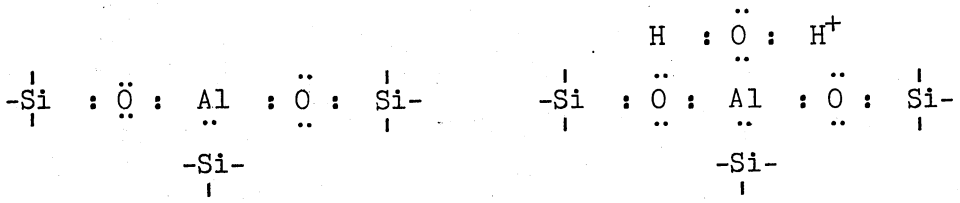

(Lewis Site) (Bronsted Site)

The strength of Lewis and Bronsted sites vary from site to site; however, the reason for this behavior is not known (6). As can be seen, the Bronsted site is a hydrated Lewis acid site (23, 39, 56). This implies that the activity of silica alumina depends strongly on the water content of the catalyst. Holm, et al. (24), in a study of a 90% silica-10% alumina catalyst, found that the maximum activity for polymerization occurred at a pretreatment temperature of 968°F (520°C). At temperatures higher and lower than this, he observed lower activity. He attributed this behavior to the different amounts of adsorbed water on the surface. The Lewis and Bronsted sites present on silica-alumina are poisoned or inhibited by sodium and nitrogen compounds. Small quantities of sodium are usually present in the silica alumina. All studies reviewed (6, 32, 42) concluded that sodium atoms, present in small quantities, poison the most active acid centers first, then, as sodium concentration increases, the weaker sites are poisoned. Also, the active sites on silica alumina are susceptible to poisoning by ammonia, pyridine, and quinoline (7). These compounds are strong bases which adsorb on both the Lewis and Bronsted sites. Levchuk and Buyanova (32)

reported on the temperature dependence of ammonia adsorption. They found that as temperature increased, the ammonia adsorption decreases and at 572°F (300°C) to 752°F (400°C) the ammonia blocked out only the more active sites.

Porcelain

Porcelain is defined as a fired ceramic ware conventionally white having a vitreous body (35). The chemical equation of porcelain is $K_2O \cdot Al_2O_3 \cdot SiO_2$. The approximate analysis is given below (35).

K_2O and/or Na_2O	-	4%
Al_2O_3	-	26%
SiO_2	-	70%

As can be seen from the analysis porcelain is a silica alumina with a high sodium and/or potassium content. No information was found on the catalytic surface properties of porcelain; but Levchuk, et al. (32) found that silica alumina with a sodium content of 2.1 wt% sodium and 25 wt% Al_2O_3 has appreciable acid strength. This indicates that porcelain in terms of catalytic activity probably has both Lewis and Bronsted sites similar to those of a high sodium content silica-alumina catalyst.

Porcelain is not really known to be a catalyst support. In fact, its role is often used as that of an "inert" packing material in reactors and towers.

Cobalt-Molybdenum on Alumina

The $CoO/MoO_3/\gamma Al_2O_3$ catalyst is used extensively in hydrotreating of heavy petroleum fractions. This catalyst is a member of a broader

group which consists of two metal ions: one from Group VII and one from Group VI(A). The most common elements used in this type of catalyst are Co, Ni, Fe, Mo and W (4). The role of these metal ions differ with the type of reaction. In some reactions, only one of the metal ions is believed involved in the reaction. In other reactions, both metal ions are required. One metal forms the reaction site and the other metal acts as a promoter for the formation of the active site. The exact function of the promoter is not well understood, but is is generally observed that the activity for certain reactions is much less in the absence of the promoter.

This study is concerned with the sulfided $CoO/MoO_3/\gamma Al_2O_3$ catalyst; specifically, the nature of the active sites present during hydrodesulfurization and hydrodenitrogenation. No information was found in the open literature describing the sites required for hydrodenitrogenation, but the nature of the sites for hydrodesulfurization has been studied extensively.

The sulfided $CoO/MoO_3/\gamma Al_2O_3$ catalyst is considered to have two types of active sites in hydrodesulfurization reactions. One site is believed responsible for hydrogenation and/or isomerization reactions, while at the other site, hydrodesulfurization is believed to occur.

Very little research has been done on the nature of isomerization/-hydrogenation sites on the $CoO_3/MoO_3/\gamma Al_2O_3$ catalyst. Ratnasamy, et al. (46) thought these sites might be metallic or sulfided cobalt. Mitchell (8) also believed the isomerization/hydrogenation site is associated with the Co^{+2} ions. Schuit and Gates (54) have suggested that the isomerization/hydrogenation site is the same as the desulfurization site. The most extensive study of this type of site was done by

Voorhoeve and Stuiver (68). They studied the hydrogenation of benzene and cyclohexane over a sulfided $NiO/WO_3/\gamma Al_2O_3$ catalyst and proposed the intercalation model. Although this model is based on a nickel-tungston catalyst, the results have been extended to the sulfided $CoO/MoO_3/\gamma Al_2O_3$ catalyst. They proposed that the sulfiding of MoO_3 or WO_3 resulted in the formation of MoS_2 or WS_2 crystals. These crystals have a layer structure in which the Mo or W atoms are surrounded by six sulfur atoms in a prismatic structure. Intercalation is the accommodation of metal ions in the catonic sites between the sulfide layers. In an ideal crystal of MoS_2 or WS_2, intercalation cannot occur. This is because the resulting electron structure is not favorable. But in real crystals of MoS_2 or WS_2, many defects are common, especially at the edges. Into these defects Co^{+2} or Ni^{+2} ions are intercalated. This alters the electron structure and results in the exposure of Mo^{+3} or W^{+3} ions with one or two anionic sites vacant. Voorhoeve and Stuiver proposed the following structures:

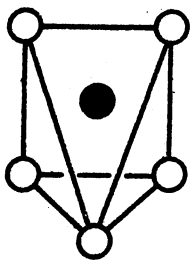

one anionic vacancy

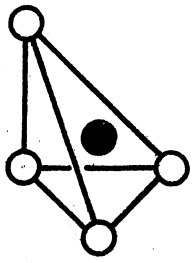

two anionic vacancies

● - W or Mo

○ - Sulfur

and suggested that these sites may also be responsible for the hydrodesulfurization reaction.

The majority of work has centered on the nature of the hydrodesulfurization sites. The cobalt is believed to act as a promoter while molybdenum forms the active site where the reaction occurs (20, 38, 50). As was stated earlier, the role of the promoter is not well understood, but generally the hydrodesulfurization ability of the sulfided $CoO/MoO_3/\gamma Al_2O_3$ catalyst is greater than that of sulfided $MoO_3/\gamma Al_2O_3$ or $CoO/\gamma Al_2O_3$ catalyst (9). Three major models have been proposed to explain the nature of the hydrodesulfurization site. These are the monolayer model, monolayer-intercalation model, and synergy model. Each of the models is discussed below.

The monolayer model was porposed by Schuit and Gates (54). It is based on infrared spectra, reflection spectra, and magnetic susceptibility data. The reaction studied was the hydrodesulfurization of thiophene. In this model, a monolayer of MoO_3 is chemically bound to the support surface. On top of the monolayer there exists a capping layer of O^{-2} ions. This layer is caused by the excess positive charge due to the Mo^{+6} ions in the monolayer. Cobalt, initially present as CoO, is incorporated into the solid alumina support as a Co^{+2} ion (tetrahedrally coordinated). The oxygen is not incorporated into the solid lattice but remains in the capping layer. The incorporation of the Co^{+2} into the support lattice frees an aluminum ion, Al^{+3}. This ion becomes bound to the monolayer of molybdenum. The presence of the tetrahedrally coordinated aluminum ion increases the stability of the monolayer. The formation of the monolayer structure occurs during the calcining step of preparation. When the catalyst is sulfided with an

H_2/H_2S mixture some of the O^{-2} ions in the capping layer are replaced with S^{-2} ions. The presence of hydrogen results in the removal of some of the sulfur atoms exposing active molybdenum sites (Mo^{+3}). Two types of active sites are proposed for a γAl_2O_3 support; one consisting of a single Mo^{+3} ion and another consisting of two adjacent Mo^{+3} ions. Due to electron configurations these Mo^{+3} sites are not possible without the cobalt promoter. Schuit and Gates (54) propose that the hydrodesulfurization site is four adjacent Mo^{+3} ions. Two of these sites are formed as described above. The other two sites are Mo^{+3} ions formed by the reaction

$$2S^{-2} + 2Mo^{+4} + H_2 \longrightarrow 2SH^- + 2Mo^{+3}$$

The reaction proposed for hydrodesulfurization of thiophene is

$$4Mo^{+3} + 2SH^- + C_4H_4S \longrightarrow C_4H_6 + 4Mo^{+4} + 3S^{-2}$$

Whether subsequent hydrogenation of C_4H_6 occurs at this site or another site is not clear. The possibility exists that the single Mo^{+3} site acts as a hydrogenation site. This type of site would be similar to that proposed by Voorhoeve and Stuiver (68), but no experimental evidence is available to confirm this.

The monolayer-intercalation model was proposed by De Beer, Van Sint Fie, Van der Steen, Zwaga and Schuit (9). This model is based on a study of sulfided catalyst promoted by cobalt, nickel and zinc. In this model, the active sites on the calcined catalyst start as a monolayer structure. During the first hours of operation or during the presulfiding process, the cobalt diffuses out of the solid alumina support lattice. This results in the intercalation of the MoS_2 crystal with cobalt. It also reduces the stability of the MoS_2 crystals and causes

the formation of smaller crystals. The presence of cobalt in the MoS_2 crystal and the smaller crystals cause the formation of intercalation type active sites. These sites were described in detail by Voorhoeve and Stuiver (63).

The "synergy" model was proposed by Hagenbach, Courty and Delmon (18). This model resulted from a study of pure MoS_2 and pure Co_9S_8 with no support present. The existence of two completely separate phases in a sulfided $CoO/MoO_3/\gamma Al_2O_3$ catalysts is proposed; one pure MoS_2 and the other pure Co_9S_8. X-ray studies show that pure MoS_2 alone is a very disorderly crystal, but the presence of small amounts of Co_9S_8 causes the MoS_2 to form a more ideal crystal. This modified MoS_2 crystal is more active in electron transfer. At the interface between MoS_2 and Co_9S_8 phases cause a "synergic" effect exists. This is a transfer of electrons across the interface between the MoS_2 and Co_9S_8 phases. This transfer of electrons results in the MoS_2 phase becoming more catalytically active. This model proposes that the activated MoS_2 phase is the active site for hydrodesulfurization.

The nature of the active site on a sulfided $CoO_3/MoO_3/\gamma Al_2O_3$ catalyst is largely unresolved. Three major models have been proposed: monolayer, intercalation and synergic. In all of these models, the active site is associated with the molybdenum phase. The role of cobalt differs in each of these models, but in each model it alters the structure of the MoS_2 phase to make it more active.

Summary

The nature of the active sites on alumina, silica-alumina, porcelain and $Co/Mo/\gamma Al_2O_3$ catalyst has been considered. This review

has established the following points.

1. Studies of pure alumina at low pressure has shown five possible types of sites; first, an Al^{+3} ion, associated with an O^{-2} ion; second, a highly energetic structurally unique O^{-2} ion; third, two strong adsorption sites whose exact structure is not known and finally a passive Bronsted site active only at higher temperatures.
2. The presence of alkali metals reduces the surface activity of silica-alumina and alumina, by reducing the numberof strong acid sites.
3. Porcelain can be considered a silica-alumina with a high sodium content. Therefore, the type of active site expected on porcelain is a weak acid site.
4. MoS_2 phase of a sulfide $Co/Mo/\gamma Al_2O_3$ catalyst is most likely where hydrodesulfurization occurs.
5. No studies of the surface structures responsible for hydrodenitrogenation on a $Co/Mo/\gamma Al_2O_3$ catalyst has been made.
6. As of now, no overall theories or correlations exist to explain or predict the activities of surface sites. This is due to the complexity of the active surface.

Next the efficiency of a trickle bed reactor will be considered.

Reactor Efficiency

The trickle bed reactor is widely used in hydrogenation and hydrodesulfurization of heavy distillates in the petroleum industry. The advantages and disadvantages of this type of unit have been listed and

discussed by Satterfield (51). The ideal trickle bed reactor can be characterized as follows:

1. Liquid phase is in plug flow.
2. Catalyst particles are completely bathed in liquid.
3. No mass transfer limitations exist in any phase or at any interface.

Very seldom does a real trickle bed reactor behave in an ideal manner (33). Problems in mass transfer and liquid distribution can exist and these problems cause a decrease in reactor efficiency.

Contacting Efficiency

In trickle bed reactors, three types of flows have been observed.

1. gas continuous flow
2. rippling or slugging flow
3. dispersed bubble flow

In pilot plant and laboratory scale equipment, gas continuous flow is normally observed (51). In this type of flow, the liquid trickles over the packing, and the gas phase is continuous. In the ideal reactor, the liquid phase should uniformly and freshly wet every catalyst particle in the bed. In the real reactor this is seldom, if ever, observed. Instead of flowing uniformly as described above, the flow tends to coalesce into rivulets (53). Thus, some of the catalyst is not freshly and continuously wetted by the rivulets. Also the liquid flow tends to migrate to the wall of the reactor (51). The extent of wall migration was found to depend on the ratio of the diameter of the reactor to the diameter of the catalyst particles. Satterfield (51) reported that for a tube particle diameter ratio (D_T/D_p) of 10, an estimated 30%-60% of

the flow migrated to the wall and therefore was not effectively controlled with catalyst.

The extent of contacting between the solid and the liquid is best measured by two variables: liquid holdup and contacting efficiency. Liquid holdup is defined by Satterfield (51) as a measure, although approximate and incomplete, of the effectiveness of contacting between the liquid and the catalyst. Physically it is the fraction of the reactor volume occupied by the liquid phase (volume of liquid present/-volume of empty reactor) (58). Liquid holdup increases as the liquid flow rate increases. Early liquid holdup measurements were made on packed beds using nonporous supports (39). Many correlations have been proposed to predict liquid holdup in nonporous beds. Schwartz, in a recent comparison study (59) of porous and nonporous supports, concluded that correlations for nonporous packed beds cannot be extended to trickle bed conditions. In this study, Schwartz evaluated the liquid holdup of n hexane on both porous and nonporous supports. He found that for a 0.06 cm diameter particle in a tube diameter of $\frac{1}{2}$ inch (1.35 cm) the liquid holdup varied from 41% at a liquid mass flux of 0.3 kg/m^2sec to 61% at a liquid mass flux of 5 kg/m^2sec. Ross, in an earlier paper (47), compared liquid holdup found in a laboratory reactor, a pilot plant reactor, and a commercial reactor. In each case, the catalyst pellet size was the same, but the column diameter varied. The following table summarizes Ross' results

TABLE I

SUMMARY OF ROSS' TRICKLE BED REACTOR STUDY

Type	Column Diameter	Liquid Mass Flux (kg/m^2hr)	Liquid Holdup
Laboratory Reactor	2 in.	2×10^3	40%
Laboratory Reactor	4 in.	8.4×10^4	59%
Pilot Reactor	4 in.	1.8×10^3	28%
Pilot Reactor	4 in.	3.3×10^3	29%
Commercial Reactor	6.5 ft	9.6×10^3	26%
Commercial Reactor	6.5 ft	2.1×10^4	28%

He attributed this variance to the different liquids used and liquid distribution problems in larger columns, Henry, et al. (20) and Mears (38) have proposed correlations to account for liquid holdup effects on reactor efficiency. These will be discussed later.

Contacting efficiency is another parameter used to measure the extent of contacting between liquid and solid. Most earlier studies were again conducted with nonporous support materials. In porous material contacting efficiency is diffucult to measure and many definitions have been proposed. Schwartz, et al. (58) have defined contacting efficiency as the ratio of the freshly wetted surface area to the total surface area. They measured the contacting efficiency for (20-28) mesh support and found the contacting efficiency was uniform at 66% for porous material (270 m^2/gm) over the liquid mass flux range of

0.3 to 5 kg/m^2sec.

As can be seen, the extent of liquid holdup has not been generalized, so no exact correlation exists for its prediction in a porous trickle bed reactor. The same is true of predicting contacting efficiency in a trickle bed reactor. Also an exact expression for the effects of these parameters on reactor efficiency has not been developed.

Mass Transfer

In an ideal reactor, no mass transfer limitations can exist within a phase or at an interface. In real trickle bed reactors, mass transfer resistances can and do occur in the liquid film and in the pores. Satterfield (51) and Schuit, et al. (54) have concluded that for typical hydrodesulfurization conditions mass transfer resistance of the sulfur bearing compounds through the external liquid film does not seem to be significant, but that diffusion in the catalyst pores can result in a significant mass transfer resistance. Pore diffusion resistance is measured by the effectiveness factor. Satterfield (50) and others have defined this term as the ratio of the actual reaction rate to that which would occur if all of the surface through the inside of the catalyst were exposed to the catalyst outer boundary reactant concentration and temperature. As can be seen, a low effectiveness factor implies high pore diffusion resistance. This tends to reduce the concentration of the higher molecular weight compounds while increasing the concentration of the lower molecular weight compounds in the pore.

For hydrodenitrogenation, values of the effectiveness factor vary from study to study depending on catalysts, feedstocks, and reactor

conditions. Van Zooneen and Douwes (67) noted that a four fold reduction in particle size did not increase hydrodenitrogenation of a straight run gas oil. This implies that the effectiveness factor was close to one. Also, Van Zoonen and Douwes varied pore diameter from 66 to 464 Å and found this had no effect. Jones and Friedman (27) studied hydrogenation of a coal derived liquid at 770°F (410°C) and 3000 psig over a Ni/Co/Mo catalyst. They found a 3 fold reduction in a catalyst diameter resulted in a 4 fold increase in hydrodenitrogenation activity. This implies significant pore diffusion and an effectiveness factor much less than one. Satchell (49), in his study of hydrodenitrogenation of a coal liquid, raw anthracene oil, over a Co/Mo catalyst, concluded that the effectiveness factor was one at 650°F (343°C) and 0.95 at 700°F (371°C). Both measurements were made at a pressure of 1000 psig. Aboul-Gheit and Abdou (1) in their work on hydrodenitrogenation of pure nitrogen compounds spiked in paraffins found that pore diffusion was significant in catalyst particle sizes larger than 60-85 mesh.

Experimental data on the effectiveness factor for hydrodesulfurization vary from one to about 0.3, and some studies indicate that pore diameter affects the effectiveness factor. Van Deemter (66) in a study of gas oil, found that reducing the diameter of the Co/Mo catalyst from 0.197 inch (0.5 cm) to 0.137 inch (0.35 cm) changed the effectiveness factor from 0.36 to 0.99. This indicated pore diffusion resistance in the larger catalyst particle. Sooter's work (63) on hydrodesulfurization of raw anthracene oil indicated an approximate effectiveness factor of one. In this study he reduced the catalyst particle size from 8-10 mesh to 40-48 mesh and observed no change in hydrodesulfurization. Addington and Thompson (2) in a study of gas oil at 780°F (416°C) and

1500 psig found an effectiveness factor of 0.6 for a 0.125 inch (0.318 cm) Co/Mo catalyst. Schuit and Gates (54), reported a study of hydrodesulfurization of gas oil by Cecil, Mayer, and Cart. In this study, Cecil, et al., reported an effectiveness factor of 0.4 for a cylindrical catalyst 0.062 inch (0.16 cm) in diameter. They also reported that changing the pore diameter from 78 Å to 103 Å increased the effectiveness factor to 0.8. In a recent study of hydrodesulfurization of a coal derived liquid (FMC oil), Ahmed (3) found no difference in the hydrodesulfurization ability of two Co/Mo/γAl_2O_3 catalysts; one with a pore diameter of 33 Å and another with a bimodal pore diameter of 30 Å and 860 Å. However, both catalysts resulted in a final sulfur content lower than the analytical ability of the laboratory instrument. Therefore, analysis of pore diffusion is difficult. Wan (69), Sooter (63) and others (64) in a study of hydrodesulfurization of a coal derived liquid found that increasing pore diameter from 25 Å to 33 Å increased sulfur removal slightly.

Axial Dispersion

In an ideal plug flow reactor, the liquid phase has no velocity gradient in the radial direction and the velocity in the axial direction is constant at any cross section. No slippage or eddies occur in the axial or radial direction. In the real reactor the axial velocity at a cross section is not constant. This results in intermixing or back-mixing which can reduce the reactor efficiency.

Various models have been proposed to predict deviation from plug flow (axial dispersion). Schwartz and Roberts (57) have reviewed these models and have found the axial diffusion model proposed by

Levenspiel (33) is adequate for most trickle bed reactor applications. The problem with this model (and all other models) is that it requires a liquid dispersion coefficient. Since this is not easily found for coal liquids, the literature must be searched to find some indication of when plug flow exists.

Mears (37) has suggested the following criteria for predicting if flow in a trickle bed reactor is within 5% of plug flow.

$$\frac{h}{dp} > \frac{20m}{P_{e_L}} \ln \frac{C_{in}}{C_{out}} \quad \Big| \quad P_{e_L} = \frac{dpL_v}{D_L}$$

where

h - reactor height

dp - diameter of catalyst particle

m - reaction order

P_{e_L} - peclet number

D_L - dispersion coefficient

L_v - liquid superficial velocity

Again, one must have a dispersion coefficient, but in the study of a gas oil, Mears found that at $Re_L = dpL_v\rho/\mu = 8$ if $h/dp > 350$, the axial dispersion effects could be neglected. Sooter (63) and Satchell (49) both concluded that axial dispersion was negligible in their studies using a raw anthracene oil in a 20 inch (50.8 cm) reactor bed with 8-10 mesh particle size. But a recent study by DeBruijn (10) found significant axial dispersion (backmixing) and channeling in a 0.807 (2.1 cm) column packed with 1/16 inch (0.159 cm) extrudate catalyst. This study was based on the hydrodesulfurization of Kuwait gas oil.

Summary

This section has considered the effects of liquid distribution, mass transfer and axial dispersion on reactor efficiency. The following conclusions can be drawn:

1. The type of flow in this study is a gas continuous flow.
2. As of now, no correlations exist for the prediction of contacting efficiency in porous trickle bed reactors.
3. Mass transfer of sulfur bearing compounds through the liquid film on the catalyst particle is negligible.
4. Pore diffusion, as measured by the effectiveness factor, varies from study to study for both hydrodenitrogenation and hydrodesulfurization.
5. Larger pore diameter in general causes the effectiveness factor to increase for hydrodesulfurization.
6. An indication of the existence of axial dispersion problems can be obtained by applying Mear's criteria for axial dispersion. This should be done with some caution because this is a relatively recent correlation and it has not yet been used extensively.

Next operation parameters will be reviewed.

Operational Parameters

Hydrodesulfurization and hydrodenitrogenation ability have been shown to be a function of several operational variables. Many studies of various feedstocks have been performed. These feedstocks have varied from heavy residue to light distillates for petroleum and various coal derived liquids. The effects of operational parameters on petroleum

oil fractions have been considered by Schuit and Gates (54), Schuman and Shalit (55). Since this is a study of a coal derived liquid, the effects of space time, temperature, pressure and hydrogen mass flow rate on hydrodesulfurization and hydrodenitrogenation of coal derived liquids will be considered.

Space Time

For hydrodesulfurization, as space time increases, the percent removal of sulfur also increases. Johns, Jones, and McMunn (26) in a pilot plant study of a coal derived liquid from the FMC process reported an increase in sulfur removal when space time was increased from 1.3 to 5 hours (weight basis). Wan (69) and Sooter (63) in their studies of hydrodesulfurization of raw anthracene oil also observed that an increase in volume hourly space time over the range 0.216-1.802 hours resulted in an increase in sulfur removal.

In the study of hydrodenitrogenation an increase in space time also resulted in an increase in removal, but the literature does not agree on the dependence of hydrodenitrogenation on space time. A study by Jones and Friedman (28) using a coal derived liquid from the COED process found the kinetics of hydrodenitrogenation could be described by a first order expression with respect to total nitrogen concentration. This indicates a strong dependence of hydrodenitrogenation on space time. Wan (69) in his study of raw anthracene oil observed a strong dependence on space time at a volume hourly space time smaller than 0.4 hours, but at space times greater than 0.4 hours he found a rather weak dependence. Satchell's (49) study of raw anthracene oil hydrodenitrogenation found a second order dependence between total nitrogen content and volume hourly

space time in the range 0.375 to 1.5 hours.

Temperature

Hydrodesulfurization of coal derived liquids has been studied over a range of temperatures from 600°F (319°C) to 930°F (499°C). In general the higher the temperature, the greater the sulfur removal, as would be expected. Sooter (63) in his study of hydrodesulfurization of raw anthracene oil at 1000 psig, found that percent sulfur removal increased from 2.1% to 77.2% when the temperature was increased from 600°F (316°C) to 800°F (427°C). Qader, et al. (16) found greater than 90% removal of sulfur at 788°F (420°C) in a study of hydrogenation of a coal derived liquid in a fixed bed reactor. Qader and Hill (44) observed 62% removal of sulfur at 662°F (350°C) and 100% removal between 841°F (450°C) and 1022°F (550°C) in a batch autoclave reactor study of hydrogenation of a coal tar at 1500 psig.

Similar temperature effects have been reported for hydrodenitrogenation of coal derived liquids. Satchell (49) in his study of raw anthracene oil at 1000 psig observed an increase in conversion from 16.5% to 71% nitrogen removal with increasing temperature in the range of 600°F (316°C) to 800°F (427°C). Qader and Hill (44) also observed this effect over a temperature range of 662°F (350°C) to 932°F (500°C) at a pressure of 1500 psig. Here percent nitrogen removal increased from 32% at 662°F (350°C) to 99% at 932°F (500°C).

Pressure and Hydrogen Flow Rate

Pressure and hydrogen flow rate are two more factors which affect the hydrodesulfurization and hydrodenitrogenation ability. The hydrogen

is usually supplied at a high rate and a high pressure. This maintains a high hydrogen partial pressure and insures hydrogen will be present in stoichiometric excess for the hydrodenitrogenation and hydrodesulfurization reaction.

For hydrodesulfurization of coal derived liquids the reports vary as to effect of pressure. Wan (69) and Sooter (63) in their raw anthracene oil studies found that hydrodesulfurization increased as pressure increased from 500 psig to 1000 psig. But an operating pressure in the range of 1000 psig to 1500 psig did not cause an increase in hydrodesulfurization ability. Sooter (63) suggested that this was caused by the liquid becoming saturated with hydrogen. A study on FMC oil (64) reported increasing pressure in the range of 500 psig to 1500 psig resulted in improved sulfur removal. Scotti (60) found 96% removal of sulfur with pressures between 1800 psig and 2400 psig using a coal derived liquid from the COED process. Qader and Hill (44) in their batch autoclave study of coal tar found that increasing pressure from 1000 psig to 3000 psig resulted in an increase in the percent sulfur removal from 90% to 99%.

The effect of pressure on hydrodenitrogenation indicate that increasing pressure causes an increase in nitrogen removal. A study of hydrodenitrogenation of COED oil (28) found that increasing the pressure from 2000 to 3100 psig increased nitrogen removal by a factor of two. Qader and Hill (44) also reported an increase in removal with increasing pressure. They found that increasing the pressure from 1000 psig to 3000 psig resulted in an increase in nitrogen removal from 50% to 80% for coal tar. Satchell (49) also observed an increase in hydrodenitrogenation as pressure increased from 500 psig to 1500 psig. At a volume

hourly space time of 1.5 hours and a temperature of 700°F (341°C), the nitrogen removal increased from 38% to 63% when the pressure was increased from 500 psig to 1500 psig.

Hydrogen flow rate can have two effects on reactor performance. First, it controls the hydrogen concentration available for hydrodenitrogenation and hydrodesulfuruzation. Also, the hydrogen mass flow rate may affect film thickness and turbulence. This can of course affect the rates of mass transfer through the liquid film.

Wan (69), in his study of raw anthracene oil, varied the hydrogen flow rate from 3980 to 39800 scf H_2/bbl oil. For sulfur Wan found no significant effect, but for nitrogen removal Wan observed a slight increase from 61.2 to 69.2%. The reactor was operating at 800°F (427°C), 1000 psig, and 0.901 hour volume hourly space time. Sooter (63) in his study of the same feedstock reported no significant effect on the hydrodesulfurization ability when the hydrogen flow rate was varied from 1500 to 20,000 scf H_2/bbl oil. The operating conditions in this study were 1000 psig, 650°F and 1.5 hours volume hourly space time. Satchell (49), in the same experiments, found that varying hydrogen flow rate from 1500 to 20,000 scf H_2/bbl oil at 700°F (371°C), 1000 psig and 1.5 hours volume hourly space time had no significant effect on hydrodenitrogenation of raw anthracene oil.

Summary

In this section, operational parameters were reviewed and the following conclusions can be drawn.

1. All of the data reviewed suggested that as space time increases the hydrodesulfurization and hydrodenitrogenation increases.

This indicates that the reactants are not reaching the equilibrium limitations.

2. The majority of the hydrodenitrogenation and hydrodesulfurization studies have been made between temperature of 600°F (316°C) and 900°F (482°C). In general, the higher the temperature the greater the activity for hydrodesulfurization and hydrodenitrogenation.
3. Hydrodenitrogenation increases as pressure increases in the range from 500 psig to 3100 psig. The amount of increase depends on the type of liquid studied.
4. The effect of pressure on hydrodesulfurization of a coal derived liquid varies with the type of liquid.
5. For raw anthracene oil, the hydrogen flow rate has been varied from 1500 scf/bbl to 39,800 scf/bbl, no effect has been observed on hydrodesulfurization and hydrodenitrogenation levels.

Next, kinetics of hydrodenitrogenation and hydrodesulfurization will be considered.

Kinetics of Hydrodesulfurization and Hydrodenitrogenation

The observed kinetics in a real trickle bed reactor, in which mass transfer resistance and heat effects are negligible, can be affected by three things:

1. The presence of flow distribution problems.
2. The presence of a broad spectrum of nitrogen or sulfur compounds.

3. The presence of inhibitors and/or promoters.

The existence of flow distribution problems in a trickle bed reactor can cause an apparent higher order for reaction kinetics. This was first suggested by Ross (47) in his comparison of commercial, pilot plant, and experimental reactors. Recently, two correlations have been proposed to account for this effect on reaction kinetics. Henry and Gilbert (20), following the suggestion of Ross, proposed that the observed reaction rate is proportional to the liquid holdup. They developed the following relation:

$$\ell n \frac{C_{in}}{C_{out}} \alpha \frac{-k_v h^{1/3}}{(LHSV)^{2/3}}$$

where

C_{in}, C_{out} - concentration of reactant in entering and leaving liquids, moles/cm^3

k_v - rate constant, cm^3 of liquid/(cm^3 of catalyst pellet volume)(sec)

h - catalyst bed length, cm

LHSV - liquid hourly space velocity, hr^{-1}

This accounts for the fact that the catalyst particle is not completely surrounded by fresh liquid at all times. They applied the above relation to hydrodesulfurization and hydrodenitrogenation data. From this they concluded that the above relation did account for effects of liquid distribution on reaction kinetics. In a later study, Mears (38) suggested that a better criteria is the external fraction of the catalyst area freshly wetted by this liquid. Using wetting correlations from packed bed studies he obtained the following relation:

$$\ell n \frac{C_{in}}{C_{out}} \alpha \quad h^{.32}(LHSV)^{-.68}(dp)^{.18}(\nu)^{.05}(\sigma_c/\sigma)^{.21}\eta$$

where

C_{in}, C_{out} - concentration of reactant in entering and leaving liquids, moles/cm^3

h - catalyst bed length, cm

LHSV - liquid hourly space velocity, hr^{-1}

d_p - diameter of catalyst particle, cm

ν - kinematic viscosity, cm^2/sec

σ - surface tension of liquid, gram/sec^2

σ_c - critical value of surface tension for packing, grams/sec

η - effectiveness factor, unitless

This equation contains the factor (η) which is the pore diffusion effectiveness factor. Mears also established that the extent of liquid holdup does not affect the criteria for freedom from axial dispersion which he had proposed earlier (37). Re-evaluating the work of Henry and Gilbert (20), he found that part of the higher order behavior was due to axial dispersion instead of liquid holdup. Mears concluded that the above relation was good only when axial dispersion and heat effects are negligible.

Another factor affecting the observed kinetics of a trickle flow reactor is the presence of a broad spectrum of sulfur or nitrogen compounds. When one is dealing with a real oil fraction, more than one type of sulfur or nitrogen compound can be present. The rate at which the compounds react depends on the rate constant and concentration of each species. The species with the higher rate constant and/or

concentration will react the fastest, while compounds with a lower rate constant and/or concentration will react at a slower rate. This effect would cause an apparent higher order. Schuit and Gates (54) have reported this effect in a review of hydrodesulfurization kinetics. Here a number of pure sulfur compound studies showed first order kinetics while studies of petroleum oil fractions containing multiple sulfur compounds showed second order behavior. Flinn, Larson and Beuthur (12) also found second order behavior with respect to total nitrogen concentration in a trickle bed study of hydrodenitrogenation of light furnace oil. They concluded that this was due to the presence of a broad spectrum of nitrogen compounds.

The kinetics of a reaction can also be affected by the presence of inhibitors and promoters. Inhibitors are compounds which tend to block or compete for active sites with the sulfur or nitrogen compounds. On the other hand, promoters tend to maintain the active structure and remove the inhibiting compounds from the active sites. Schuit and Gates (54), in a review of industrial hydrodesulfurization kinetics, reported hydrogen sulfide improved the hydrodenitrogenation ability of sulfided $CoO/MoO_3/\gamma Al_2O_3$ and $NiO/WO_3/\gamma Al_2O_3$ catalysts in the studies of Goudriaan, et al. (14) and Satterfield, et al. (52). Satterfield, et al. (52) also found that hydrogen sulfide acted as a promoter for hydrodenitrogenation of pyridine above 616°F (325°C) but below 616°F (325°C) it acted as an inhibitor. They proposed that below 616°F (325°C) the hydrogen sulfide competed with pyridine for the hydrogenation sites; while at temperatures greater than 616°F (325°C), the hydrogen sulfide may maintain the sites or cause the removal of strongly absorbed nitrogen compounds from the site. McIlvried (36) reported the

hydrodenitrogenation of pyridine is inhibited by the presence of ammonia and nitrogen compounds.

Many authors have studied the hydrodesulfurization of oil fractions (petroleum, shale oil, and coal derived liquids). Most kinetic studies of oil fraction hydrodesulfurization have concluded that it is a second order reaction with respect to total sulfur concentration (54). Recently Sooter (63) in a study of raw anthracene oil in a trickle bed reactor found a reaction order greater than or equal to two would fit his data. DeBrujin (10) in a recent trickle bed study of hydrodesulfurization of a Kuwait gas oil found second order behavior when backmixing was not significant. But a study by Qader (44) of hydrodesulfurization of coal tar in a batch autoclave reactor found first order behavior with respect to total sulfur concentration.

Very little information is available for hydrodenitrogenation of oil fractions, and the available data is contradictory. Flinn, Larson and Beuther (12) found second order behavior with respect to total nitrogen concentration for a light furnace oil. But for a heavy Kuwait gas oil they found first order behavior with respect to total nitrogen concentration. Both studies were done in trickle bed reactors. Satchell (49) in a study of raw anthracene oil proposed that hydrodenitrogenation was second order with respect to total nitrogen concentration. Jones and Friedman (28) found first order behavior with respect to total nitrogen concentration in a trickle bed reactor study of a coal derived liquid from the COED process. Frost and Jensen (13) also observed first order behavior in a trickle bed study of shale oil. Qader and Hill (45) in a study of coal tar hydrogenation in a batch autoclave reactor found first order behavior with respect to total

nitrogen concentration.

Summary

In this section, the factors affecting reactor kinetics have been reviewed. The following conclusions can be drawn:

1. The effect of flow distribution problems on reactor kinetics has been described by correlations given by Henry, et al. (25) and Mears (38). Both studies are relatively new and have not been widely tested.
2. An apparent higher order for hydrodenitrogenation and hydrodesulfurization can be caused by the presence of a broad spectrum of sulfur and nitrogen compound types.
3. The presence of hydrogen sulfide tends to inhibit hydrodesulfurization, while it acts as a promoter for hydrodenitrogenation.
4. Second order behavior is normally observed for hydrodesulfurization of oil fractions (petroleum, shale oil and coal derived liquids).
5. Both first and second order behavior has been observed for hydrodenitrogenation of oil fractions.

CHAPTER III

EXPERIMENTAL APPARATUS

This study was conducted using a trickle bed reactor previously designed and constructed for another related study (49, 63). The system was designed to allow isothermal operations at pressures up to 1500 psig and to allow the oil and hydrogen flow rates to be measured and controlled accurately. The existing system is shown in Figure 1. The experimental equipment used in this study is listed in Table II along with vendor and model numbers. The equipment identification number given each item corresponds to the equipment numbers shown in Figure 1. (In the following description, item number will be given after the name of the equipment for convenience.)

The treat gas and oil entered the top of the trickle bed reactor, 40, and flowed through the reactor to the sample bombs, 16, 18, where the gas and liquid phases were separated. The liquid was collected in the sample bomb 18 and the treat gas was scrubbed and vented to a hood. The system's pressure was maintained by a pressure regulator, 4, on the inlet treat gas line. The treat gas rate was regulated by a microvalve, 31, on the sample bomb off gas line. The flow rate of the oil was set by the positive displacement pump's, 36, speed. A detailed description of the equipment follows.

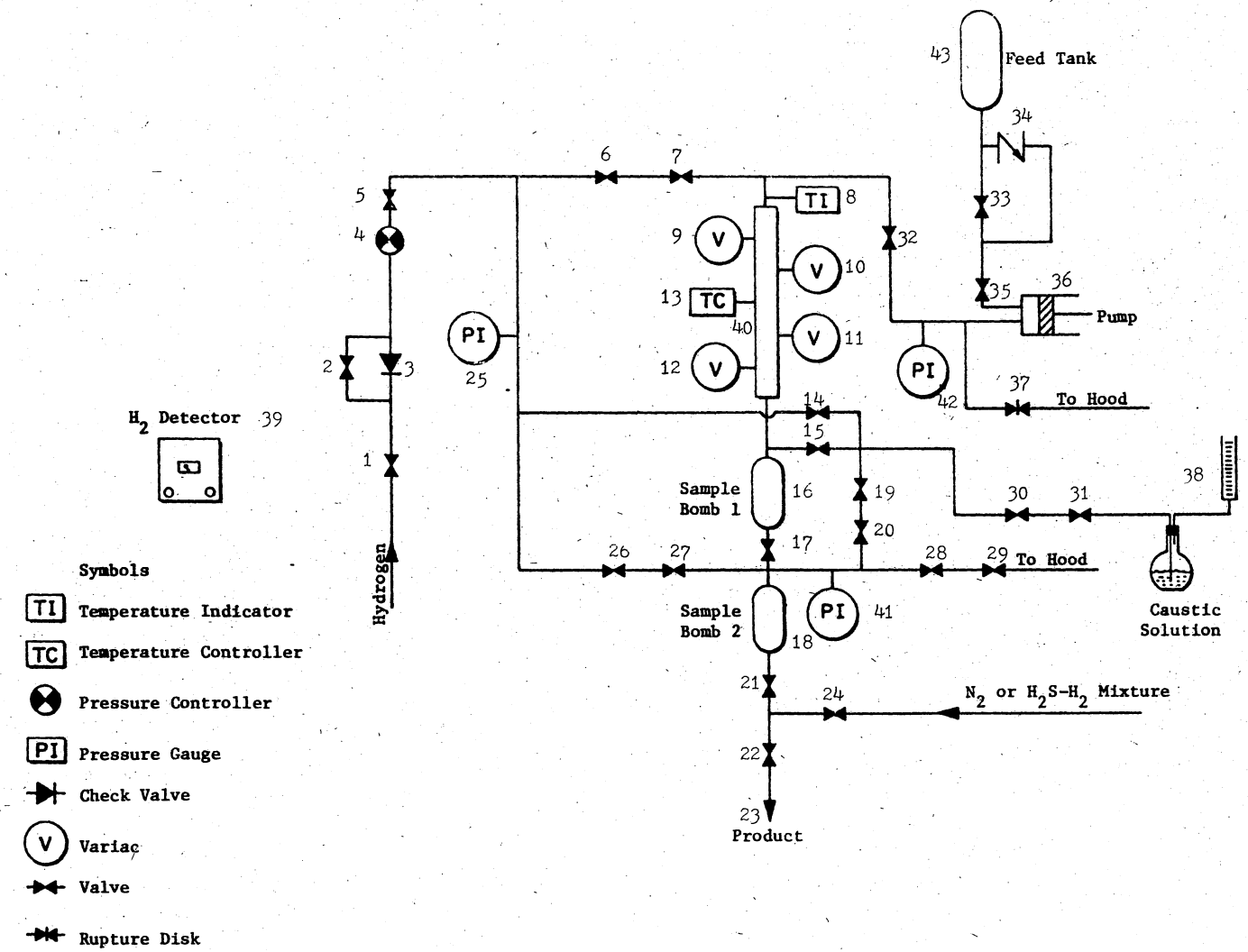

Figure 1. Schematic Flow Diagram of the Experimental System

TABLE II

LIST OF EXPERIMENTAL EQUIPMENT

Tubing	1/4 inch O.D. Stainless Steel Tubing
1	Valve - Whitey SS4354
2	Valve - Autoclave 10V-4071
3	Check Valve - Autoclave 10-6904-316-CW
4	Pressure Reducing Regulator - Grove Mitey Mite Model 94
5	Valve - Whitey 3TS4
6	Valve - Whitey 3TS4
7	Valve - Autoclave 10V-4071
8	Temperature Display - Leeds and Northrup 900 Series Numatron with a Conax J-SS4-G-T3 Thermocouple
9	Powerstat - Curtin Type 316 with Marsh Resistance Heater
10	Powerstat - Curtin Type 316 with Marsh Resistance Heater
11	Powerstat - Curtin Type 316 with Marsh Resistance Heater
12	Powerstat - Curtin Type 316 with Marsh Resistance Heater
13	Temperature Programmer - Hewlett-Packard Model 240 with Marsh Resistance Heaters
14	Valve - Whitey IVS4
15	Valve - Autoclave 10V-4001
16	Sample Bomb - Hoke DOT3A1800
17	Valve - Autoclave 10V-4071
18	Sample Bomb - Hoke DOT3A1800
19	Valve - Autoclave 10V-4001
20	Valve - Whitey 3TS4

TABLE II (continued)

21	Valve - Whitey 1VS4
22	Valve - Whitey 1VS4
23	Valve - Whitey 1VS4
24	Valve - Whitey 1VS4
25	Pressure Gauge - Heise Dourdon Tube Gauge, 5000 psig maximum pressure
26	Valve - Whitey 3TS4
27	Valve - Whitey 1VS4
28	Valve - Whitey 3TS4
29	Valve - Whitey 1VS4
30	Valve - Autoclave 10V-4071
31	Valve - Whitey 22RS4
32	Valve - Autoclave 10V-4071
33	Valve - Whitey 1VS4
34	Check Valve - Whitey 5354
35	Valve - Autoclave 10V-4071
36	Ruska Pump Model 2236
37	Rupture Disc - Autoclave 3000
38	Bubble Meter - Fisher 25 ml
39	MSA Hydrogen Detector Model I-501
40	Reactor - 1/2 inch 316 stainless steel (see Figure 2) with aluminum block heaters (see Figure 3) installed with Carr Fiberglass insulation
41	Pressure Gauge - Ashcroft Duragauge, 3000 psig maximum pressure
42	Pressure Gauge - Ashcroft Maxisafe, 3000 psig maximum pressure
43	Oil Storage - Hoke 84D2250

Reactor

A critical, but simple, piece of equipment is the reactor, shown in Figure 2. It consists of a 33-1/4 inch (84.5 cm) long, 1/2 inch (1.27 cm) O.D., stainless steel tube with a 1/8 inch (.3175 cm) stainless steel thermal well running down the center of the reactor. The thermal well was welded shut on the bottom. The top of the thermal well was secured in the 1/2 inch (1.27 cm) stainless steel cross by means of a modified 1/4 to 1/8 inch (1.27 to .318 cm) reducer. The centerline thermal well was used to obtain temperature profiles of the reactor bed. The reactor bed was held in place by fifty mesh stainless steel screens located at the top and bottom of the stainless steel tubes as shown in Figure 2.

Reactor Heating System

In this study, the reactor, 40, was maintained at isothermal conditions as closely as possible. This was done by massive aluminum blocks grooved and wrapped with electrical resistance heaters and insulation. A typical block is shown in Figure 3. The location of the blocks and the mode of thermal control are given in Table III. The energy inputs to the blocks were controlled by a Hewlett-Packard Model 240 and by powerstats, 9, 12. The control thermocouple for the temperature programmer was placed in a small hole 1-3/5 inch (4.06 cm) deep in block III. Control with the variacs was maintained manually to achieve flat temperature profiles.

The insulation used around the reactor consisted of a 1 inch (2.54 cm) layer of felt insulation and a 2 inch (5.06 cm) layer of

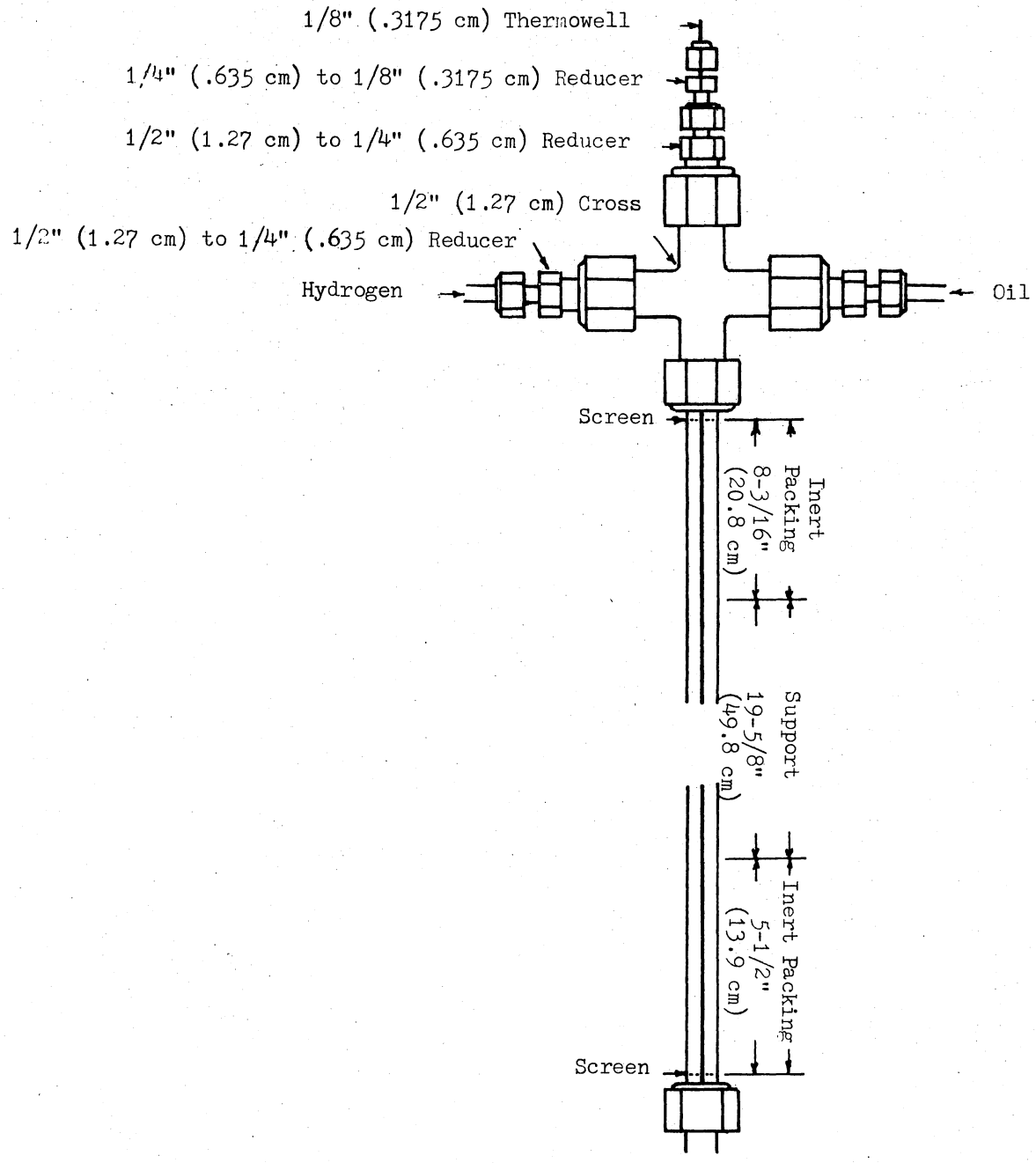

Figure 2. Reactor Design

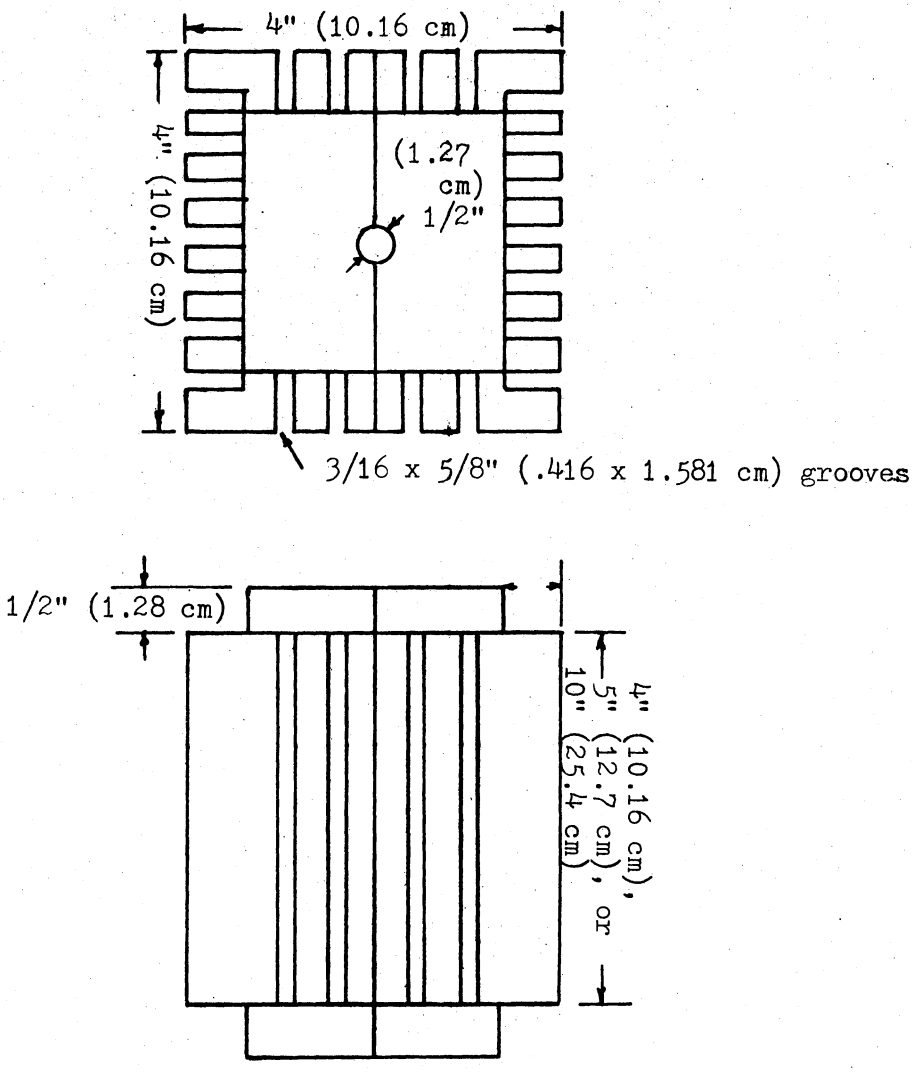

Figure 3. Reactor Heater Block Design

fiberglass insulation wrapped around the heating blocks. Each layer of insulation was held in place by asbestos tape.

TABLE III

REACTOR HEATERS

Block Number From Reactor Inlet	Block Height in inches (cm)	Mode of Control
I	4 (10.16)	Powerstat
II	5 (12.70)	Powerstat
III	10 (25.40)	Temperature Controller
IV	5 (12.70)	Powerstat
V	4 (10.16)	Powerstat

Temperature Measurements

The reactor temperature profile was measured with a Conax J-SS4-G-T3 iron constantan thermocouple. This was done by moving the thermocouple to a position in the thermal well, allowing the thermocouple to equilibrate, and then noting the digital readout from a Leeds and Northrup 900 Series Numatron, 8.

Pressure and Flow Control

The system pressure was measured on a 0-5000 psig Heise Gauge, 25, located upstream of the reactor. The pressure read from this gauge

was taken as the nominal reactor pressure. The inlet pressure to the reactor was controlled by using an internally loaded Mitey Mite Pressure Controller, 4. The upstream pressure was maintained by the hydrogen manifold regulator. The off gas rate was controlled by a Whitey Micro-valve, 31, designed for fine flow control. A 25 ml bubble meter, 38, was used to measure the off gas rate from the sample bomb, 18.

Oil and Treat Gas

Feed Systems

The oil was fed from a 2250 ml stainless steel storage tank, 43, to the reactor by a Ruska 2236 Metering, Positive Displacement Pump, 36. Because of the possibility of blockage and excessive pressure build up, a rupture disk, 37, rated at 3000 psig was placed on the delivery line close to the pump. The rupture disk is vented to the hood by a 1/2 inch (1.27 cm) stainless steel tube.

The treat gas (hydrogen or nitrogen) was fed directly from the bottles through a manifold, which allowed the changing of a bottle of treat gas without interruption of the run. Since hydrogen gas was used as a treat gas, an excess flow valve, 3, and a MSA hydrogen detector, 39, Model I-501, were installed as safety devices. The excess flow valve, 3, was placed near the manifold outlet to prevent excessive leakage of hydrogen gas if a rupture occurs downstream. The hydrogen detector, 39, gave an alarm when the hydrogen level had accumulated to 50% of the lower explosvie level. In addition to these precautions a quarter turn valve, 1, was installed between the excess flow valve and the manifold. This provides for a rapid shut off of the feed system in case of emergency.

Sampling System

The sampling system provides a means of obtaining a sample without causing an interruption in operation. The system consists of two sampling bombs, 16, 17, in series. The bombs were one liter stainless steel bombs, rated at 1800 psig at ambient temperature. Figure 4 shows the sample bomb design. A 1/4 inch (0.635 cm) stainless steel tube passes through a reamed 1/2 to 1/4 inch (1.27 to 0.635 cm) reducer. The 1/4 inch (0.635 cm) tube extends down into the bomb. This design allows the liquid and gas phases to separate; the liquid collecting at the bottom of the bomb and the gases going to the vent. Two bombs were necessary to provide a means of sampling while allowing continuous operation. A detailed description of the sampling procedure is given in the experimental section.

Feedstock

The feedstock used in this study was a raw anthracene oil obtained from the Reilly Tar and Chemical Corporation. This feedstock is similar to a solvent fraction produced from a solvent refined coal process. As such, this process stream may require rehydrogenation and cleanup. This coal derived liquid has been studied extensively at this institution and is the best feedstock available for the purpose of this study. The properties determined in this study are shown in Table IV. The raw anthracene oil was found to have a sulfur content of .47 wt%, nitrogen content of 1.055 wt% and nil ash content. Note oxygen analysis was found by difference. These values differ slightly from values reported previously in related studies (49, 63).

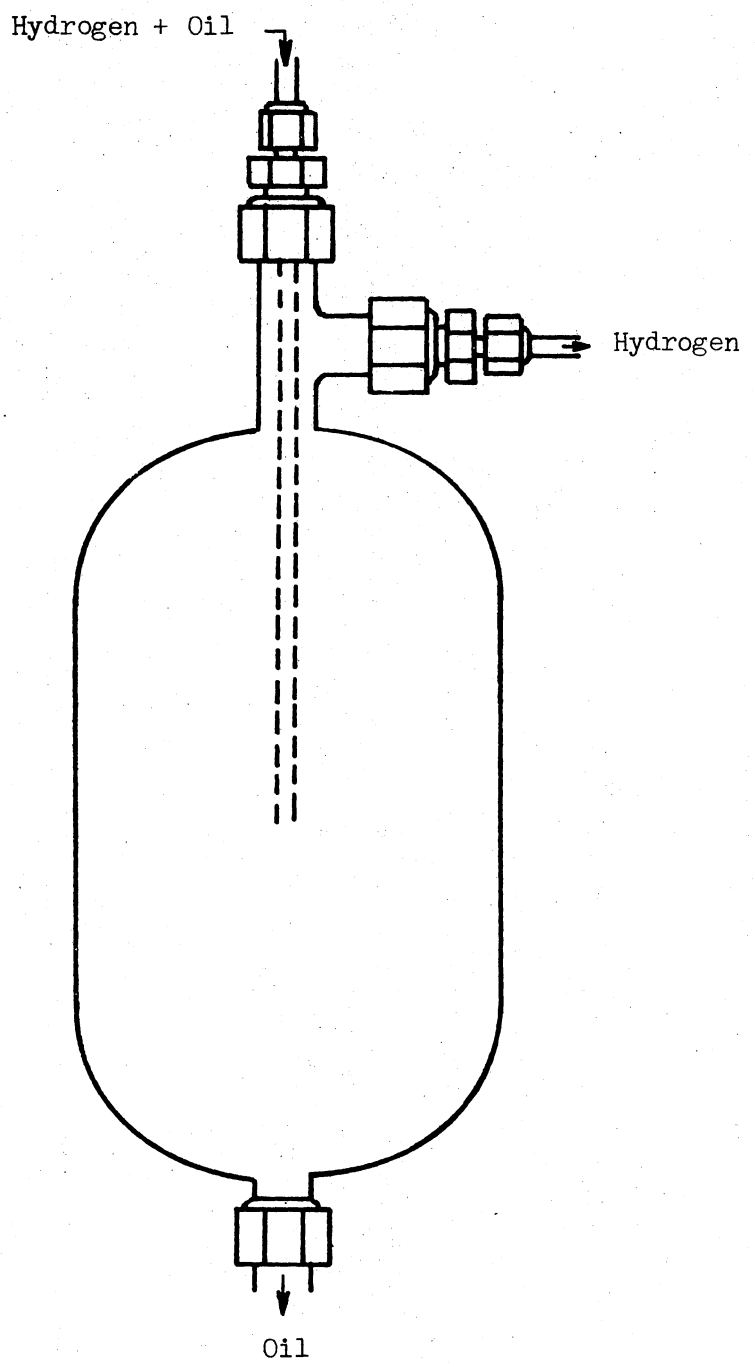

Figure 4. Sample Bomb Design

TABLE IV

FEED OIL PROPERTIES

Carbon, wt %	90.28
Hydrogen	5.57
Sulfur	.47
Nitrogen	1.055
Oxygen	2.6 (Diff)
Ash	Nil

	Distillation	
Volume Distilled	50 mm of Hg	760 mm of Hg*
First Drop	228°F	285°F
10 Vol %	282°F	445°F
20	337°F	507°F
30	367°F	542°F
40	397°F	576°F
50	419°F	600°F
60	441°F	628°F
70	465°F	653°F
80	493°F	685°F
90	534°F	730°F

* Estimated from ASTM D1160 at 50 mm of Hg

Support Properties

The support was a Ketjen Gamma Alumina (007-1.5E) obtained from AKZO Chemi BV. This support was chosen because it was used extensively as a support in commercial hydrodesulfurization catalyst. The properties are listed in Table V. These properties were obtained from the manufacturer. Figure 5 shows the results of mercury penetration porosimetry performed by the American Instrument Co., Inc. The curve was developed from the volume of mercury penetrated into the support for a given pressure. Figure 5 is a plot of $dV/d(\ell nr)$ vs. r . Here $dV/\ell(\ell nr)$ is the differential change in the volume of mercury penetrated (caused by increasing pressure) divided by natural log of the average pore radius corresponding to the pores filled with mercury at a given level of pressure. Figure 5 shows that the Ketjen support (007-1.5E) has a most frequent pore distribution of 34 Å.

Experimental Procedure

Support Preparation

In this study, the activity of an extruded Ketjen Gamma Alumina Support (007-1.5E) was studied. The support was prepared so that there was only one variable; the absence of active metals. Previous active metal impregnations on supports have been done by a method recommended by Leach (29). In this recommended method, MoO_3 was dissolved in an ammonia and water solution. The pH was adjusted to 5.5 with nitric acid acid, and next $Co(NO_3)_2 6H_2O$ was dissolved in the solution. The solution was diluted with distilled water and the support was added.

TABLE V

ANALYSES OF THE KETJEN GAMMA ALUMINA (007-1.5E)

Chemical Composition:		
Loss on Ignition (1 hr 650°C)	:	1.4 % w.b.*
Na_2O	:	0.03 % d.b.*
SO_4	:	0.5 % d.b.*
Refractories	:	balance
Physical Properties:		
Estimated Reactor Density	:	0.49 g/ml
Compacted Bulk Density	:	0.57 g/ml
Surface Area (1 hr 600°C)	:	300.0 m^2/g
Pore Volume (hg) (1 hr 120°C)	:	0.65 ml/g
Average Length	:	7.6 mm
Average Diameter	:	1.7 mm
Side Crushing Strength	:	3.7 lbs/mm
Bulk Crushing Strength	:	8.0 kg/cm^2
Abrasion	:	1.2 %

*d.b. = dry base
w.b. = wet base

(Vendor Supplied Data)

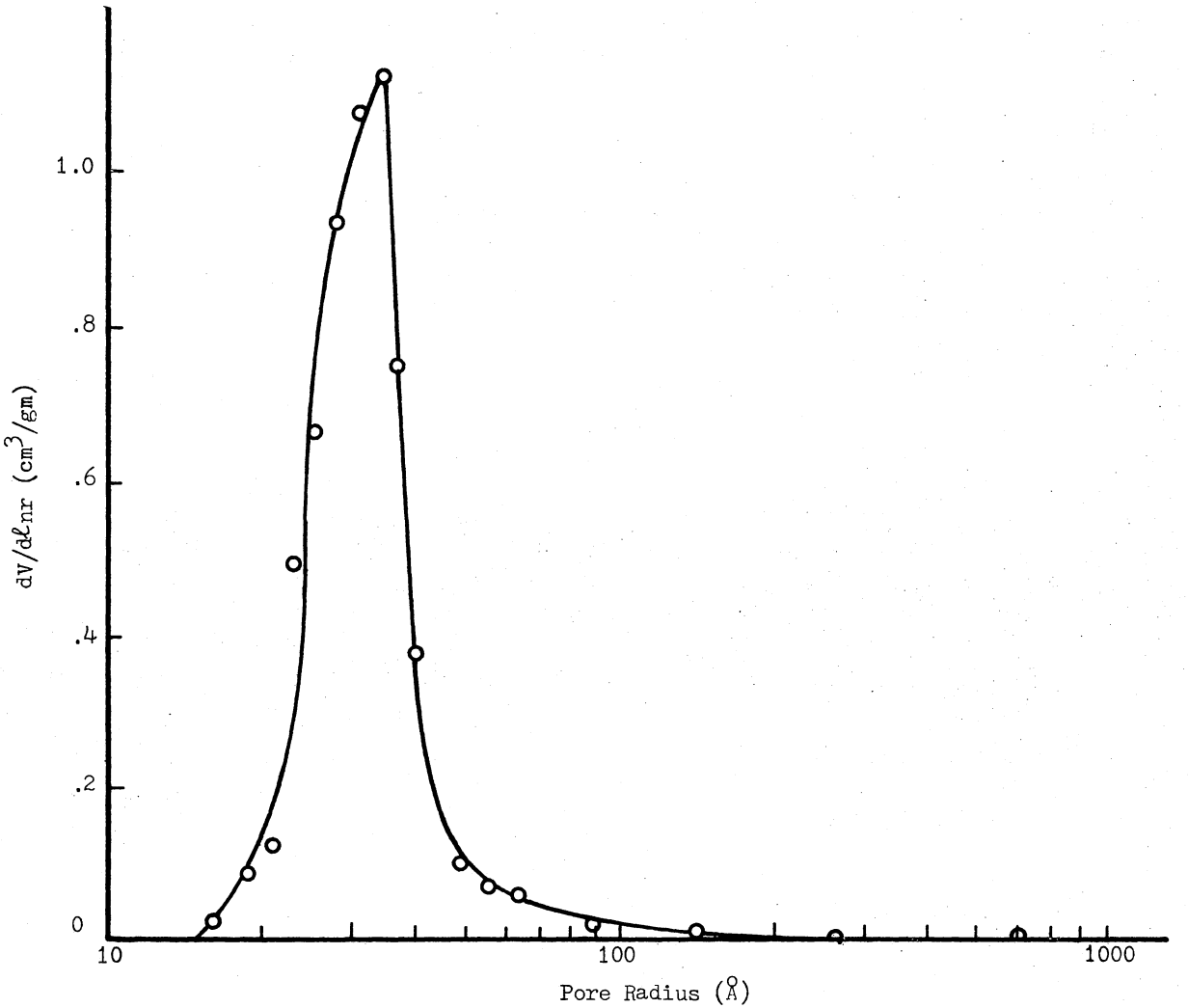

Figure 5. Pore Size Distribution for Ketjen Alumina Support (007-1.5E)

In the present study, the following procedures were used:

1. Crushing and Screening: In other studies the catalysts were usually crushed and screened to achieve an 8-10 mesh size. However, when the crushed extrudate was screened it was usually undersized and passed through the 8-10 mesh screen. For this reason, the support was not crushed or screened but used in the extrudate form.
2. Solution Preparation: 5 ml of 30% aqueous NH_3 was added to 15 ml of distilled water. The pH of the resulting solution was adjusted to 5 with nitric acid. The solution was diluted to 40 ml with distilled water.
3. Support Treatment: The above solution was poured over 25 gm of alumina support. This was allowed to stand for 24 hours. Next the mixture was dried in a furnace at 212 ^{o}F (100^{o}C) for 24 hours. Next the temperature was slowly increased to 900^{o}F (482^{o}C) and maintained at 900^{o}F (482^{o}C) for one hour.

Note the resulting solution contains the same type of ions as present in the method recommended by Leach (29), except Co and Mo ions are absent. The object was to essentially reproduce the regular Leach method except for the active metals addition. A solution for pH of 5 was determined by finding the final pH of the Co/Mo impregnation solution.

The equipment and chemicals used in this preparation are given in Table VI.

TABLE VI

EQUIPMENT AND CHEMICALS FOR
SUPPORT PREPARATION

Leco Furnace	Model Number 540-231
Beckman pH Meter	Model 76
Ammonia Hydroxide	Reagent, Dupont
Nitric Acid	Analytical Reagent, Maclinckrodt

Support Loading

After the support has been prepared as above it was carefully weighed and stored in a desiccator. Next, the reactor tubing was rinsed with acetone and allowed to dry. A fifty mesh screen was wedged between the top of the reactor and the 1/2 inch (1.27 cm) cross. With the thermal well held centrally in the reactor, 8-3/16 inch (20.8 cm) of 8-10 mesh crushed ceramic rashig rings were added. The reactor was tapped vigorously during this process to insure uniform packing. Next, 19-5/8 inch (49.8 cm) of the Ketjen extrudate was added, again the reactor was tapped vigorously during this process. Next, 5-1/2 inch (13.9 cm) of 8-10 mesh crushed ceramic rashig rings were added and tapped. Finally, the 50 mesh screen was placed on the bottom and a straight union screwed in place. This entire arrangement is shown in Figure 2.

Next, the reactor was installed in the system by connecting the 1/4 inch (0.635 cm) oil and hydrogen feed lines at the top and the 1/4

inch (0.635 cm) product line at the bottom. Once this was done, the system was pressurized to 1800 psig with nitrogen, and all fittings were checked for leaks with soap solution. This done, the pressurized system was allowed to set for 8-12 hours. If no significant pressure drop (< 20 psi) was observed, the insulation was installed. At this point, the heater circuits were checked for continuity with a volt-ohm meter.

Support Activation

The reactor was slowly heated to 450°F (232°C) and maintained at this temperature for 12 hours while prepurified nitrogen passed over the support bed. This calcining step was done to remove adsorbed water from the support bed. Next the Mitey Mite Pressure Regulator, 4, and Heise Gauge, 25, were isolated from the system, and the reactor was purged with hydrogen for 10 minutes. After this support was treated with a 5 mole % H_2S and the H_2S/H_2 gas flow rate was maintained at 8 cm^3/sec for 2 hours. The system was then purged with hydrogen gas at 100 psig for 10 minutes.

The support bed was presulfided only in experimental run BCW. The ACW and CCW support beds were not presulfided.

Start Up

The Heise Gauge, 25, and the Mitey Mite Pressure Regulator, 4, were reconnected to the system, and the reactor was heated to the operating temperature of 750°F (399°C). Also during this heating period the Ruska Meter Pump, 36, was filled with the feedstock, raw anthracene oil. When the reactor had reached the desired temperature, the system was pressurized with the treat gas to 1500 psig. The Ruska Pump, 36, feed

was set to the desired rate and turned on. The hydrogen flow rate was then adjusted with the Whitey Microvalve, 31, on the off gas line.

Normal Operation

Once the reactor, 40, was receiving oil and treat gas, the system was allowed to stabilize for 48 hours. This period allowed the reactor temperature and pressure to stabilize. Also when active metals are present on the support this period allowed the catalyst bed to stabilize. During the line out period the temperature profile and pressures of the reactor were recorded every half hour until the system stabilized at the desired temperature and pressure. Once this was achieved the temperature profile and pressure were recorded every hour.

Table VII summarizes the valve settings during normal operations. Valve locations can be found in Figure 1.

TABLE VII

NORMAL OPERATION VALVE POSITIONS

Valve	Position	Valve	Position	Valve	Position
1	Open	19	Open	27	Open
2	Open	20	Open	28	Closed
6	Open	21	Closed	29	Open
7	Open	22	Closed	30	Open
14	Closed	23	Closed	31	Open
15	Closed	24	Closed	32	Open
17	Open	26	Closed	33	Closed

Sampling Procedure

After the 48 hour line out period, the collection of samples began. As stated earlier, the system has been designed to allow sampling without disturbing normal operating conditions. The following procedure was used to obtain a sample. Item numbers correspond to those given in Figure 1.

1. Valve 19 and 17 were closed and valve 15 was opened. This isolates sample bomb, 18, and allows the gas to flow through valve 15.
2. Valve 28 was opened slowly. This allowed the pressure in the sample bomb, 18, to drop to atmospheric pressure, as observed on pressure gauge, 41.
3. Once the pressure in sample bomb, 18, was atmospheric, valve 24 and 21 were opened. This allows nitrogen to bubble through the sample bomb, 18, removing NH_3 and H_2S for 30 minutes.
4. After the nitrogen purge, valve 28 and 24 were closed and the sample was collected by opening valve 22.
5. After the sample was collected valve 21, 22 and 6 were closed. Valve 26 was slowly opened until sample bomb, 18, had returned to normal pressure.
6. Valve 26 was closed and valve 6 was opened.
7. Valve 17 and 19 are opened and valve 15 was closed. This returns the system to normal operating conditions.

Reactor Shut Down

The following procedure was used during reactor shut down.

1. Valve 1 was closed, securing the hydrogen flow.
2. Next, the pump and all heating systems were de-energized.
3. The system pressure was allowed to fall to 200 psig.
4. The reactor was allowed to cool to ambient temperature.
5. System pressure was then reduced to atmospheric pressure.

Sample Analysis

In this study, four types of analyses were performed. These were ASTM D1160 Distillations, sulfur analysis, nitrogen analysis and hydrogen analysis.

ASTM D1160 Distillation

This analysis was done on a standard ASTM D1160 distillation unit. The pot and vapor temperatures were recorded as the sample is distilled. The existing apparatus has been modified to allow the collection of equal volume fractions of the distillate without interruption of the vacuum distillation. All distillations were performed at a pressure of 50 mm of Hg absolute. A detailed description of the procedure is given in Appendix C. Due to insufficient pot heating rates, the vapor temperatures obtained in these distillations were low and erratic, but the pot temperature data was accurate. Because of these difficulties, a correlation was developed to correct the pot temperature to the vapor temperature. This is discussed in Appendix A.

Sulfur Analysis

The total sulfur concentration of the product samples was determined by a Leco Automatic Sulfur Analyzer. The general procedure for

sulfur analysis has been described in the Leco Bulletin (30). The system consists of a Model 521-500 Induction Furnace, a Model 532-000 Automatic Titrator and an oxygen purifying train. In this system, the sample was combusted in an atmosphere of purified oxygen in the induction furnace. This caused the sulfur species in the sample to form SO_2. The SO_2 and other combustion products were then passed to an automatic titrator, where the SO_2 in these gases was automatically titrated by an iodate method. This method was based on an ASTM combustion method E3065 (30). The detailed procedure will now be discussed.

Solution Preparation

Three solutions were required for sulfur analysis: starch solution, HCL solution and KIO_3 solution. The starch solution was prepared daily by dissolving 2 gm of arrow root starch in 50 ml of distilled water. This solution was added to 150 ml of boiling distilled water and the resulting solution was boiled for 1 to 2 minutes. It was then allowed to cool to room temperature. Next six grams of KI were dissolved in the solution. The HCL solution was made by placing 15 ml of concentrated HCL in a 1 liter volumetric flask. This flask was filled to the 1 liter mark with distilled water. This solution was usually prepared in large quantities and can be kept about a month. The KIO_3 solution was prepared by placing 0.444 gms of KIO_3 in 1 liter volumetric flasks and then filling the flask with distilled water to the 1 liter mark. Like HCL this solution was also made in large quantities and kept for up to a month.

System Preparation

Next the combustion tube, photocell and titrate vessel were cleaned with distilled water and allowed to dry. The photocell was aligned by adjusting the photocell resistance to 30,000-50,000 ohms. After this both the furnace and the automatic titrator were turned on and allowed to warmup for 30 minutes. The HCL solution was added to the titrate vessel to bring the level to a predetermined mark on the titrate vessel. Next, purified oxygen was allowed to bubble through the HCL in the titrate vessel for 15 minutes. This insured that the vessel was clean. Also the heating element on the tube connecting the furnace to the titrator was energized and allowed to warmup for 15 minutes.

Sample Preparation

The sample itself is prepared by following, exactly, the order given here:

1. to a crucible add 0.282 ±0.005 gm of MgO
2. weigh crucible
3. add 0.1 ±0.005 gm of sample to MgO layer
4. weigh crucible
5. cover sample with 0.282 ±0.005 gm of MgO
6. add 1.5 ±0.005 gm of iron chips
7. add 0.77 ±0.005 gm of tin accelerator
8. cover crucible
9. sample was ready for combustion.

Calibration

Before any samples were ran, three things were done. First, the endpoint was set. The setting of the endpoint establishes the reference color which the photocell and automatic titrator will maintain by addition of KIO_3 solution. This was done by filling the titrate vessel to the mark with HCL solution and adding 2 ml of starch solution. Purified O_2 was allowed to bubble through the vessel at 1.2ℓ/min. The endpoint control knob was turned to the extreme left position, and the titrator switch was set at endpoint. The endpoint control knob was turned slowly to the right until the addition of KIO_3 solution results in a medium blue solution. Once this was established it is not adjusted for the rest of the day. The reaction which occurs here was as follows:

$$KIO_3 + 5KI + 6HCl \longrightarrow 3I_2 + 6KCl + 3H_2O$$

$$I_2 + \text{Starch} \longrightarrow \text{Blue Complex.}$$

Second, a blank was determined. The blank is a measure of the amount of sulfur present in the crucible and combustion chemicals when no sample is present. Here the crucible was prepared as above but no sample was added. Again the titrate vessel was filled to the mark with the HCL solution. Then 2 ml of starch solution was added and the mixture was agitated by bubbling O_2 at a rate of 1.2ℓ/minute. The titrator switch was set at the endpoint, giving the reference blue color. The titrator switch was set at neutral and buret was filled with KIO_3. At this point, 0.7 gm of sodium azide was added. This was to eliminate interference from nitrogen oxides and chlorine (31). The crucible was placed in the combustion tube and the combustion process occurred. The resulting gases were carried over to the titrate vessel, and the SO_2

in these gases undergo the following reaction

$$SO_2 + I_2 + 2H_2O \longrightarrow H_2SO_4 + 2HI$$

This removed the blue color. This change was sensed by the photocell and the appropriate amount of KIO_3 was added to maintain the endpoint color. The amount added from buret was the blank value. This was done at the beginning and end of each day analyses were made.

Finally, a furnace factor was found. This factor accounts for the extent of sulfur oxidation, since total oxidation of all sulfur to SO_2 is unlikely. In order to find the furnace factor, a reference oil sample of known sulfur content was analyzed. The reference oil used in this study was a coal derived liquid supplied by Pittsburg and Midway Coal Mining Co. The sample was prepared and ran in the same way in which the blanks were determined. The furnace factor was calculated as follows:

$$\text{Furnace Factor (F)} = \frac{(\text{weight of sample})(\text{weight percent sulfur})}{(\text{buret reading} - \text{blank reading})}$$

This factor was determined at the beginning and end of each day analyses were made.

Sample Analysis

Once these three tasks had been completed, the analyzer was ready to run unknown samples. The procedure was identical to that for blank determination. The weight percent sulfur in the unknown samples was found as follows:

$$\text{weight percent sulfur} = \frac{F(\text{buret reading} - \text{buret blank})}{\text{weight of sample}}$$

Two analyses of each sample were made. Additional analysis was done

when poor agreement was obtained from these two. The reported value was taken as the average of the two analyses.

The accuracy and precision of the sulfur analysis done in this manner depends to a large extent on the skill of the operator. This skill can only be developed by operating the analyzer. The chemicals and gases used in this section are given in Table VIII. Also a sample calculation of the furnace factor and weight percent sulfur are given in Appendix E.

Nitrogen and Hydrogen Analysis

Hydrogen and nitrogen analyses were done on a Perkin-Elmer Model 240 Elemental Analyzer. The complete procedure for the analyses have been described in the Perkin-Elmer Manual (41). The analytical system consists of a combustion furnace, reduction furnace and a detector system. In this system, the sample was burned in a purified oxygen atmosphere in the combustion zone of the furnace. The resulting combustion gases were carried through the combustion tube packing by a purified helium gas. The combustion tube packing removed sulfur oxides and halogens. Next, the combustion product gas passes through a reduction tube where nitrogen oxides were reduced to nitrogen gas. This gas was passed to the detector system. The detector system analyzes for hydrogen in the form of water and nitrogen in the form of N_2. This was done automatically in a self integrating, steady state, thermal conductivity analyzer. This analyzer consists of three pairs of thermal conductivity analyzers in series (see Figure 6). The platinum filaments of each pair of cells were connected differentially in a bridge circuit so that the difference in the gas contents of the two cells will result

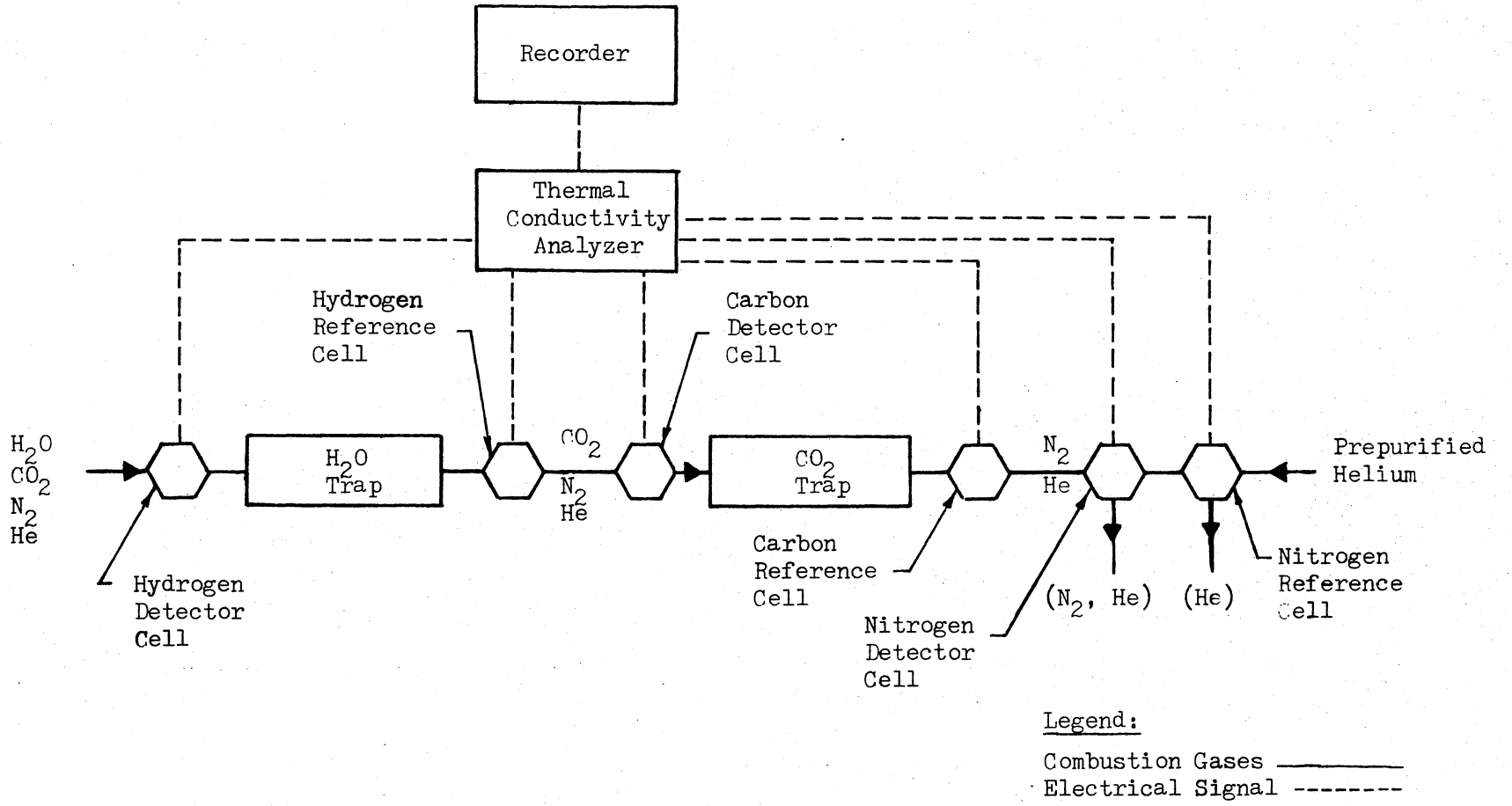

Figure 6. Schematic of Analytical System of Nitrogen, Carbon and Hydrogen Analyzer

in an electrical signal. A magnesium perchlorate trap between the first pair of detectors absorbed any water from the combustion gas before it entered the second cell. Therefore, the signal obtained from the first pair of cells corresponds to the amount of water in the combustion gas. Next, the gas passed to the carbon cell. Here the removal of CO_2 in the absorbing trap resulted in an electrical signal proportional to the carbon content. Finally, the combustion gases from the carbon cell were passed to the nitrogen detector cell. The gas was compared to pure helium resulting in the electrical signal proportional to the nitrogen content.

The electrical signal resulting from the detector cells were recorded on a Leeds and Northrup Speed Max XL Recorder. The recorder output consisted of two signals: a zero and a read signal. The first signals obtained from the analyzer were the zero signals. The zero is the background signal from the detectors. This is the signal caused by prepurified helium flowing through the detector cells. One zero signal was recorded from each pair of detection cells in the following order: nitrogen, carbon, hydrogen. The second group of signals from the analyzer are the read signal, again the one signal is recorded from each pair of cells. The read signal corresponds to the signal caused by the combustion gases. Again, the order of their appearance was nitrogen, carbon and hydrogen. All samples were weighed with a Perkin-Elmer Autobalance, Model AD-2.

Tube Packing

Four types of tubes are required for nitrogen and hydrogen analyses. The recommended make up of these tubes are shown in Figure 7,

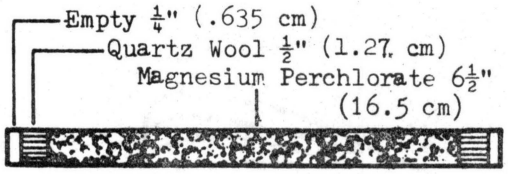

WATER TRAP

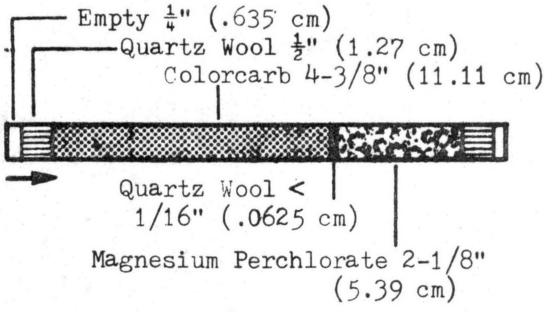

CO_2 TRAP; He, O_2 SCRUBBER

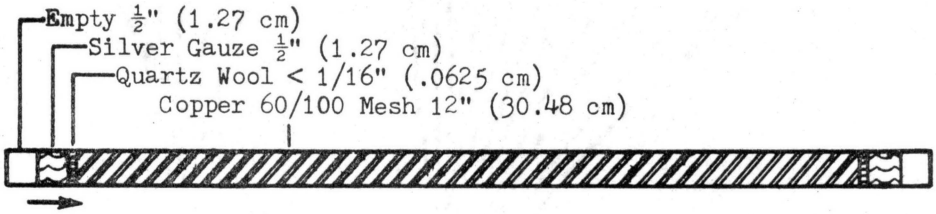

REDUCTION TUBE

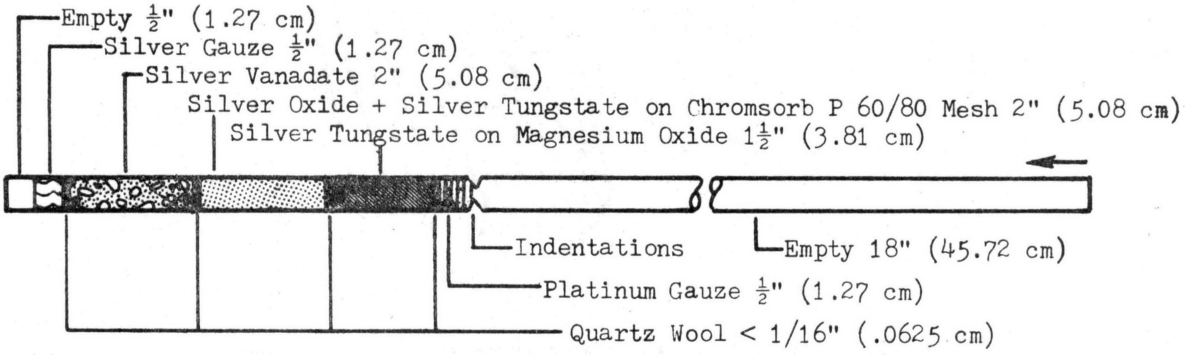

COMBUSTION TUBE - BASIC

Figure 7. Recommended Makeup for Combustion and Reduction Tubes, Traps, and Scrubbers

and the chemicals and materials are listed in Table VIII. During preparation, the tubes were tapped vigorously to insure that flow channeling (short circuiting) of the combustion gases did not occur.

Calibration

Before samples were analyzed, the instrument was calibrated, daily. First, blank values for both nitrogen and hydrogen were found by analyzing an empty platinum sample boat. The empty boat was placed in a combustion ladle and inserted into the combustion tube. (The combustion ladle is a device for moving the sample into the combustion zone. It is constructed of quartz with a magnet sealed in one end and a sample holding area at the other. The magnet allows the ladle and sample to be inserted into and withdrawn from the combustion zone remotely.) The analyzer was then cycled through the analysis program cycle. The blank values were then calculated from the recorder output as follows:

$$\text{Nitrogen:} \quad (\text{Blank})_N = (\text{Read})_N - (\text{Zero})_N$$

$$\text{Hydrogen:} \quad (\text{Blank})_H = (\text{Read})_H - (\text{Zero})_H$$

This was repeated until consistent blanks were obtained. The purpose of the blanks was to take into account any adsorbed nitrogen or hydrogen (water) on the ladle or boat.

Once the nitrogen and hydrogen blanks had been found, the calibration factors for nitrogen and hydrogen were determined. This was done by analyzing a sample of known nitrogen and hydrogen content. In this study, the calibration standard was acetanilide (NAS Standard Sample #141). A 2 to 3 mg sample of acetanilide was carefully weighed into a platinum boat. The sample was then analyzed. And from the recorder

TABLE VIII

LIST OF GASES AND CHEMICALS USED

Hydrogen	prepurified, 99.95%, 220 psig (Air Products)
Nitrogen	purity, 99.997%, 3500 psig (Air Products)
Hydrogen sulfide	5.14% mixture in H_2, 2000 psig (Matheson)
Inert packing	1/4 inch, semi porcelain, Rashig rings (Maurice A. Knight Co.)

Chemicals used in analytical work:

Sulfur Analysis

Oxygen	purity, 99.5%, 2100 psig (Sooner Supply)
Magnesium oxide powder	Analytical grade, Mallinckrodt Chemical Works
Potassium iodate	Analytical grade, Fisher Scientific Company
Potassium iodide	Analytical grade, Baker Chemical Company
Concentrated HCl solution	Fisher Scientific Company
Sodium azide	Chemical purpose, Eastman Kodak Company
Iron chips	Leco Corporation, part #501-007
Tin accelerator	Leco Corporation, part #501-076
Crucible	Leco Corporation, part #528-036
Crucible porous lid	Leco Corporation, part #528-012

Nitrogen and Hydrogen Analysis

Oxygen	Purity, Ultra High Purity (99.99%), 2700 psig (Linde)
Helium	Purity, High Purity (99.995%), 270 psig (Linde)
Aluminum Capsules	Perkin-Elmer, Part No. 009-0709
Platinum Gauze	Perkin-Elmer, Part No. 240-1147
Silver Gauze	Perkin-Elmer, Part No. 240-0092

TABLE VIII (continued)

Magnesium Perchlorate	Reagent Grade, Fisher Scientific Company
Silver Vanadate	33-130 Reagent, Coleman Instruments
Tungstic Anhydride	Purified, Fisher Scientific Company
Quartz Wool	Perkin-Elmer, Part No. 240-1118
Colorcarb CO_2 Absorber	Perkin-Elmer, Part No. 240-0115
Copper (60-100 Mesh)	Perkin-Elmer, Part No. 240-0017
Silver Oxide - Silver Tungstate on Chromosorb Reagent	Perkin-Elmer, Part No. 240-0113
Silver Tungstate-Magnesium Oxide	Perkin-Elmer, Part No. 240-1344
Acetanilide	Organic Analytical Standard, BDH Chemicals Ltd.
Quartz Combustion Tube (9 mm I.D. x 11.2 mm O.D.)	Thermal American Quartz
Quartz Reduction Tube (9 mm I.D. x 11.2 mm O.D.)	Thermal American Quartz
Pyrex Tube (9 mm I.D. x 11.2 mm O.D.)	Perkin-Elmer, Part No. 240-1217

output the calibration factors were calculated as follows:

$$\text{Nitrogen:} \quad K_N = \frac{(\text{Read})_N - (\text{Zero})_N - (\text{Blank})_N}{(\text{Percentage of N})(\text{Sample Weight})}$$

$$\text{Hydrogen:} \quad K_H = \frac{(\text{Read})_H - (\text{Zero})_H - (\text{Blank})_H}{(\text{Percentage of H})(\text{Sample Weight})}$$

Next, to insure that the calibration had been done correctly, the nitrogen and hydrogen content of the raw anthracene feedstock was found and compared to a known value. Because raw anthracene oil is a liquid, it was analyzed in aluminum capsules. Since aluminum capsules and tungstic anhydride were used instead of a platinum boat, the blank value of an empty aluminum capsule was found. This was done by analyaing an open aluminum capsule and one microscope of tungstic anhydride (20 mg). The tungstic anhydride served two purposes. First, it acted as an oxidant and second it protected the quartz ladle from the aluminum. (At the high temperatures (3631°F, 2000°C) of the combustion furnace, aluminum attacks quartz.) The open capsule and the tungstic anhydride were placed in the quartz ladle and the ends of the ladle were plugged with loose wads of quartz wool. This was to insure that the aluminum capsule did not come out in the combustion zone of the furnace and damage the quartz tube. The open capsule was analyzed and the blank values found from recorded output as follows:

$$\text{Nitrogen:} \quad (\text{Blank})_N = (\text{Read})_N - (\text{Zero})_N$$

$$\text{Hydrogen:} \quad (\text{Blank})_H = (\text{Read})_H - (\text{Zero})_H$$

As for platinum boats this was done to determine the amount of nitrogen and hydrogen (H_2O) absorbed on the aluminum capsules surface. This was

repeated until consistent blanks were obtained.

A sample of raw anthracene oil was heated for 15 minutes with a heating lamp, and a 8-10 mg sample of the raw anthracene oil was weighed into an aluminum capsule. The capsule was sealed in an atmosphere of helium with the Perkin-Elmer Capsule Sealing Unit Model 042-1250, and the sealed capsule was placed in the ladle. Next, 20 mg of tungstic anhydride was added and the ends of the ladle were plugged with a loose wad of quartz wool. The sample was analyzed and the recorder output was used to find the percent nitrogen and hydrogen as follows:

$$\text{Nitrogen: Weight Percent Nitrogen} = \frac{(\text{Read})_N - (\text{Zero})_N - (\text{Blank})_N}{K_N\,(\text{Sample Weight})}$$

$$\text{Hydrogen: Weight Percent Hydrogen} = \frac{(\text{Read})_H - (\text{Zero})_H - (\text{Blank})_H}{K_H(\text{Sample Weight})}$$

These values were compared to the values given in Table IV. If the calculated values were within ± 2% of the nitrogen or hydrogen content, the machine was ready to analyze unknown samples.

Sample Analysis

The procedure and calculations for analysis of unknown samples were identical to those given for the raw anthracene calibration check. Each sample was analyzed twice, and repeats were performed as necessary. The average value was reported.

All chemicals and gases used in the nitrogen and hydrogen analyses are given in Table VIII. Also, sample calculations are given in Appendix E.

The Perkin-Elmer analyzer is a very sensitive instrument capable of great accuracy. The degree of accuracy depends to a large extent on the operator's experience, skill, and care. This experience and skill comes only with time and many hours of experience.

CHAPTER IV

EXPERIMENTAL RESULTS

In this section the results of experimental runs ACW, BCW and CCW will be presented. The discussion of these results will be given in the next section. All experimental runs in this study were made at a temperature of 750°F (399°C), a pressure of 1500 psig, and at volume hourly space times of 0.46 hrs., 0.92 hrs., and 1.84 hrs.

Run ACW

The purpose of run ACW was to evaluate the hydrodesulfurization, hydrodenitrogenation and hydrogenation ability of a non-presulfided alumina support. The support was prepared, loaded and calcined in the manner described in the previous section, except this support loading was not presulfided with a H_2/H_2S mixture. The data obtained from this run are given in Figures 8 through 12. In Figure 8 the weight percent nitrogen and sulfur in the product oils are presented as a function of space time. This figure shows that alumina in the presence of hydrogen results in significant removal of nitrogen and sulfur from raw anthracene oil. Specifically, the nitrogen level of the raw anthracene oil was reduced from 1.05 weight percent to 0.78 weight percent nitrogen at a volume hourly space time of 1.84 hours. The sulfur concentration dropped from 0.47 weight percent sulfur to 0.25 weight percent sulfur at a volume hourly space time 1.84 hours.

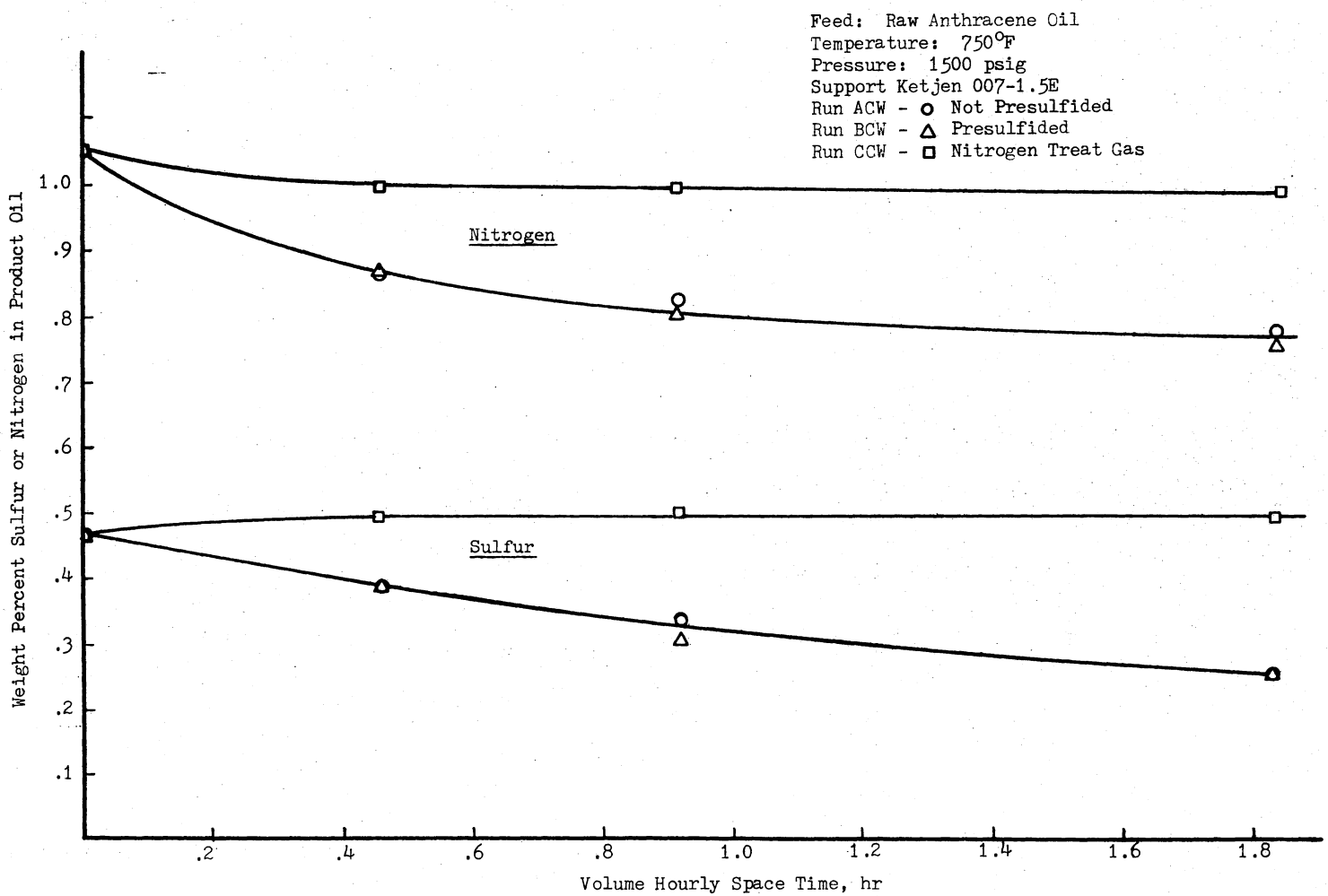

Figure 8. Sulfur and Nitrogen Response

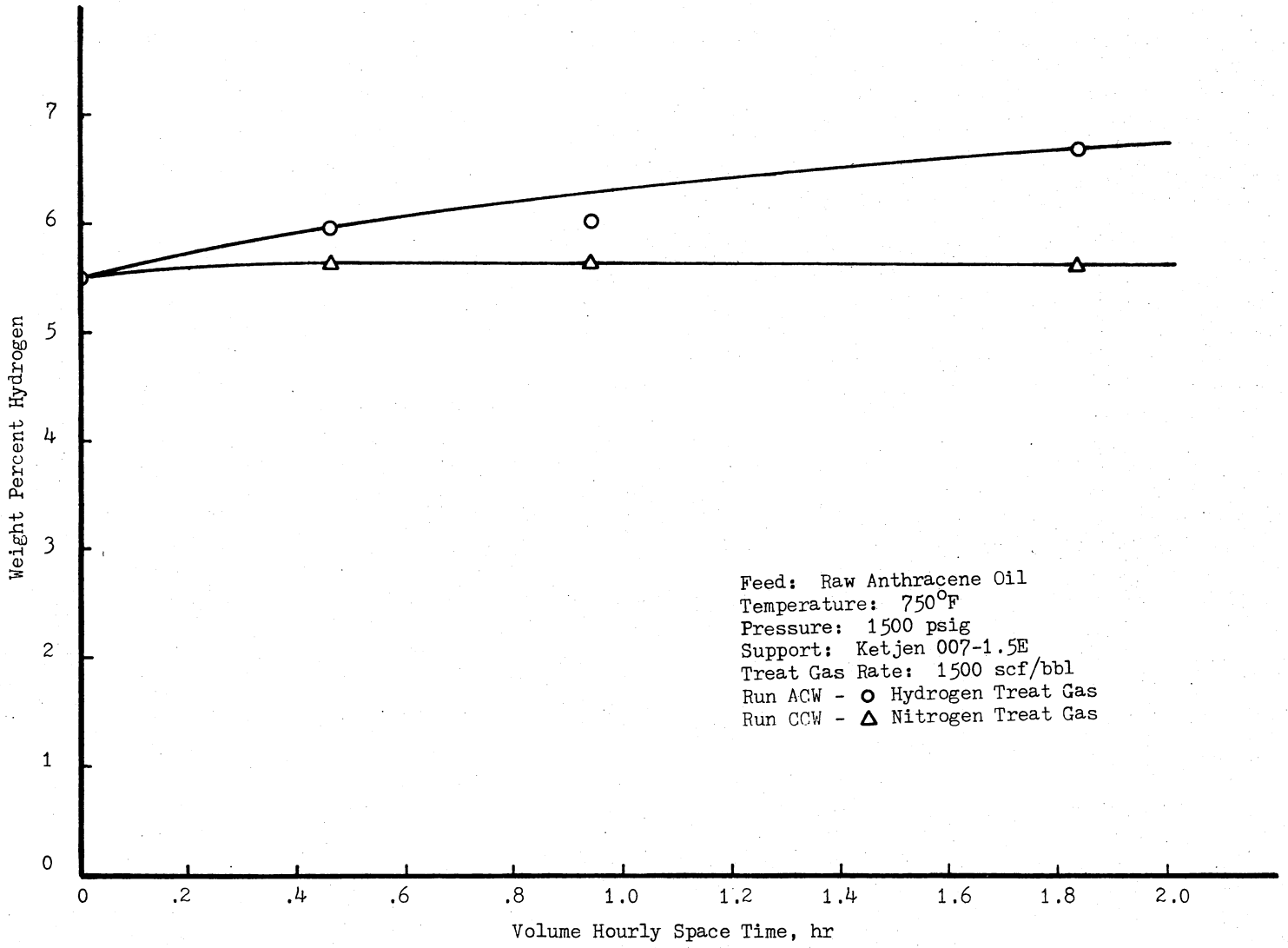

Figure 9. Hydrogen Response

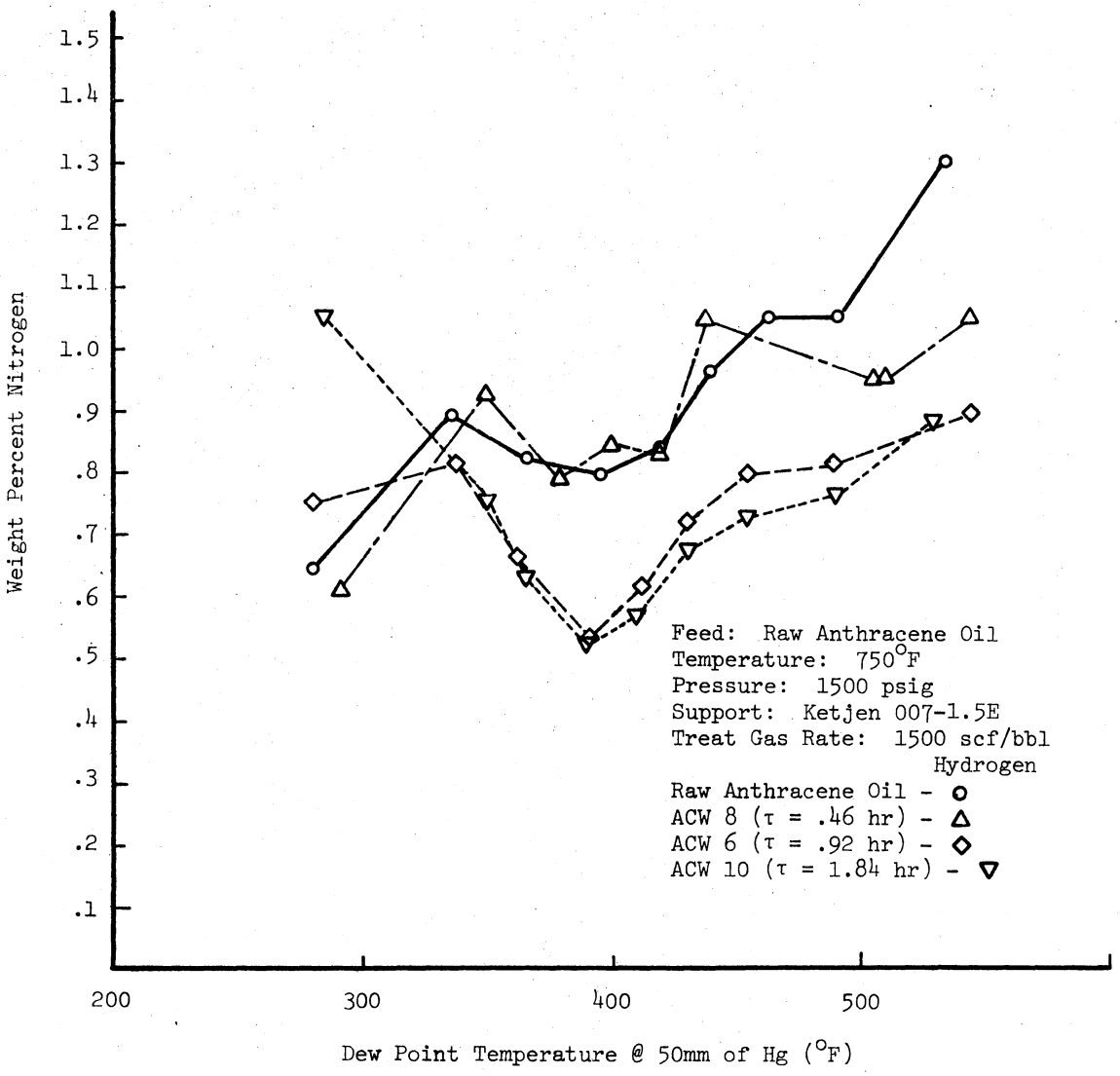

Figure 10. Nitrogen Content of Distillation Fractions of Run ACW

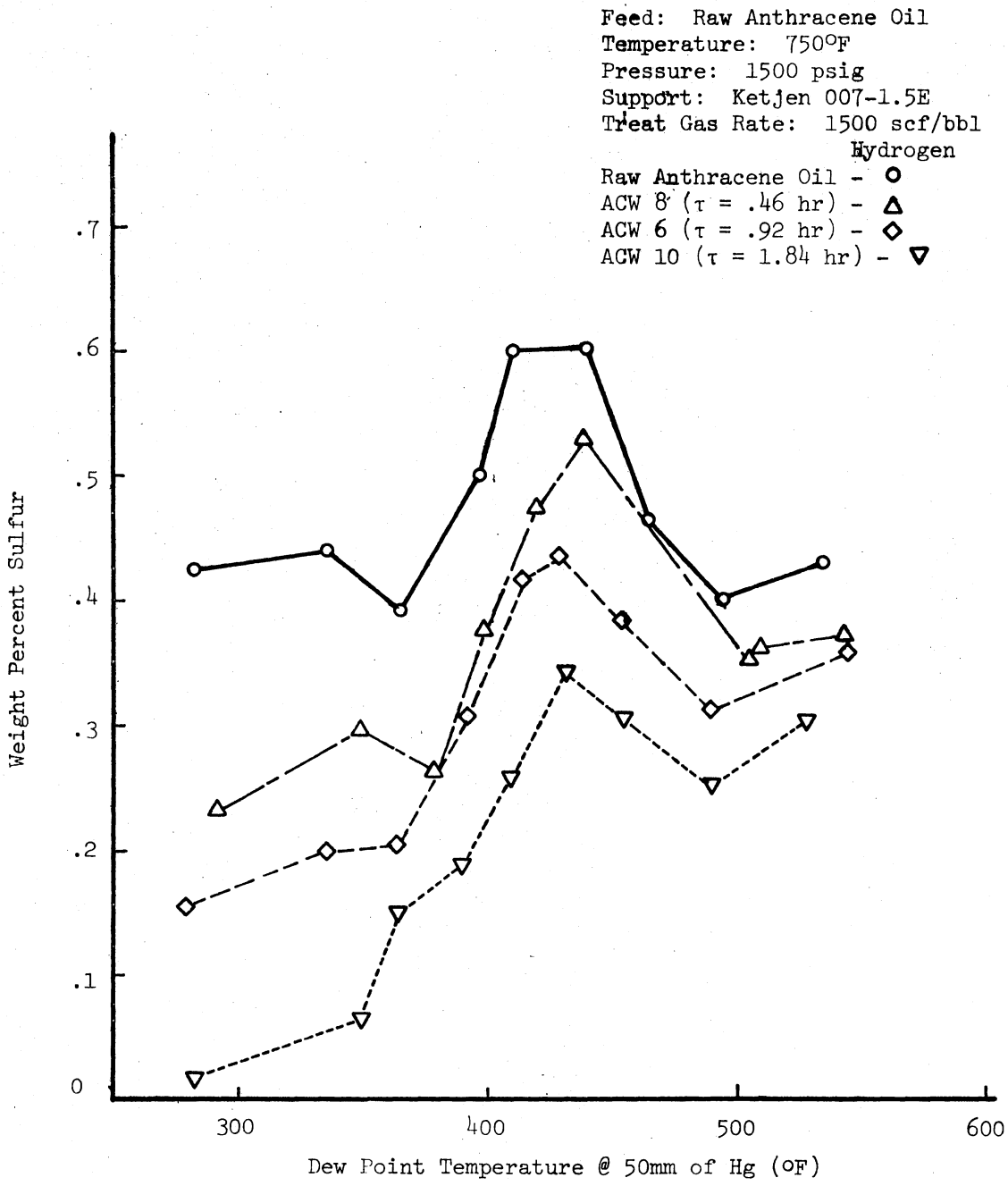

Figure 11. Sulfur Content of Distillation Fractions of Run ACW

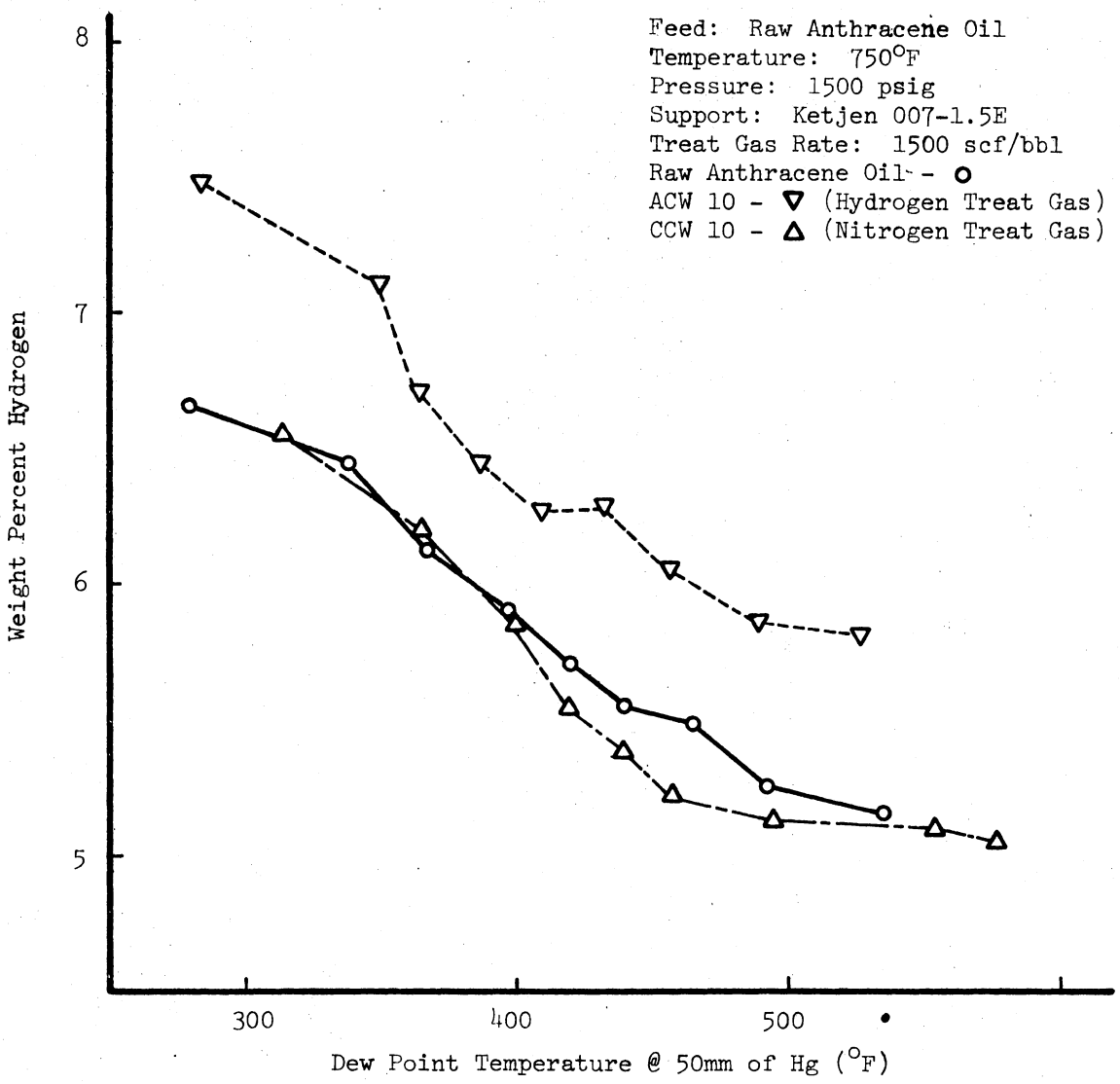

Figure 12. Hydrogen Content for the Distillation Fractions of ACW 10 and CCW 10

Figure 9 gives the hydrogenation ability of alumina; here weight percent hydrogen in the product oil versus space time is plotted. This figure shows that significant hydrogenation of raw anthracene oil occurs in the presence of alumina support. Note the hydrogen content of the oil has increased from 5.6 weight percent to 6.4 weight percent hydrogen at the space time of 1.84 hrs.

Figures 10 through 12 are distillation fraction curves. These curves have been corrected for insufficient pot heating rates in the manner described in Appendix A. Figure 10 gives percent nitrogen in the fraction versus vapor temperature for volume hourly space times considered in this study (τ = 0.46 hr; 0.92 hr., and 1.84 hrs.). The raw anthracene feed oil is also shown. By comparing the sample curves to the feed curve the extent to which nitrogen compounds have been affected can be gauged. Figure 10 shows a significant decrease in the nitrogen concentration in the heavy (450°F to 550°F) and middle (350°F to 450°F) fractions while the light (250°F to 350°F) fraction nitrogen content actually increases. The percent sulfur in the distillation fractions versus vapor temperature is given for the same space times in Figure 11. Also shown in this feed is the sulfur content of the raw anthracene feed oil. A comparison of the sample curve to the feed curve shows significant sulfur removal has occurred in all fractions, but more was removed in the light (250°F to 350°F) and middle (350°F to 450°F) fractions than in heavy (450°F to 550°F) fractions.

Finally, the percent hydrogen in the fraction versus vapor temperature is presented in Figure 12. This was evaluated at the greatest space time considered: τ = 1.84 hrs. The hydrogen content of the raw anthracene feed oil fraction is also given. A comparison shows that a

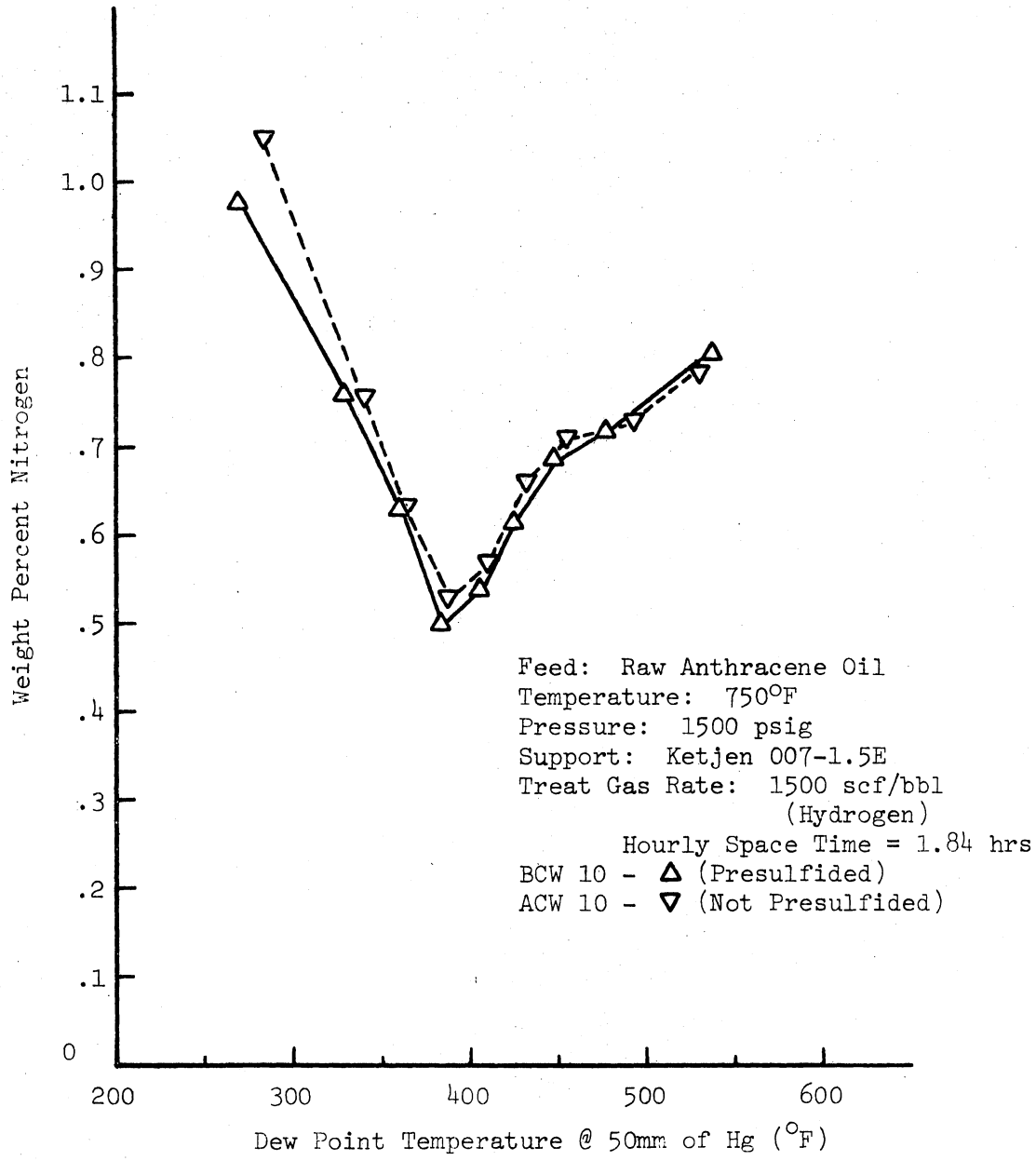

Figure 13. Nitrogen Content of Distillation Fractions of Samples ACW 10 and BCW 10

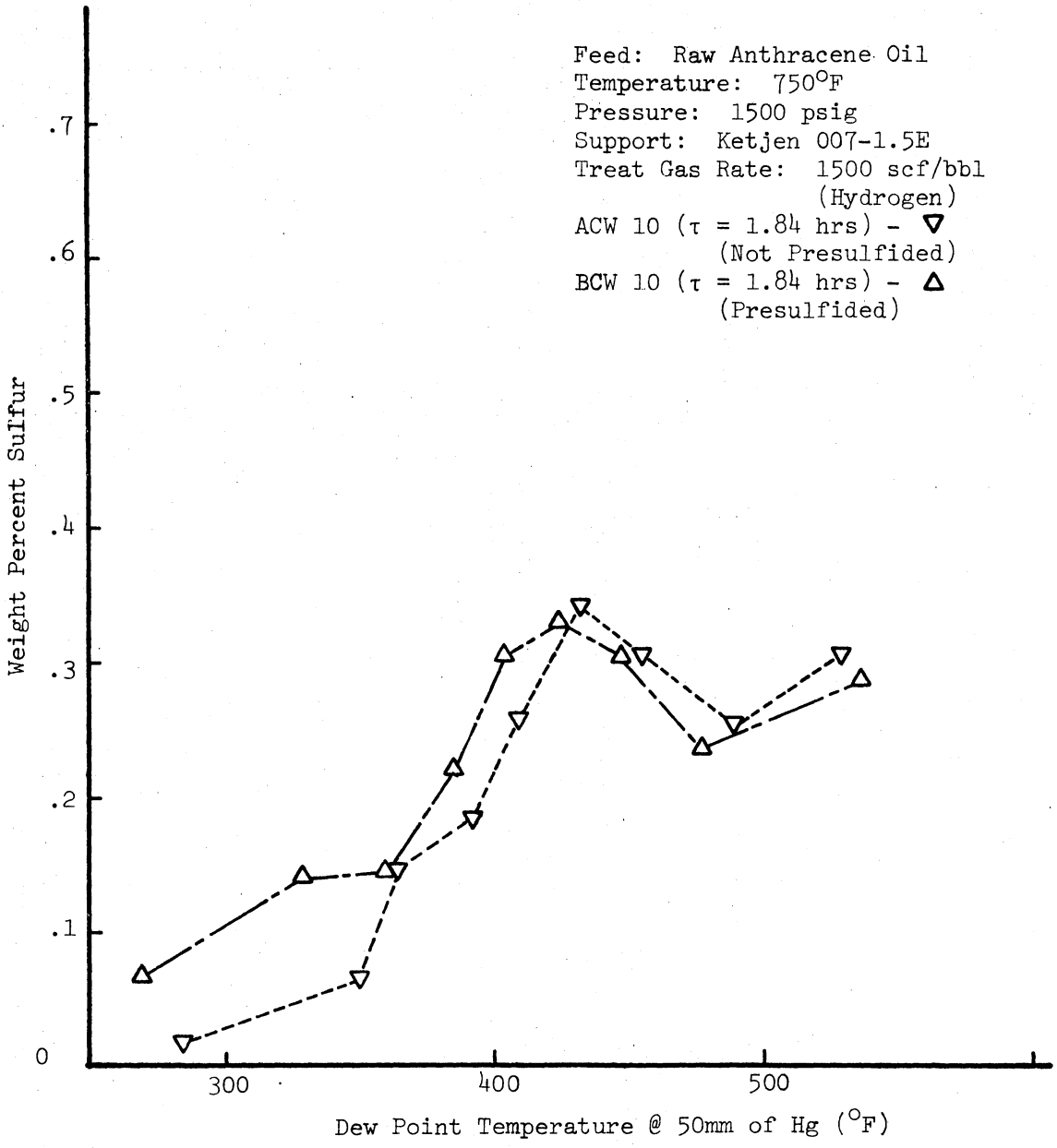

Figure 14. Sulfur Content of Distillation Fractions of Samples ACW 10 and BCW 10

spectrum of hydrogen addition has occurred, but more has been added to the light (250°F to 350°F) and heavy (450°F to 550°F) fractions than to the middle (350°F to 450°F) fractions. The complete tabulated data for Run ACW is presented in Appendix B. In this series all samples were analyzed for sulfur and nitrogen content, but only selected samples were analyzed for hydrogen content.

Run BCW

The BCW series has two purposes. First, in this run the support loading was presulfided, whereas in run ACW it was not. This allows a comparison of the effect, if any, of presulfiding on hydrodesulfurization and hydrodenitrogenation ability of alumina support. The second purpose was a reproducibility check. If Run BCW showed no effect due to presulfiding, then this run could be used as a reproducibility check on experimental and analytic procedures. Figure 8 gives hydrodesulfurization and hydrodenitrogenation as a function of space time. This figure shows that there is essentially no difference between the presulfided runs and the non-presulfided run in terms of sulfur and nitrogen removal.

Nitrogen and sulfur contents of the distillation fractions for a volume hourly space time of 1.84 hours are presented in Figures 13 and 14, respectively. Also shown in these figures are the result of run ACW at a volume hourly space time of 1.84 hours. A comparison of the curves shows no significant difference due to presulfiding. Note the vapor temperatures given in these figures were obtained by the method described in Appendix A. The complete tabulated data for Run BCW can be found in Appendix B. In this run all samples were analyzed for

sulfur and nitrogen, but none were analyzed for hydrogen content. In order to assess, indirectly, the hydrogen results from run ACW, a plot of the corrected vapor temperature versus the percent volume of the distillate was made for samples ACW 10 and BCW 10. This is shown in Figure 15. This type of analysis is often used to measure the amount of hydrogenation/hydrocracking which has occurred. As can be seen, these curves are essentially the same as raw anthracene oil curve. The reason is that large amounts of hydrogen addition must occur to significantly change the boiling curve. In the presence of alumina not enough hydrogen was added to the feedstock and not enough hydrocracking occurred to significantly vary the boiling curve. For this reason weight percent hydrogen analysis should be done on all samples.

Run CCW

Run CCW was made to assess the extent which thermal reactions (such as cracking and condensation) affect the nitrogen and sulfur compounds present in raw anthracene oil. All conditions were the same except that the treat gas was nitrogen instead of hydrogen and the bed was not presulfided. The flow rate of the nitrogen was the same as the hydrogen flow rate in runs ACW and BCW. The nitrogen gas was supplied to maintain the trickle bed conditions in the reactor and prevent the reactor from being filled with liquid. Figure 8 presents the weight percent nitrogen and sulfur of the product oils as a function of space time. This figure demonstrates that alumina in the absence of hydrogen has very little affect on the overall nitrogen and sulfur content of the feed oil. Specifically Figure 8 shows that the nitrogen level is only reduced from 1.05 wt% to 1.01 wt% at a volume hourly space time of 1.84

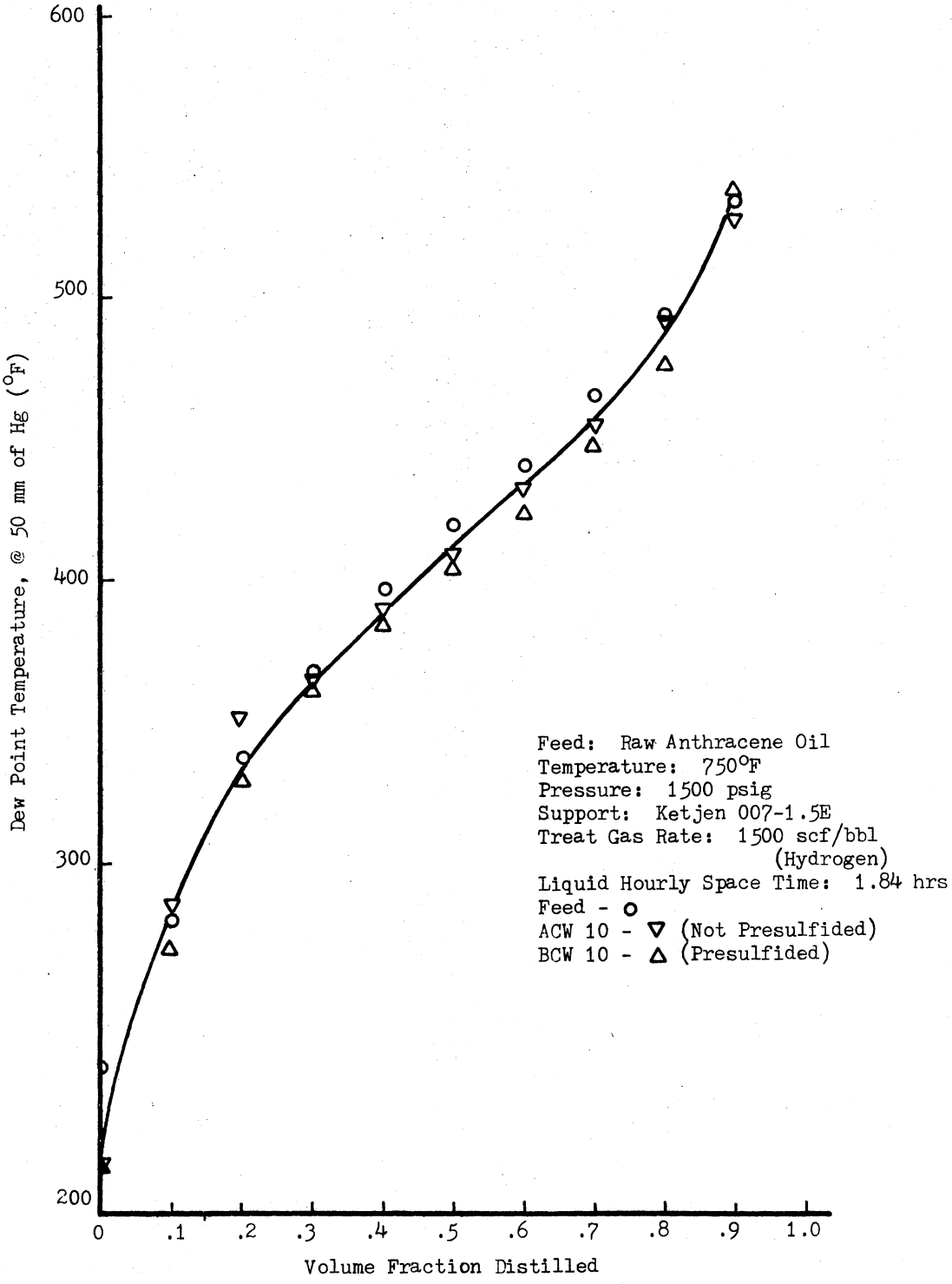

Figure 15. Boiling Curve For Samples ACW 10 and BCW 10

hours and the sulfur concentration actually increases slightly in the absence of hydrogen. The effect of space time on hydrogen concentration in the product samples is given in Figure 9. This figure shows that the absence of hydrogen has not significantly affected the total hydrogen concentration of the feed. As the space time increases the hydrogen concentration remains the same.

The nitrogen content of the distillation fractions are given in Figure 16 for the three volume hourly space times considered in this study. Also shown is the feed oil nitrogen concentration. A comparison of the sample curve to the feed curve shows the extensive movement of nitrogen compound from the heavy ($450^{\circ}F$ to $550^{\circ}F$) fraction to the light ($325^{\circ}F$ to $375^{\circ}F$) fraction.

Figure 18 presents the sulfur content of the distillation fractions as a function of space time. The sulfur content of the raw anthracene feed oil is also given in this figure for comparison. These curves indicate that alumina in the absence of hydrogen does not significantly affect the sulfur content of the distillation fractions.

The weight percent hydrogen of the distillation fractions versus vapor temperature was presented in Figure 12. This was evaluated at only one space time (τ = 1.84 hrs). Also shown is the hydrogen content of the raw anthracene feed oil. Apparently in the absence of a hydrogen treat gas the hydrogen content of the heavy ($400^{\circ}F$ to $575^{\circ}F$) fractions decrease while those of light ($300^{\circ}F$ to $400^{\circ}F$) fractions remain the same.

Also shown are Figures 17 and 19, which represent an analytical/experimental procedure check for nitrogen and sulfur content. Figures 17 and 19 give the nitrogen and sulfur content of the distillation

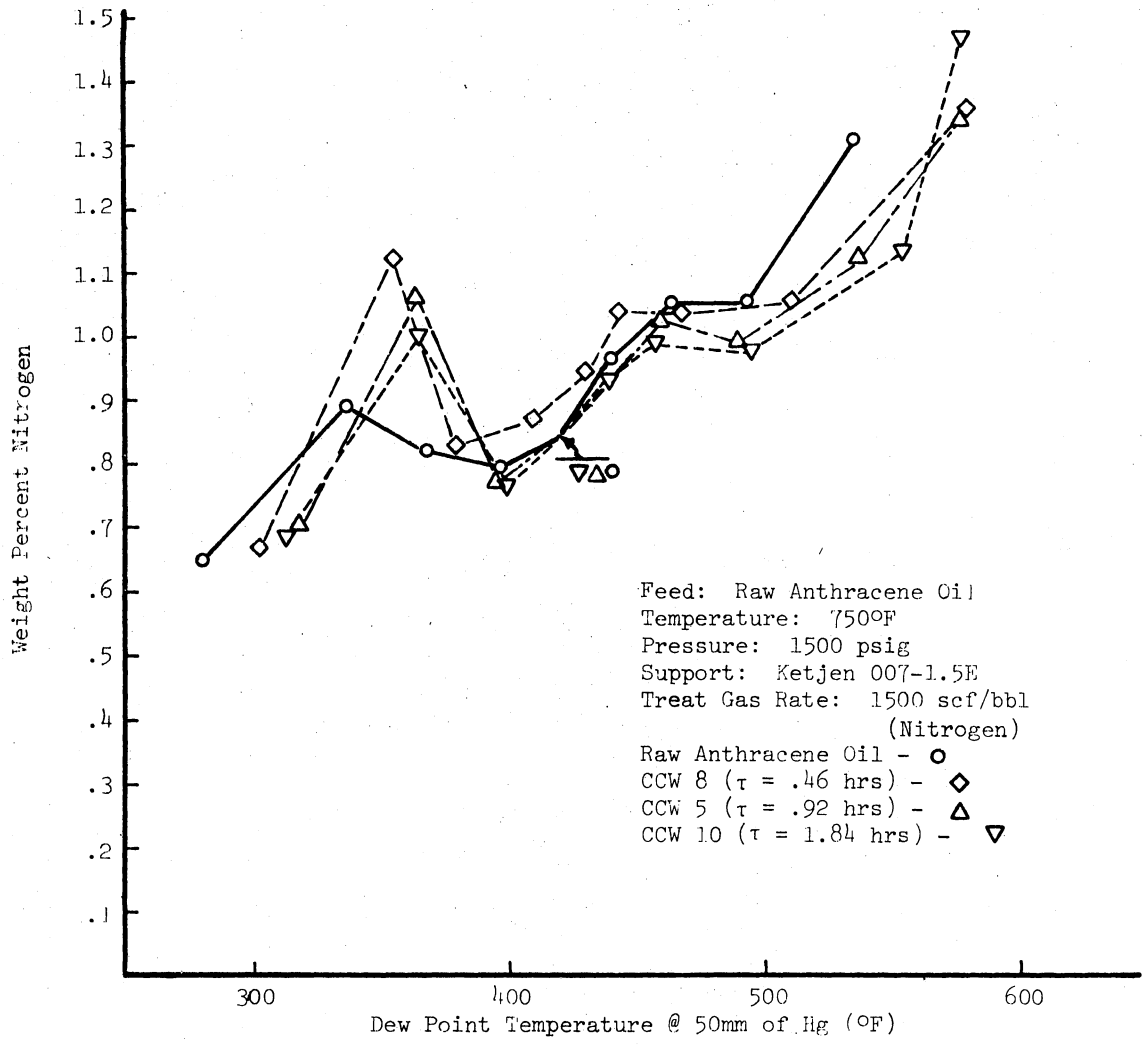

Figure 16. Nitrogen Content of Distillation Fractions for Run CCW

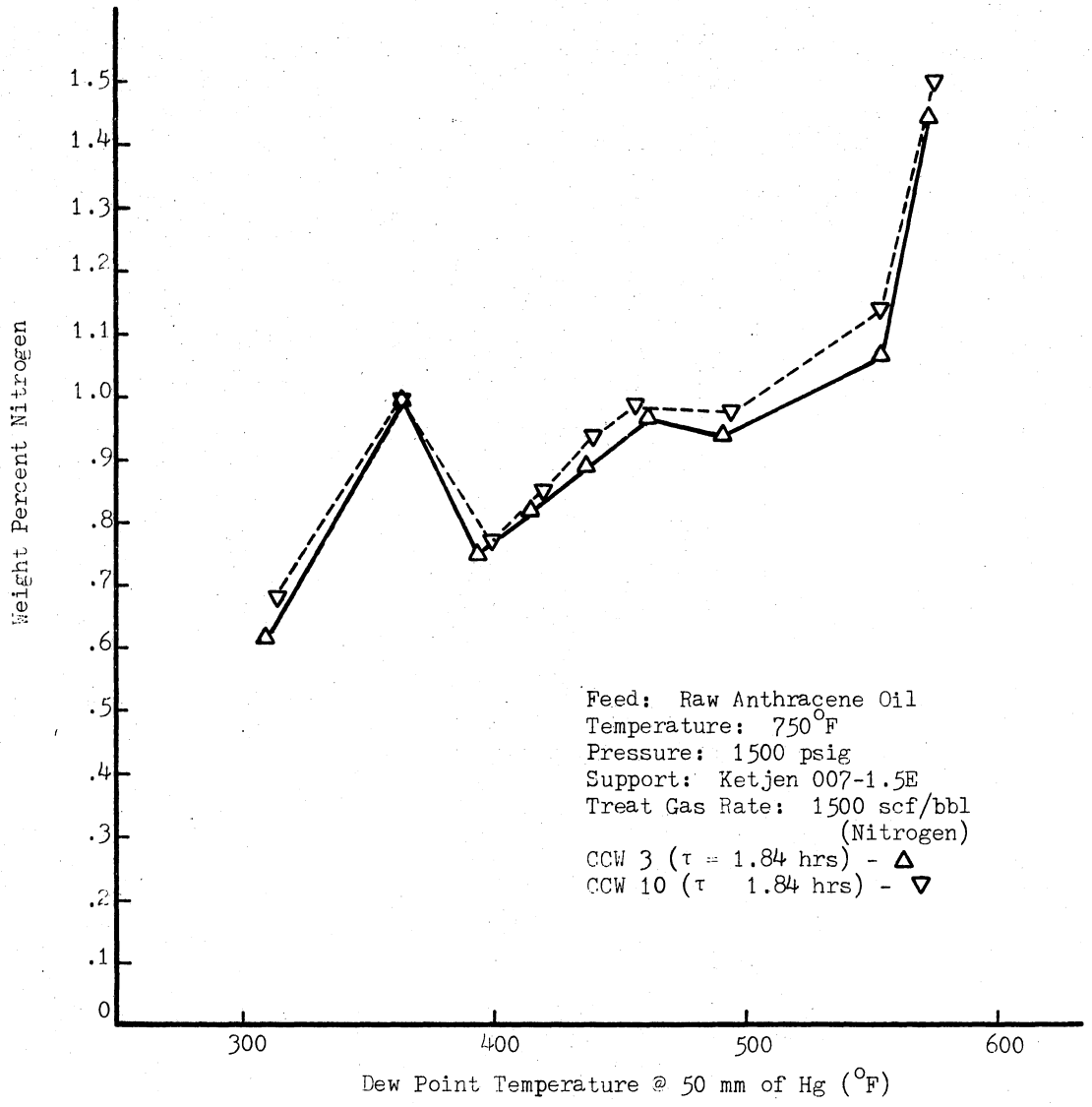

Figure 17. Nitrogen Content of Distillation Fractions for Samples CCW 3 and CCW 10

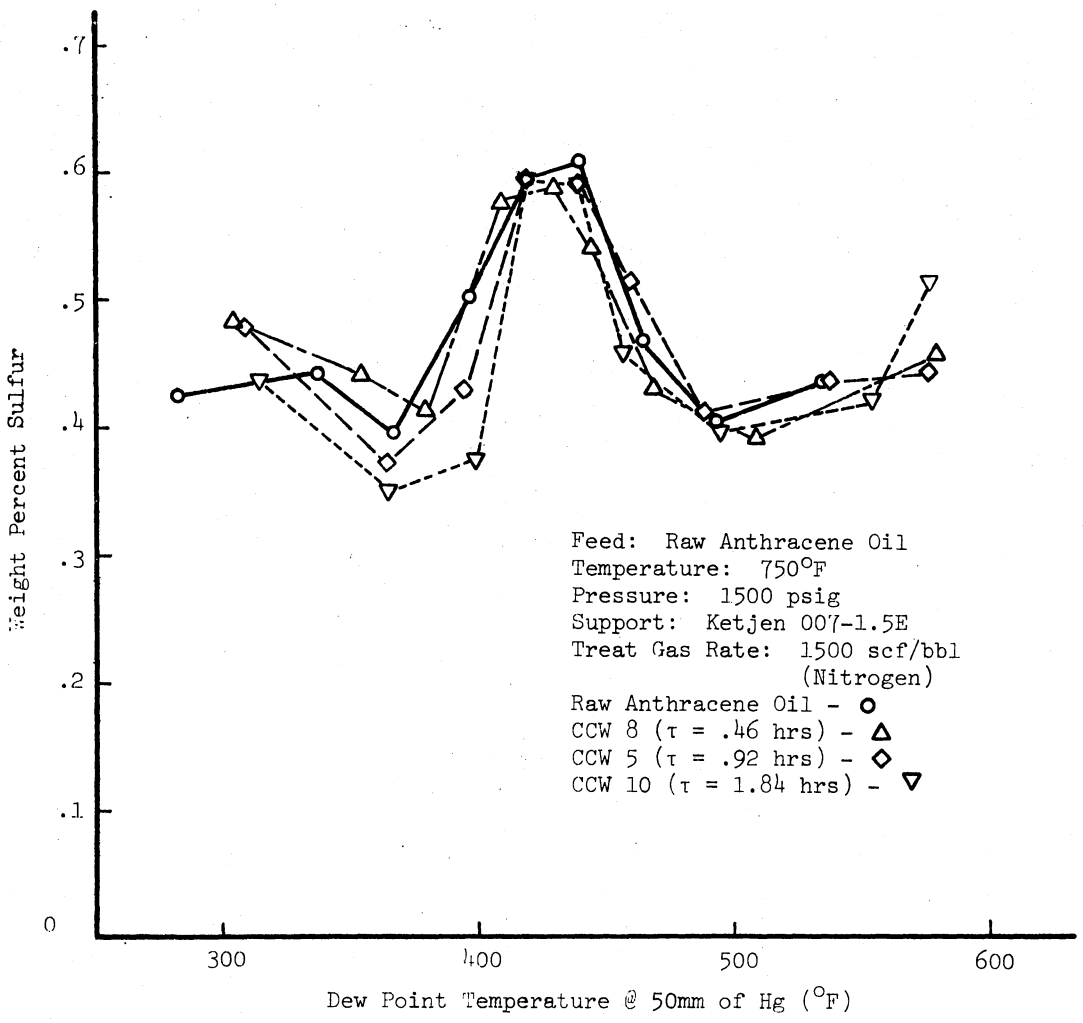

Figure 18. Sulfur Content of Distillation Fractions of Run CCW

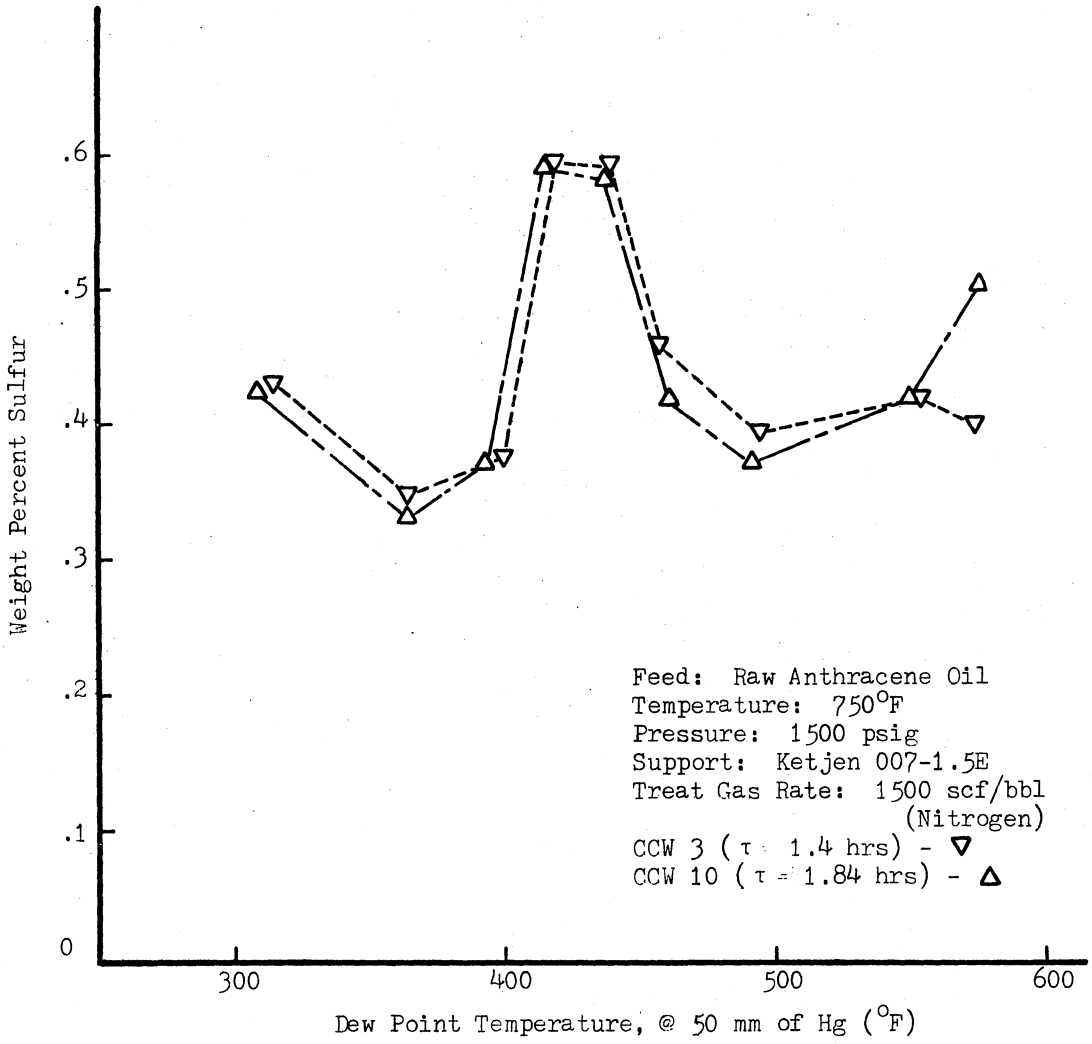

Figure 19. Sulfur Content of Distillation Fractions of Samples CCW 3 and CCW 10

fractions of two samples; CCW 3 and CCW 10. These samples were obtained at identical conditions; the only difference between the two samples was the time at which the samples were taken. Sample CCW 3 was made 36 hours into the run and CCW 10 was taken at 72.5 hours. As can be seen the agreement is very good.

The distillation data vapor temperatures were obtained by the procedure described in Appendix A. The complete data obtained for Run CCW are tabulated in Appendix B. All samples in the CCW series were analyzed for nitrogen and sulfur, but only selected samples were analyzed for hydrogen content.

In the next section these results will be discussed in detail and the activity of the alumina support will be compared to other materials.

CHAPTER V

DISCUSSION

In this section the results of experimental Runs ACW, BCW and CCW are discussed. These results allow the evaluation of four items:

1. The precision of the operational and analytical phases.
2. The hydrodesulfurization, hydrodenitrogenation and hydrogenation ability of a non-presulfided alumina support.
3. The hydrodesulfurization and hydrodenitrogenation ability of a presulfided alumina support.
4. The effect of a non-presulfided alumina support on sulfur and nitrogen compounds when hydrogen treat gas is not used.

A comparison of these results to those of Satchell (49), Sooter (63) and Chirakaparambil (7) will also be made. From this, ideas can be developed as to the effects of the nature of the active sites. Before these four points are discussed, the performance of the trickle bed reactor will be considered to access the extent which non ideal behavior affects the results of this study.

Trickle Bed Reactor Performance

Three flow dynamic factors affect the performance of a trickle bed reactor. They are liquid distribution, mass transfer and axial dispersion. This study is not intended to measure the effects of these factors, but an indication must be obtained as to what extent these

factors affect reactor performance.

Sooter (63) and Satchell (49) in their studies of hydrodenitrogenation and hydrodesulfurization of raw anthracene oil using $CoO/Mo_3O/\gamma Al_2O_3$ catalysts attempted to assess the effects of these variables. Their studies are very useful because they used the same reactor system and similar operating conditions. Sooter, in his study of hydrodesulfurization, applied Mear's criteria (37) for axial dispersion. Sooter found that a 20 inch (50.8 cm) catalyst bed at a volume hourly space time of .375 hr met Mear's criteria, but the same catalyst bed at space times of .75 hr and 1.5 hrs did not meet the criteria, for absence from axial dispersion effects. In order to measure the effects of axial dispersion two runs were made; one with a 10 inch (25.4 cm) bed of 8-10 mesh catalyst and one with a 20 inch (50.8 cm) bed of 40-48 mesh catalyst. Both were operated at volume hourly space times of 0.375, 0.75, and 1.5 hours. The results obtained from the 20 inch (50.8 cm) bed with the 40-48 mesh catalyst were identical to those obtained for a 20 inch (50.8 cm) bed with an 8-10 mesh catalyst, while the 10 inch (25.4 cm) bed with 8-10 mesh catalyst showed a slight decrease in sulfur removal from 88.7% to 85.2%. Satchell also ran with a 20 inch (50.8 cm) bed of 40-48 mesh and a 10 inch (25.4 cm) bed of 8-10 mesh catalyst. He observed no change in the nitrogen removal ability in either case. Both Satchell and Sooter reasoned that by reducing particle size from 8-10 mesh to 40-48 mesh, axial dispersion should have been eliminated or reduced. Since no increase in hydrodesulfurization or hydrodenitrogenation was observed, they concluded axial dispersion did not significantly affect reactor performance. These studies also indicated that mass transfer resistance in the pore as indicated by the

effectiveness factor was not a limiting factor. Both concluded that the effectiveness factor for hydrodesulfurization and hydrodenitrogenation was close to one and that liquid distribution problems did not affect reactor performance.

Sooter's (63) and Satchell's (49) results indicate at least two possibilities. Either axial dispersion, mass transfer and liquid distribution problems do not significantly affect trickle bed reactor performance under the experimental conditions or the interaction of variables mask the effect of these variables on reactor performance, (i.e., a decrease in one variable is cancelled by an increase in another variable). A recent wetting correlation proposed by Mears (38) has suggested the second possibility. This correlation is

$$\log \frac{C_{in}}{C_{out}} \alpha (h)^{.32} (LHSV)^{-.68} dp^{.18} \nu^{-.05} (\sigma_c/\sigma)^{.21} \eta \ ,$$

where

C_{in}, C_{out} - Concentration of reaction in feed and product, mole/cm^3

h - catalyst bed length, cm

LHSV - liquid hourly space velocity, hr^{-1}

dp - diameter of catalyst particle, cm

ν - kinematic viscosity, cm^2/sec

σ - surface tension of liquid, grams/sec^2

σ_c - critical value of surface tension for packing, grams/sec^2

η - effectiveness factor, unitless.

This equation is valid only when axial dispersion and heat effects are negligible. Considering Sooter's and Satchell's 20 inch (50.8 cm) bed

runs at a volume hourly space time of .375 hour with an effectiveness factor close to one, this relation predicts an increase in conversion due to increased wetting when the catalyst particle size is reduced from 8-10 mesh to 40-48 mesh. In all runs the length of the reactor, volume hourly space time, kinematic viscosity and the surface tension should have remained constant. If Mear's correlation is accepted, two possible explanations are implied. First, the possibility exists that the effectiveness factor is not one and that its increase masks the effect of reducing particle size. Consider Mear's wetting correlation reducing the particle size by a factor 5 would increase conversion. But if the effectiveness factor was not close to one, reducing particle size would cause the effectiveness factor to increase. This would cause a decrease in conversion. These two factors could be offsetting so the change in the conversion is nil.

Another possible explanation is that the reactor used in this study had such good liquid distribution (wetting) that decreasing particle size did not affect wetting. The latter possibility is rather hard to accept when one considers the literature on liquid distribution (59, 47, 58) and the physical situation which exist in the reactor. Any time a continuous solid surface such as the reactor wall is used in a packed bed this surface forms a region of decreased flow resistance. This is because the bed packing cannot intermesh with the reactor wall as with other packing particles. Therefore more void space exists near the pipe wall. In this reactor two such solid surfaces exist; the tube wall and the thermal well. As can be seen in Figure 2 the oil in this study enters from the side of the reactor. The maximum oil flow rate in this study was 100 cm^3/hr. If 20 drops per cm^3 are assumed, this amounts to

roughly 1 drop per second. Due to this very low oil flow rate, the entrance configuration and the lower flow resistance next to the wall, the possibility exists that the oil flow is confined to region next to the tube wall. Figure 2 also shows that the treat gas enters on the other side of the reactor. Because of the region of low flow resistance next to the thermal well, the majority of the gas flow could possibly be flowing down the sides of the thermal well. This could possibly explain why Sooter (63) and Satchell (49) did not observe any effect when they increased the gas flow rate from 1500 scf/bbl to 20,000 scf/bbl. This simply caused the majority of the gas to flow in the region next to the thermal well. Therefore, increased contact of the oil with the gas and the catalyst might not have occurred.

As stated earlier, the purpose of this study is not to determine which of these or other possibilities are valid. But in view of the above considerations, one cannot say with certainty that axial dispersion, mass transfer and liquid distribution do not affect reactor performance in this study. The evidence offered thus far in previous studies by Sooter (63) and Satchell (49) is simply not conclusive. However, within the range that they could change their variables of time, particle sizes, flow rates, etc.; no effects could be observed.

Precision Analysis

The purpose of this section is to discuss the precision of the data presented in this study. This study had two phases; an operational phase and an analytical phase.

Operational Phase

In the operational phase, support preparation and operation of the trickle bed reactor were the main activities. A good indication of the operational phase precision can be obtained by considering Runs ACW and BCW. These runs were initially made to assess the effect of presulfiding on the hydrodenitrogenation and hydrodesulfurization ability of an alumina support. Figures 8, 13 and 14 show no significant effect due to presulfiding. With this in mind the results of these runs were used as an indication of the operational phase precision.

Runs ACW and BCW were made on the same trickle bed reactor, but with different support loadings and different operator work schedules. Therefore, these runs should give an excellent indication of the overall reproducibility of support preparation, loading and operator performance. Close examination of Figure 8 shows that runs ACW and BCW were almost identical in sulfur and nitrogen removal. Specifically, the maximum observed deviation of the nitrogen results from the mean was ± 1.1% absolute and that of the sulfur results was ± 3.1% absolute. Table IX shows that the variation in experimental conditions for runs ACW and BCW were also almost identical. These results indicate that the experimental precision of support preparation, support loading and reactor operation was extremely good.

Analytical Phase

The second phase of this study was the analytical phase. This phase had three goals. First, all samples were to be analyzed for weight percent sulfur and nitrogen. Second, selected samples were distilled at 50 mm of Hg and the resulting distillation fractions

TABLE IX

VARIATION OF EXPERIMENTAL CONDITIONS
FOR RUNS ACW AND BCW

Experimental Variable	ACW	BCW
Temperature, ^{o}F	746-753	747-753
Pressure, psig	1475-1483	1472-1480
Mass of Support Loaded, gm	22.48	22.38
Treat Gas Rate, SCF/bbl (Hydrogen)	1290-1631	1500-1896

analyzed for weight percent sulfur and nitrogen. Finally, selected samples and sample distillations were analyzed for weight percent hydroden. As can be seen, four types of analyses are involved in these goals: ASTM D1160 distillation analysis, nitrogen analysis, sulfur analysis and hydrogen analysis. By considering each type of analysis separately, an indication of the analytical precision of the data from that analysis can be obtained.

The main goal of the ASTM D1160 distillation analysis was to obtain vapor temperatures corresponding to different volumes of distillate. In this study, this goal was not met, but estimates of the vapor temperatures have been obtained. An insufficient heating rate or boil up rate from the distillation pot resulted in the reflux level falling below the head thermal couple which resulted in low and erratic vapor temperature readings. A full discussion of these effects and the development of a correlation to correct for these effects are given in Appendix A. Because of these difficulties an estimate of the precision

of the original experimental temperatures obtained is not possible, but the correlation developed in Appendix A has corrected the pot temperature to within ± 10°F of correctly obtained experimental vapor temperatures. However, the precision of the vapor temperatures are of less importances because the purpose of the distillation data is to measure how the nitrogen, sulfur, and hydrogen content of the various boiling fractions are affected by reactor operating conditions. As can be seen in Appendix A the proposed correlation gives vapor temperatures satisfactorily for this purpose. A detailed procedure for ASTM D1160 distillation of coal liquids has been given in Appendix C to eliminate the need for the pot-vapor temperature correlation.

An estimate of the nitrogen analysis precision can be obtained from the percent nitrogen analysis of raw anthracene oil. The determination of the percent nitrogen in the raw anthracene oil is made as a calibration check when the nitrogen analyzer is calibrated and this is done daily. The results of 32 different raw anthracene nitrogen analyses are shown in Appendix D. The average value for the weight percent of nitrogen is 1.055%. The standard deviation is ± 0.020%. This is ± 1.9% of the nitrogen content. In this study, the range of nitrogen contents of the samples has varied from 0.5% to 1.44% weight percent. Smith (61) in a study of this nitrogen analysis technique found that the accuracy and the precision did not significantly vary until levels of 0.1% nitrogen were reached. Therefore, the overall precision of the nitrogen data presented in this experiment can be estimated at ± 1.9% of the nitrogen content throughout the range of interest.

The experimental precision of the sulfur analyzer has been established by Sooter (63), and Ahmed (3) has verified Sooter's findings.

Table X shows a comparison of the results obtained in this study to those obtained by Sooter (63).

TABLE X

ANALYTICAL PRECISION OF THE SULFUR ANALYSIS

	This Study			Sooter's Study		
Sample	wt%'s	Dev.	%Dev.	wt%'s	Dev.	%Dev.
ACW 10A	0.0185	± .0035	± 18.9	0.02	± .004	± 20.0
ACW 10B	0.0655	± .0035	± 5.34	0.06	± .00491	± 8.2
ACW 10C	0.147	± .004	± 2.72	0.15	± .00525	± 3.5
ACW 10D	0.184	± .004	± 2.17	0.20	± .00838	± 4.0

As can be seen, the precision obtained in this study is comparable to that obtained by Sooter (63).

The precision of the hydrogen analysis was obtained from the hydrogen content of raw anthracene oil. During start up of the analyzer, a calibration check is made by finding the weight percent hydrogen in the raw anthracene oil. Only five data points are available to calculate the standard deviation of the hydrogen analysis. This is due to the limited number of samples that were analyzed for weight percent hydrogen. The data from these runs are listed in Appendix D. The average hydrogen content of the raw anthracene oil is 5.57 wt% with a

standard deviation of ± .1085%. This is ± 1.95% of the hydrogen content. In this study the hydrogen content varied from 7.58 wt% to 5.14 wt%. Smith's study (61) again indicates no significant variation of accuracy or precision in this range. In conclusion, the hydrogen data presented in this study has an estimated precision of ± 1.95% of the hydrogen content.

An overall indication of both the experimental and analytical phase precision can be obtained by considering Figures 13, 14, 17 and 19. Figures 13 and 14 are the nitrogen and sulfur content of two samples ACW 10 and BCW 10. As can be seen in Appendix B, these samples were taken under identical conditions but on different runs. Thus these figures indicate both experimental and analytical phase precision. Figure 13 shows the nitrogen data for ACW 10 and BCW 10. These curves are in close agreement.

An overall indication of experimental and analytical precision for the CCW run can be obtained by considering Figures 17 and 19. In these figures, the nitrogen and sulfur content of the distillation fractions of two samples, CCW 3 and CCW 10, are shown. These samples were taken at identical conditions on the same run. The only difference between the two samples was the time at which the samples were taken. Sample CCW 3 was taken at 36 hours into the run and CCW 10 was obtained at 72.5 hours. These curves show remarkable agreement. This indicates that both experimental and analytical precision of run CCW was very good.

In this section, the precision of each phase of the study and overall precision was considered. The vapor temperatures were found to be ± 10°F of the experimental vapor temperatures. The nitrogen data

presented can be expected to have a deviation of ± 1.9% of the nitrogen content. The sulfur data can be expected to have a deviation consistent with that found by Sooter (Table X). And the hydrogen results can be expected to have a deviation of ± 1.9% of the hydrogen content. In summary, all the data presented in this study is reproducible and precise within limits of experimental reproducibility.

The Effect of Presulfiding

Run ACW and BCW were made to assess the effect of presulfiding on the hydrodesulfurization and hydrodenitrogenation ability of an alumina support. In these two runs, all conditions were the same except that in run BCW the alumina support was presulfided. This was done by passing a 5.08% H_2S/H gas mixture over the support for two hours at a volumetric flow rate of 8 cm^3/sec. The reactor temperature was maintained at 450°F during this period.

Figure 8 of the results section shows that the percent sulfur and percent nitrogen of the product samples are identical within the experimental accuracy of this study. In order to check this conclusion, distillations of samples ACW 10 and BCW 10 were made. These samples were chosen because of similarity of sampling conditions. The conditions and compositions of these samples are given in Appendix C. Figures 13 and 14 show that the distillation curves are close agreement for the higher boiling temperature fractions. But at lower vapor temperatures the agreement is not as good. Specifically in the lower boiling fraction BCW 10 has a higher sulfur content and a lower nitrogen content than ACW 10. This result could be due to the effect of presulfiding, but the possibility also exists that this was caused by excessive heating of the

light (250°F to 350°F) fraction of BCW 10 during sulfur and nitrogen analysis. Specifically, some of the lighter nitrogen compounds could have been driven off with other light compounds. This could cause the sulfur content to increase if these compounds were not as volatile.

In conclusion, the presulfiding of the alumina support has had no substantial effect on the hydrodesulfurization and hydrodenitrogenation ability of the support. The possible effect which it has on the active site of alumina will be discussed in a later section

The Effects of Alumina on Nitrogen Compounds

In this section the effects of alumina on nitrogen compounds will be considered. This will be done by comparing the results of Runs ACW and CCW. The runs differ only in that nitrogen was used as a treat gas in Run CCW. This was done to assess the extent of nitrogen removal due to hydrogenation and the amount of nitrogen removal due to thermal reactions. The percent nitrogen removal data for these runs are summarized in Table XI and Figure 8.

As can be seen the alumina in the presence of hydrogen resulted in a significantly greater degree of nitrogen removal. This indicates that thermal reactions such as cracking and condensation do not result in significant nitrogen removal at the conditions studied. Also, Table XI indicates that hydrodenitrogenation in the presence of hydrogen is only a weak function of space time. This is better seen in Figure 8. Here quadrupling the volume hourly space time from 0.46 hrs to 1.84 hrs resulted in only a 10% increase in the nitrogen removal. The nitrogen removal for Run CCW shows essentially no space time dependence. These

TABLE XI

SUMMARY OF NITROGEN RESULTS FOR
RUNS ACW AND CCW

Run	Treat Gas	Treat Gas Rate scf/bbl	Space Time 0.46 hrs % N Removal	0.92 hrs % N Removal	1.84 hrs % N Removal
ACW	Hydrogen	1500	17	22	27
BCW	Nitrogen	1500	5.2	4.7	4.6

results seem to indicate that alumina, even in the presence of hydrogen, has a limited effect on the nitrogen compounds in raw anthracene oil. But before any conclusions are drawn the nitrogen content of the distillation fractions for runs ACW and CCW must be considered.

Figure 10 gives the nitrogen content of the ACW distillation fractions at the three spece times used in this study. For a space time of .46 hrs this figure shows that most of the nitrogen removal has occurred only in the heavy (450°F to 550°F) fractions. The light (250°F to 350°F) and middle (350°F to 450°F) fractions' nitrogen content has remained relatively unchanged compared to the distillation fractions of the feedstock. More extensive nitrogen removal occurs in both the middle and heavy fractions for a space time of .92 hrs, while in the light fraction the nitrogen content has actually increased slightly. The results for a space time of 1.84 hrs show a slight decrease in the nitrogen removal of the heavier fractions, but essentially no increase in the nitrogen removal in the middle fractions. The light fractions at this space time show a surprising result. As can be seen

at a space time of 1.84 hrs, the nitrogen content of the light fraction actually increases above that of the heavy fractions. A better understanding of these results can be obtained by considering the distillation curve for Run CCW (without hydrogen) shown in Figure 16. Table XI indicates that Run CCW resulted in essentially no nitrogen removal. Therefore, one might expect to find the nitrogen content of the nitrogen distillation curves to be essentially the same as the raw anthracene curves. This is not observed. As can be seen in Figure 16 extensive movement of nitrogen compounds has occurred in the heavy (450°F to 550°F) and light (250°F to 350°) fractions while essentially no change has occurred in the middle (350°F to 450°F) fractions. Apparently some of the nitrogen compounds in the heavier (450°F to 550°F) fractions have been cracked, causing the formation of two fragments. One of the fragments, containing nitrogen, becomes a stable low boiler. The other fragment undergoes a condensation reaction with other fragments to form a high boiler. This results in an increase in the nitrogen content in the 325°F to 375°F vapor temperature range and an increase in the high boiler vapor temperature. As can be seen the magnitude of this increase decreases somewhat with increasing space time. This could be due to hydrodenitrogenation caused by intermolecular hydrogen transfer. This could account for the slight nitrogen removal observed in Run CCW.

Now again consider the distillation data from Run ACW. As can be seen from the distillation data of Run CCW extensive cracking of heavy fractions has occurred. With these results in mind, Run ACW shows the existence of simultaneous cracking, hydrogenation, and hydrodenitrogenation. For Run ACW no shift to the heavy fractions was observed, but the nitrogen content of the light fractions increased especially for

τ = 1.84 hrs. This indicates that cracking of the heavy fractions caused the formation of fragments. These fragments are hydrogenated to form lighter compunds instead of condensing to form heavier boilers. Also apparent from Figure 10 is that the nitrogen compounds formed by the cracking/hydrogenation reaction did not undergo extensive hydrodenitrogenation. This result could be caused by reaction dynamics, the nature of the nitrogen compound formed or the nature of the active site on alumina. These possibilities will be discussed in a later section.

Another interesting comparison can be made by considering the nitrogen content of the distillation fractions obtained by Satchell (49). These results are shown in Figure 20. In one study, a $CoO/MoO_3/\gamma Al_2O_3$ catalyst was used. This catalyst caused a full spectrum of nitrogen removal in all distillation fractions. Here no increase in the nitrogen content of the lighter fractions was observed. This indicates that the nature and/or the number of active sites on the alumina support is different from that of an activated $CoO/MoO_3/\gamma Al_2O_3$ catalyst as one would expect. Also shown in Figure 20 are Satchell's distillation results from a run in which crushed and sieved 8-10 mesh ceramic beryl saddles were used as a substitute for the catalyst. This curve shows slight nitrogen removal in the lighter fractions and essentially no nitrogen removal in the heavier fractions. Overall this run resulted in an 8.5% nitrogen removal at a volume hourly space time of 1.5 hours. A comparison of this result with those given in Table XI for alumina indicates that alumina has a greater ability for hydrodenitrogenation. This is possibly due to the difference in the nature of the active sites on the alumina and ceramic beryl saddles. This will be discussed in a later section.

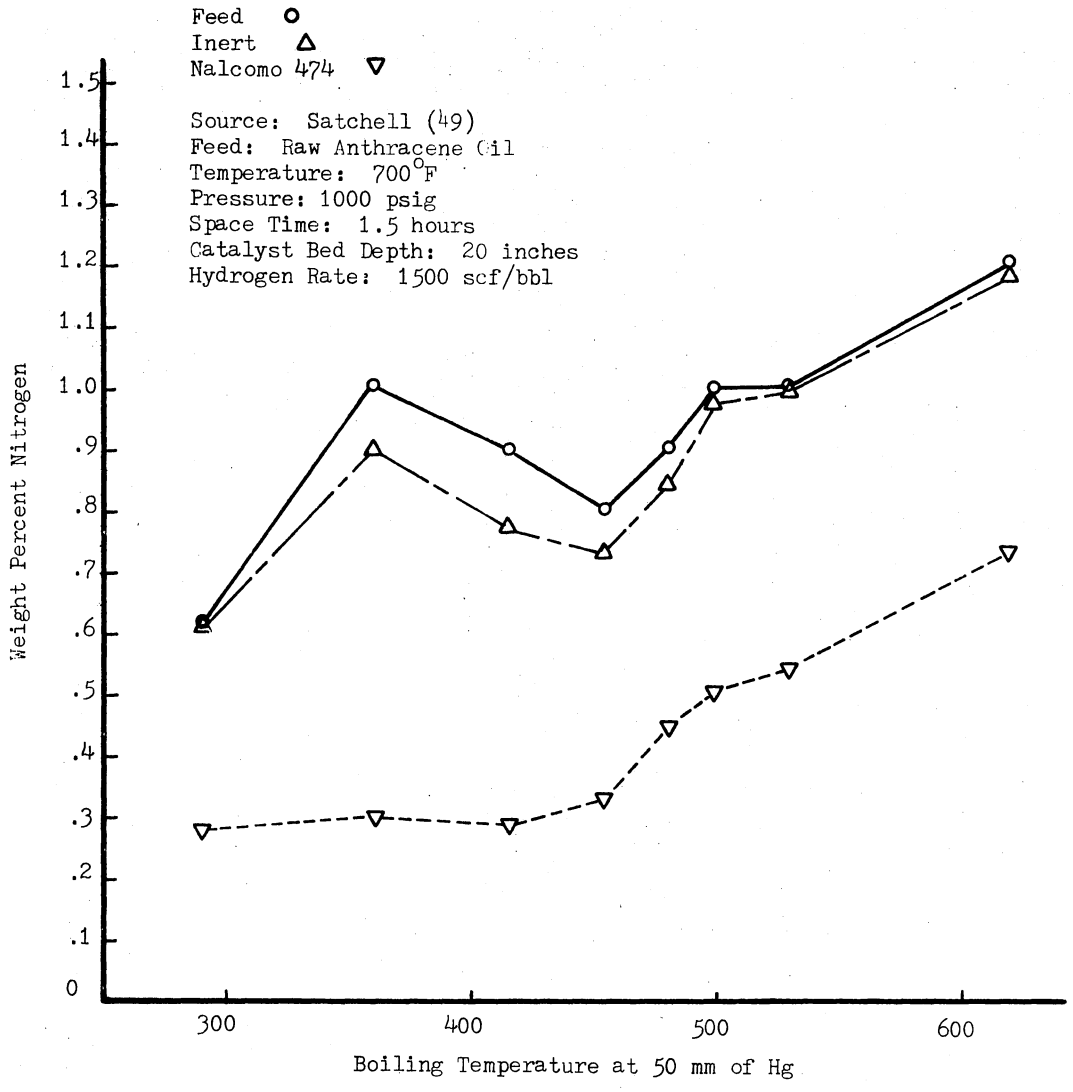

Figure 20. Nitrogen Content of Distillation Fraction for a Ceramic Porcelain and a $CoO/MoO_3/\gamma Al_2O_3$ Catalyst (Source: Satchell (49))

So far in this discussion no attempt has been made to identify the nitrogen compounds involved in the observed results. A recent study by Greenwood and Scheppele (8) has shown that the feedstock used in this study contains a wide spectrum of nitrogen compounds. Preliminary results of this study show the existence of at least 82 different nitrogen molecules ranging in molecular weight from 79 to 261 atomic mass units. Their study has also shown the nitrogen content of the raw anthracene oil is made up of the contributions from many types of nitrogen with no one single type of nitrogen compound dominating. (Specifically, 82 different nitrogen compounds have been found in the acid and base fractions.) For this reason, the specification of which nitrogen compound has undergone what reaction is difficult. But speculation is possible as to what products were formed, because the product nitrogen compounds seem to have a very limited boiling range. Consider first the results of ACW shown in Figure 16. Recall that in this run the cracking and condensation of heavy ($450^{\circ}F$ to $550^{\circ}F$) boiler has caused the formation of low stable boiling in the $325^{\circ}F$ to $375^{\circ}F$ range. This compound is most likely a quinoline type compound (I) (15). The boiling point of quinoline type compounds would fall in this range. Figure 16 also shows that cracking and condensation has occurred over a wide range of heavy ($500^{\circ}F$ to $600^{\circ}F$) nitrogen compounds. For this reason the exact compound which is undergoing the cracking and condensation reaction to form the quinoline type compound is difficult to determine without a mass spectroscopic study of the distillation fractions. The results of Run ACW shown in Figure 10 show evidence of extensive cracking/hydrogenation and hydrodenitrogenation. Apparently the cracking/hydrogenation causes the formation of lighter nitrogen

compounds in the 250°F to 350°F fractions. Due to this boiling range these compounds are most likely quinoline (I) and hydroindole (II) type compounds.

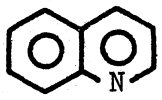

I

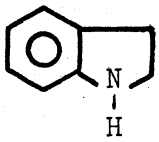

II

Again, inspection of Figure 10 shows a broad spectrum of nitrogen compounds in the 400°F to 550°F range have been affected by hydrodenitrogenation and cracking/hydrogenation. Because of this wide range the exact compounds which have undergone these reactions is difficult to determine without a mass spectroscopic study.

In conclusion, two types of reactions involving nitrogen compounds are observed over alumina in the absence of hydrogen. These are cracking and condensation. They do not affect the overall nitrogen content, but do cause extensive nitrogen compound movement within the fractions. In the presence of hydrogen, alumina showed extensive activity for cracking/hydrogenation and hydrodenitrogenation. The cracking/hydrogenation did not result in the significant nitrogen removal and caused the formation of nitrogen compounds which tend to resist nitrogen removal. Also by comparing these results to the work of Satchell, a significant difference between the active sites on alumina, $CoO/MoO_3/\gamma Al_2O_3$ catalyst, and crushed and sized ceramic beryl saddles has been observed.

The Effects of Alumina on Sulfur Compounds

In order to determine the effects of alumina on sulfur compounds in raw anthracene oil the data obtained from runs ACW and CCW will be compared. The results and conditions of these runs are summarized in Table XII and Figure 8.

TABLE XII

SUMMARY OF SULFUR RESULTS FOR RUNS ACW AND CCW

Run	Treat Gas	Treat Gas Rate scf/bbl	Space Time 0.46 hrs % S Removal (Increase)	0.92 hrs % S Removal (Increase)	1.84 hrs % S Removal (Increase)
ACW	Hydrogen	1500	16.0	32.0	46.0
CCW	Nitrogen	1500	(5.5)	(8.0)	(2.6)

For run ACW as the space time increases the percent removal of the sulfur also increases significantly. The results from run CCW actually show a slight increase in sulfur concentration. Figure 11 gives the sulfur content of the distillation fractions for Run ACW. As can be seen, there was extensive sulfur removal of the lighter fractions, but only moderate removal was obtained in the middle and heavy fractions. The sulfur content of the distillation fractions for Run CCW are

presented in Figure 18. This curve shows that in the absence of hydrogen, alumina has little affect on the sulfur compounds present in raw anthracene oil. This result is very interesting in that it indicates that sulfur compounds in the raw anthracene oil did not undergo extensive thermal cracking; whereas nitrogen compounds did under extensive cracking over the alumina support. These results explain the overall increase in sulfur content observed in Run CCW. For this run, Figures 16 and 12 show extensive cracking of non sulfur bearing compounds has occurred. Figure 12 shows the hydrogen content of the heavy (450°F to 550°F) boiler has decreased for Run CCW. This indicates cracking and condensation of a large portion of the heavy fractions. For nitrogen compounds, Figure 16 also shows cracking and condensation of nitrogen compounds, but Figure 18 shows essentially no evidence of cracking or condensation of sulfur compounds. The extensive cracking of non sulfur bearing compounds has resulted in the loss of some lower molecular weight compounds with the treat gas. Since the sulfur compounds have not been cracked their relative concentration increases. This causes the apparent increase in sulfur concentration observed in Run CCW.

Another interesting comparison can be made if the results of the study by Sooter (63) are considered. Note Sooter's temperature was higher than that used in this study, but his pressure was lower (Sooter's conditions would be more favorable to cracking than the conditions used in this study). In this study, two types of runs were made. In one, crushed and sized (8-10 mesh) ceramic beryl saddles were used as a replacement for the catalyst. Although the primary goal of Sooter's study was evaluation of the hydrodesulfurization of raw anthracene oil by a $CoO/MoO_3/\gamma Al_2O_3$ catalyst, the results obtained from his

study of ceramic beryl saddles are also significant. The sulfur content of distillation fractions is shown in Figure 21. A comparison with Figure 14 shows an interesting result. The percent sulfur removed by the ceramic beryl saddles is significantly greater than that removed by the alumina in all fractions. This can also be seen by considering Table XIII. Table XIII summarizes Run ACW of this study and Sooter's ceramic beryl saddle study.

TABLE XIII

COMPARISON OF RUN ACW TO SOOTER'S CERAMIC BERYL SADDLE STUDY

Run	Pressure psig	Temperature °F	Liquid Hourly Space Time 0.46 hrs — % Sulfur Removed	0.92 hrs — % Sulfur Removed	1.84 hrs — % Sulfur Removed
Sooter's Ceramic Study	1000	800	33	44	58
ACW	1500	750	16	32	46

The ceramic beryl saddles resulted in significantly greater sulfur removal at all space times considered. These results are very surprising when one considers the relative total surface areas of these two solids. Sooter's ceramic beryl saddles were assumed nonporous. If the surface area of this nonporous porcelain is calculated, it is found to

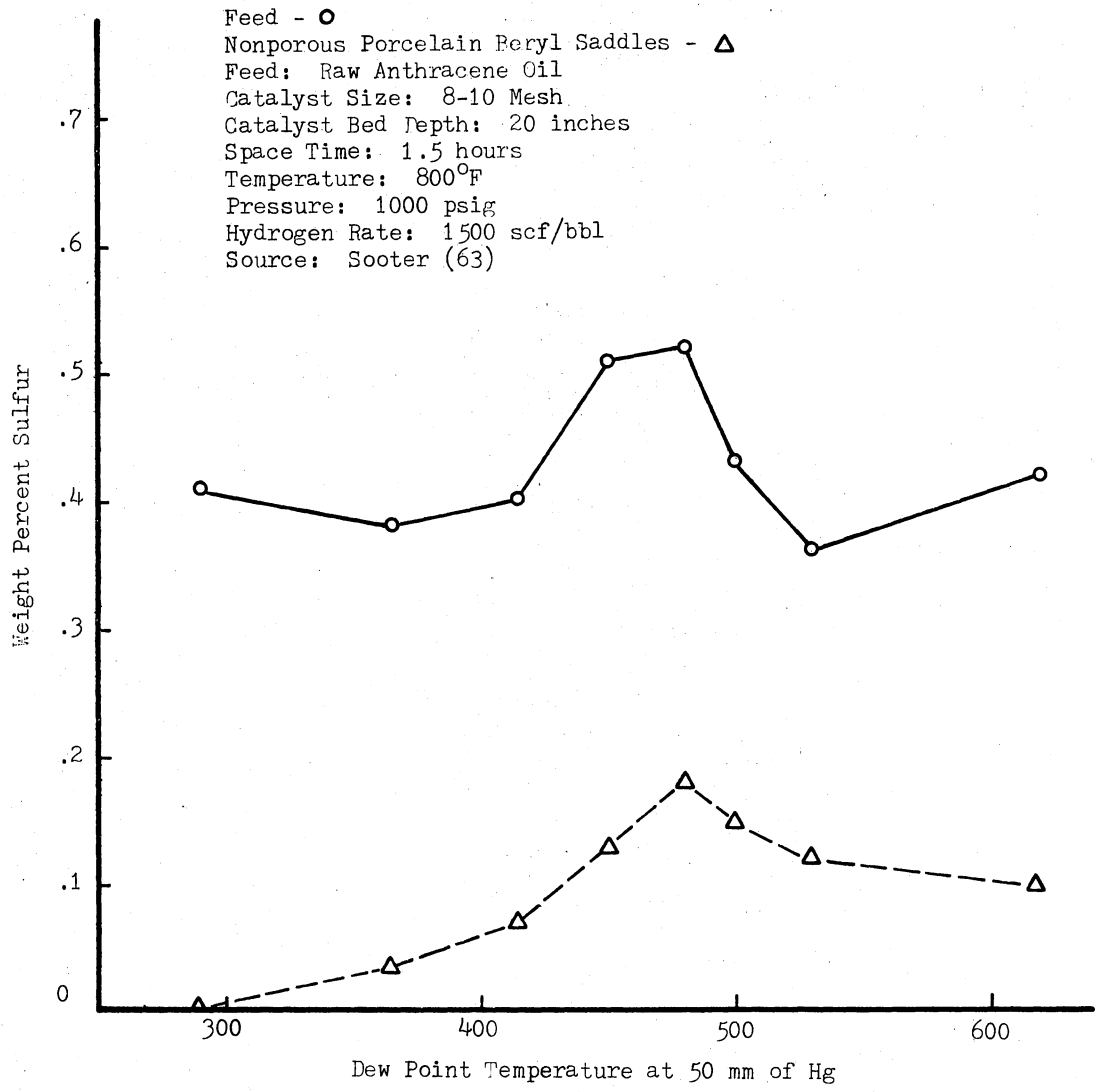

Figure 21. Sulfur Content of Distillation Fraction for Ceramic Beryl Saddles (Source: Sooter (63))

be only 1.224×10^{-4} M^2/gm compared to the surface area of the alumina which is 300 M^2/gm. This implies that although the surface area of the alumina is 2.5×10^6 times greater than that of the porcelain, the porcelain has a greater activity for hydrodesulfurization. This cannot be explained by the difference in operating conditions and is rather hard to explain in terms of surface reactions. To obtain an indication of whether the ceramic beryl saddles were porous, a simple experiment was conducted in which a beryl saddle was placed in a mixture of acetone and red dye. After five minutes the beryl saddle was removed from the mixture and allowed to dry. The saddle was then broken apart and the fractures inspected for penetration by the red dye. This experiment showed that the beryl saddles are in fact porous. This experiment does not provide an estimate of how porous or the pore sizes, but it does establish that the porcelain does have an active area greater than the external particle area.

If one considers this result and Sooter's findings one can conclude that porcelain alone would be good hydrodesulfurization catalyst. But this conclusion is contradicted in a study by Chirakaparambil (7) who studied hydrodesulfurization of FMC and PAMCO oils over 8-10 mesh crushed beryl saddles similar to what Sooter used. In Chirakaparambil's study the temperature varied from 700°F (371.4°C) to 800°F (427°C) and the pressure from 500 to 1500 psig. For PAMCO oil, very little sulfur removal was observed ($\sim$ 1.5% sulfur removal) and an increase in sulfur content was actually observed for FMC oil. Chirakaparambil attributed the increase in sulfur content in FMC oil to the selective cracking of non-sulfur compounds. These results do not agree with those of Sooter (63).

The apparent disagreement between the results presented in this study and those of Sooter (63) and Chirakaparambil (7) make a comparison between the three studies difficult. In one case, porcelain was shown to cause more sulfur removal than alumina. This could be due to the porcelain having a larger surface area and/or a more active adsorption site for sulfur compounds of raw anthracene oil. Chirakaparambil, using the same beryl saddles as Sooter, observed no sulfur removal from FMC oil and only slight sulfur removal for PAMCO oil.

These results seem to indicate that the hydrodesulfurization activity possibly depends on the nature of the sulfur compounds and the specific feedstocks used. The sulfur compounds in the raw anthracene oil was recently characterized by Greenwood and Scheppele (8). This study found only two major series of sulfur compounds; benzothiphenes (III) and dibenzothiophenes (IV).

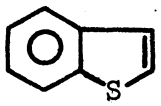

III

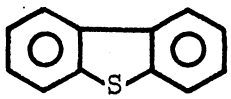

IV

Their study also showed that the dibenziothiophene (IV) was the sulfur compound with the largest concentration ($\sim$ 2 wt%). Considering the distillation curve for raw anthracene oil given in Figure 11, the broad peak between vapor temperature of 375°F and 475°F most likely corresponds to dibenzothiphene, while the sulfur concentration below 375°F is most likely due to benzothiphene. As can be seen in Figure 11, a greater amount of hydrodesulfurization has occurred in benzothiophene region than in the dibenzothiophene section. The type of sulfur compounds present in the heavy (475°F to 550°F) fractions has not been sufficiently characterized to identify a typical compound type.

Characterization studies of FMC oil and PAMCO oil have only recently been started by Greenwood and Scheppele. Initial results for FMC oil (15) indicate that types of sulfur compounds present in FMC oil are significantly different from those observed in raw anthracene oil. At present, the exact nature of the sulfur compound in FMC oil is not known, but further studies are underway. As of yet, no results have been obtained for PAMCO oil, but this oil will be characterized in the near future.

The possibility exists, considering the initial results of Greenwood and Scheppele (15), that conflicting results of Sooter (63) and Chirakaparambil (7) may be due to a significant difference in the types of sulfur compounds present in raw anthracene oil, FMC oil, and PAMCO oil. Also these results may be due to a difference in the nature of the feedstocks. FMC oil and PAMCO oil are more easily carbonized and cause the formation of carbonaceous material on the support. This can cause pore blockage and significantly reduce surface area, resulting in a loss in hydrodesulfurization activity. This has been observed with both PAMCO and FMC oil in $CoO/MoO_3/\gamma Al_2O_3$ studies (64) done at this institution. However, runs of up to 200 hours with raw anthracene oil has shown no loss in hydrodesulfurization activity (63). These results indicate FMC oil and PAMCO oil may be carbonizing and reducing the activity of the ceramic beryl saddles. At present, not enough information is available to determine which of these or other possibilities cause this effect.

In conclusion, alumina in the absence of hydrogen does not cause extensive cracking of sulfur compounds in raw anthracene oil. In contrast, alumina in the absence of hydrogen did cause extensive cracking

of nitrogen compounds. In the presence of hydrogen, extensive hydrodesulfurization does occur but not to the extent observed on porcelain. When the PAMCO or FMC feedstocks are used, essentially no sulfur removal is observed. This study does not give an indication why these differences exist, but further investigation is recommended.

The Effect of Alumina on Total Hydrogen Content

Again a comparison of data obtained from Run ACW and CCW will be made. The conditions and the results are summarized in the following table.

TABLE XIV

SUMMARY OF HYDROGEN RESULTS FOR RUNS ACW AND CCW

Run	Treat Gas	Treat Gas Rate scf/bbl	Liquid Hourly Space Time 0.46 hrs % H Addition	0.92 hrs % H Addition	1.84 hrs % H Addition
ACW	Hydrogen	1500	6.4	9.1	14.6
CCW	Nitrogen	1500	1.5	1.0	1.0

The data presented here are total hydrogen content of the reactor product oils. Figure 9 and Table XIV show that for Run ACW as the space time increases the hydrogen addition increases. The weight percent

hydrogen versus space time results for Run CCW shows a very slight increase in the weight percent hydrogen. This increase is not significant because it is not within the experimental precision of the hydrogen analyzer. The total hydrogen content of the distillation fractions of Run ACW are shown in Figure 12. This curve is for one space time, $\tau = 1.84$ hours. As can be seen, this curve shows extensive hydrogenation of all fractions, with a higher content observed in the light ends. This is most likely due to the cracking and hydrogenation of the heavy fractions. The cracking and hydrogenation form lower molecular weight compounds. This causes the hydrogen content of the light fractions to increase. The weight percent hydrogen distillation results for Run CCW are also shown in Figure 12. This curve shows a translation toward the heavy ends which is evidence of extensive cracking and condensation. This results in the formation of higher molecular weight compounds (higher boiling fractions) with a lower hydrogen content.

The results presented in this section indicate that alumina in the presence of hydrogen promotes hydrogenation of a broad spectrum of hydrocarbons in raw anthracene oil. Also these results confirm the existence of extensive cracking and condensation in the absence of hydrogen.

Effects of the Active Sites and Feed Composition

The preceding sections have shown that a definite difference exists between the results obtained in this study and the studies of porcelain and $CoO/MoO_3/\gamma Al_2O_3$ catalysts. These differences are possibly due to the nature of the active sites and the nature of nitrogen and sulfur

compounds in the feedstock. While the exact determination of the causes and effects of these differences is beyond the scope of this study, the results presented lead to some interesting speculations.

First, consider the nitrogen results. Here in the presence of hydrogen extensive cracking, hydrogenation and hydrodenitrogenation was observed. As can be seen from Figures 10 and 20, the products of these reactions differ greatly from those obtained from the ceramic beryl saddles or a $CoO/MoO_3/\gamma Al_2O_3$ catalyst. Since the feedstock in each situation was the same this indicates that the active sites on these materials differ significantly. Specifically, alumina is believed to have two major sites, a Lewis site associated with a structural defect causing formation of an exposed Al^{+3} ion and a passive Bronsted site. The exact structure of the Bronsted site has not been proposed. Rosynek and Strey (48) have observed that ammonia tends to block the Al^{+3} site of alumina at temperatures greater than 751°F (400°C). This result indicates the possibility that nitrogen compounds are being adsorbed on the Lewis sites of the alumina in this study. Although nitrogen compounds are probably adsorbed at the Lewis site of the alumina, the statement cannot be made that these are hydrodenitrogenation sites. The possibility exists that these are the hydrodenitrogenation sites, but not enough is known about the character of these sites to draw any conclusions. Later in this section, results will be presented which indicate that a strong adsorption site is necessary for a hydrodenitrogenation reaction.

Also observed in the presence and absence of hydrogen was extensive cracking of nitrogen compounds. This result agreed well with that observed by Tung and McIninch (65). They observed extensive cracking of

cumene and 1 Hexene over alumina at temperatures greater than 751°F (400°C). They attributed this activity to the existence of Bronsted sites. Figure 16 shows that in the absence of hydrogen extensive cracking and condensation of nitrogen compounds does occur, but this does not result in any significant nitrogen removal.

In the presence of hydrogen, cracking and hydrogenation actually cause the nitrogen content of the light fractions to increase. The possibility exists that the cracking and hydrogenation causes the formation of light nitrogen compounds which are not as likely to undergo the hydrodenitrogenation reaction. Three possible explanations can be given for this behavior. First, the possibility exists that cracking/-hydrogenation has caused the formation of a nitrogen compound which is not as likely to undergo the hydrodenitrogenation reaction on alumina. This compound would have a boiling range similar to quinoline and hydroindole type compounds. The resistance of this compound to hydrodenitrogenation could be due to the structure of molecule. During cracking/hydrogenation, a molecule could be formed which is not capable of being absorbed on the active hydrodenitrogenation sites on alumina. Another possibility is that cracking/hydrogenation of the heavy (450°F to 550°F) fractions could be consuming the majority of the hydrogen in the system (15). This could result in the starving of the hydrodenitrogenation reaction for hydrogen, thus resulting in lower hydrodenitrogenation. Also the possibility exists that alumina lacks enough sufficiently active sites to cause extensive hydrodenitrogenation. In this situation, because alumina has a cracking (Bronsted) site, the rate of production of the light nitrogen compounds by cracking/hydrogenation might exceed the rate of removal by hydrodenitrogenation.

Therefore, the nitrogen content in the light fraction would be increased.

Satchell's results for hydrodenitrogenation of raw anthracene oil over a $CoO/MoO_3/\gamma Al_2O_3$ catalyst, given in Figure 20, shows no evidence of accumulation of nitrogen compounds in the light ($275^{\circ}F$ to $425^{\circ}F$) fractions. This is most likely due to the difference in the nature of the active sites on a $Co/Mo/\gamma Al_2O_3$ catalyst. At the present time, not enough is known about the structure of the active Co/Mo complex or the active sites on alumina to state why these differences exist.

Also shown in Figure 20 is the result of beryl saddles. As was stated earlier, negligible nitrogen removal was observed. This implies that there are very few, if any, hydrodenitrogenation sites on the beryl saddles. The exact composition and characteristics of these beryl saddles are not known at this time. But they are a ceramic material and should have properties similar to porcelain. Porcelain is a silica-alumina with a relatively high sodium or potassium content (35). The active site on the silica-alumina material is an exposed Al^{+3} ion site. This site can be either a Lewis site or a Bronsted site, depending on the adsorbed water. These sites are known to be poisoned or inhibited by sodium compounds (6, 32, 42). Sodium compounds poison the most active site leaving the weaker site. With this in mind porcelain would most likely have a large number of weak sites, both Bronsted and Lewis types. (Note Satchell's porcelain data shows no evidence of cracking due to a Bronsted acid. This is most likely due

to the structural difference between Bronsted sites on alumina and that on silica alumina (56, 65).) The absence of hydrodenitrogenation ability indicates that hydrodenitrogenation sites are also absent. Therefore, the possibility exists that since porcelain has very few strong adsorption sites that hydrodenitrogenation reaction occurs at a strong adsorption site. This is most likely a strong Lewis site associated with an Al^{+3} site in porcelain. The fact that these sites are blocked by sodium could be the reason for the low hydrodenitrogenation observed in Satchell's ceramic beryl saddle studies.

The existence of strong adsorption sites on the alumina could explain its significant hydrodenitrogenation activity. The alumina used in this study had a low sodium content (0.03 wt% Na). Pines, et al. (17) and Tung, et al. (65) have established that the presence of alkali metals in alumina tends to reduce the number of the strong adsorption sites. Since the alumina used in this study is relatively free from sodium, it is expected to have more strong adsorption sites than those of porcelain. This could be the reason why alumina has a higher activity for hydrodenitrogenation than that of porcelain.

The sulfur results presented in this study also give rise to some interesting speculation. As will be recalled, porous alumina has shown significant sulfur removal in the presence of hydrogen. This removal is possibly due to the exposed Al^{+3} Lewis acid sites. A study by Rosynek and Strey (48) has found that the Lewis site of alumina does adsorb hydrogen sulfide and methyl mercaptan. They have proposed the following mechanism.

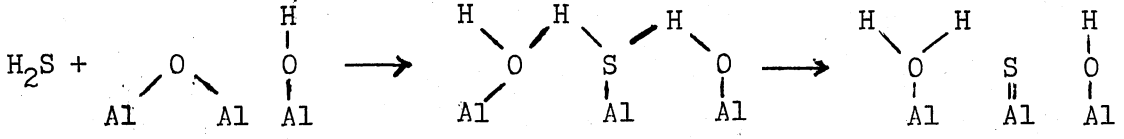

The structure of this site is very close to the $Co/Mo/\gamma Al_2O_3$ hydrodesulfurization site proposed by Schmit and Gates (54). This site is composed of a group of exposed Mo^{+3} ions surrounded by sulfided Mo atoms. A detailed description of the Co/Mo sites is given in the background study of this work on page 3.

The fact that no sulfur removal was observed in the absence of hydrogen is most likely due to the Lewis sites being in a sulfided form $\overset{S}{\underset{Al}{\|}}$ with no hydrogen gas present to reduce the site back to an active Lewis site. The lack of sulfur removal also implies the absence of hydrogen donor compounds such as tetralin in raw anthracene oil. Also the results show that, in the absence of hydrogen, sulfur compounds do not undergo extensive cracking. This indicates that the Bronsted site present on alumina possibly does not affect the sulfur compound but does cause extensive cracking of the nitrogen compounds. The reason for this behavior is most likely related to the nature of the Bronsted site and that of the sulfur and nitrogen compounds in the raw anthracene oil.

In conclusion, the ideas presented in this section are speculation and no experimental evidence exists to substantiate these ideas. Hopefully, some of these thoughts will stimulate new ideas and new experiments.

In the next section of this study, the result and discussion section will be summarized.

CHAPTER VI

CONCLUSIONS AND RECOMMENDATIONS

In this study a trickle bed reactor, operating at 750°F (399°C), 1500 psig and volume hourly space times of 0.46 hr., 0.92 hr. and 1.84 hr., has been used to evaluate the ability of a gamma alumina support to remove sulfur and nitrogen from raw anthracene oil (a coal derived liquid). Three runs were made in this study, ACW, BCW and CCW. Runs ACW and BCW were made to assess the effect of presulfiding and ability of the alumina support to cause hydrogenation, hydrodenitrogenation, and hydrodesulfurization. A hydrogen treat gas was used in both ACW and BCW. Run CCW was made to determine the effect of thermal reactions on nitrogen and sulfur compounds in the coal derived liquid. Here nitrogen was used as a treat gas.

The following conclusions and recommendations can be drawn from the results presented.

Conclusions

1. The reproducibility of the data present in this study is good.
2. Axial dispersion, mass transfer and liquid distribution may affect reactor performance and have not been shown to be absent in previous studies.
3. The presulfiding of an alumina support does not result in a significant increase in activity either for nitrogen or sulfur

removal compared to untreated support.

4. In the presence of hydrogen, alumina causes cracking/hydrogenation and hydrodenitrogenation of nitrogen compounds. The nitrogen compounds formed in the cracking/hydrogenation process seem to be less likely to undergo hydrodenitrogenation.
5. In the absence of hydrogen, extensive cracking and condensation of heavy fraction nitrogen compounds was observed. This caused the formation of a low (325°F to 375°F) boiling in nitrogen compound(s).
6. Sulfur compounds in the presence of hydrogen undergo extensive hydrodesulfurization over the alumina support.
7. In the absence of hydrogen, sulfur compounds do not appear to undergo a cracking reaction as was observed with nitrogen compounds. This indicates that selective cracking of nitrogen compounds has occurred. Also no significant sulfur removal was observed when hydrogen treat gas was not present.
8. Significant hydrogenation of all distillation fractions occur. The fact that the hydrogen content of light fractions increases more is most likely due to cracking/hydrogenation of fragments to form low boilers.
9. In the absence of hydrogen treat gas, the hydrogen content of distillation fractions confirms the existence of cracking and condensation.
10. The ceramic beryl saddles used in Satchell's (49), Sooter's (63) and Chirakaparambil's (7) studies are porous. The extent of porosity and pore size distribution are not known.
11. The conflict between Sooter's (63) and Chirakaparambil's (7)

results is probably due to a difference in the nature of the feedstocks; specifically, different types of sulfur compounds and/or feedstocks.

12. Ceramic beryl saddles have significant hydrodesulfurization ability but very poor hydrodenitrogenation ability for raw anthracene oil.

Recommendations

1. Mass spectroscopic studies of sample ACW 10 and CCW 10 distillations fractions should be made. This would indicate what light nitrogen compounds were being formed, what the precursor was and what the possible mechanisms is.
2. Mass spectroscopic studies should also be made of a sample from Chirakaparambil's FMC oil run. This would assess the amount of carbonization which has occurred.
3. Ceramic beryl saddles used by Sooter (63), Satchell (49) and Chirakaparambil (7) should be characterized as to their exact chemical composition, pore distribution and surface area.
4. An attempt should be made to tailor porcelain for an economical "throw away" bed. This bed could be used as a trap for metallic compounds and ash for coal derived liquids.
5. An investigation of flow distribution problems in the reactor bed should be made. This might include running with flow distributor in the reactor bed, running without a thermal well, and varying catalyst particle size.
6. An investigation should be made as to what effect the presence of halogen compounds in the treat gas might have on

hydrodenitrogenation. This effort would entail finding the conditions at which significant hydrodenitrogenation occurs but does not cause excessive cracking.

BIBLIOGRAPHY

1. Aboul-Gheit, A. K. and I. K. Abdou, Inst. of Petr. London Journal, 59, 188-194(1973).

2. Addlington, D. and E. Thompson, Third European Symposium on Chemical Reaction Engineering, 203(1964).

3. Ahmed, M. M. M.S. Thesis, Oklahoma State University (1975).

4. Ahuja, S. P., M. L. Derrien and J. F. Le Page, Ind. Eng. Chem. Prod. Res. Dev., 9, 272(1970).

5. Beuther, H., R. A. Flinn and J. B. McKinley, Ind. Eng. Chem., 51, 297(1964).

6. Bremer, V. H., K. H. Steinberg and Tran-Khal Chuong, Z. Anorg. Allg. Chem., 400, 115(1973).

7. Chirakaparambil, F. G., M.S. Thesis, Oklahoma State University (1974).

8. Crynes, B. L. Catalysts for Upgrading Coal Derived Liquids, Quarterly Report for the Period of June 9, 1976 - September 8, 1976.

9. De Beer, V. H. J., T. H. M. Van Sint Fiet, G. H. A. M. Van Der Stein, A. C. Zwaga and G. C. A. Shuit, J. Catal., 35, 297 (1974).

10. De Bruijn, A. Sixth International Congress on Catalysts, London, (1976).

11. Fedchuk, A. P. and V. V. Mikho, Kinet. Kata., 15, 478(1974).

12. Flinn, R. A., O. A. Larson, and H. Beuther, Hydrocarbon Proc. and Petro. Ref., 42, 129(1967).

13. Frost, C. M. and H. B. Jensen, Preprints, Div. of Petrol. Chem., ACS, 18, 118(1973).

14. Goudriaan, F., H. Gierman and J. C. Vlugter, J. Inst. Petr., 59, 40(1973).

15. Greenwood, Gil, Private Communication, Fall (1976).

16. Grimm, C. D. and L. Berg, Sixty-Eighth National Meeting, AIChe, (1971).

17. Haag, W. O. and H. J. Pines, Amer. Chem. Soc., 82, 2471(1960).

18. Hagenbach, G., P. H. Courty and B. Belmon, J. Catal., 31, 264 (1973).

19. Heiser, H. W., A. S. Russel, and H. C. Stumpf, Alumina Technical Paper No. 10, 2nd Revision (1960).

20. Henry, H. C. and J. B. Gilbert, Ind. Eng. Chem., Process Design Develop., 12, 328(1973).

21. Hightower, J. W., Preprint, Div. of Petrol. Chem., ACS, 18, 262 (1973).

22. Hirschler, A. E., J. Catal., 2, 428(1963).

23. Holm, V. C. F., A. C. Bailey and A. Clark, J. Phys. Chem., 63, 129 (1963).

24. Holm, V. C. F. and A. Clark, J. Catal., 2, 16(1963).

25. Hoog, L., J. Inst. Petrol., 36, 738(1950).

26. Johns, J. J., J. F. Jones, and B. P. McMunn, Preprints, Div. of Fuel Chem., ACS, 16(1), 26(1972).

27. Jones, J. F. and L. D. Friedman, Office of Coal Research Report No. 56, 383(1963).

28. Jones, J. F. and L. D. Friedman, "Char Oil Energy Development Final Report." Office of Coal Research Report No. 56, 25 (1970).

29. Leach, B. E., Private Communications, (1975).

30. _____, Leco Automatic Sulfur Determinator Instruction Manual, Lab. Equip. Corp. 1415 Hilltop Rd., St. Joseph, Mich. 49085.

31. Kolthoff, I. M. and E. B. Sandell, Textbook of Quantitative Inorganic Analysis, 3rd Ed. (1958).

32. Levchuk, V. S. and N. E. Buyanova, Izvestiva Akademii Nauk SSSR, Seriya Khimicheskaya, 21(1), 27(1972).

33. Levenspiel, O., Chemical Reaction Engineering, John Wiley and Sons, Inc. (1967).

34. MacIver, D. S., H. H. Tobin and R. T. Barth, J. Catal., 2, 485 (1963).

35. Mantell, C. L., Engineering Material Handbook, McGraw-Hill Book Co., Inc. (1958).

36. McIlvried, H. G., Ind. Eng. Chem. Process. Design Develop., 10(1), 125(1971).

37. Mears, D. E., Chem. Engr. Sci., 26, 1361(1971).

38. Mears, D. E., Adv. in Chem. Ser. No. 133, 218(1974).

39. Miesserov, K. G., J. Catal., 13, 169(1969).

40. Mitchell, P. C. H., The Chemistry of Some Hydrodesulfurization Catalysts Containing Molybdenum, Clamax Molybdenum Company, London (1967).

41. _____, Model 240 Elemental Analyzer Instruction Manual, Perkin-Elmer, Norwalk, Conn.

42. Parry, E. P., J. Catal., 2, 371-379(1962).

43. Qader, S. H., Hydrocarbon Processing, 48(9), 147(1969).

44. Qader, S. H. and G. R. Hill, Ind. Eng. Chem. Process Des. Develop. 8(4), 450(1969).

45. Qader, S. H., W. H. Wiser and G. R. Hill, Ind. Eng. Chem. Process. Design Develop., 7, 390(1968).

46. Ratnasamy, P., A. V. Ramaswamy, L. Banerjee, D. K. Sharma and N. Ray, J. Catal., 38, 19(1975).

47. Ross, L. D., Chem. Eng. Progress, 61, 77(1965).

48. Rosynek, M. P. and F. L. Strey, J. Catal., 41, 312(1976).

49. Satchell, D. P., Ph.D. Thesis, Oklahoma State University, 1974.

50. Satterfield, C. N., Mass Transfer in Heterogeneous Catalyst. MIT Press, Cambridge, Mass. (1970).

51. Satterfield, C. N., AIChE J. 21(2), 209(1975).

52. Satterfield, C. N., M. Modell and J. F. Mayer, AIChE J., 21(6), 1100(1975).

53. Satterfield, C. N. and F. Ozel, AIChE J., 19, 1259(1973).

54. Schuit, G. C. A. and B. C. Gates, AIChE J., 19, 417(1973).

55. Schuman, S. C. and H. Shalit, Catalyst Rev., 4, 245(1970).

56. Schwartz, J. A., J. Vac. Sci. Technol., 12(1), 321(1975).

57. Schwartz, J. G. and L. W. Roberts, Ind. Eng. Chem. Process Design Develop., 12, 267(1973).

58. Schwartz, J. G., E. Weger, M. P. Dudukovic, "A New Tracer Method for Determination of Liquid-Solid Contacting Efficiency in Trickle Bed Reactors", submitted to the AIChE Journal (1976).

59. Schwartz, J. G., E. G. Weger, M. P. Dudukovic, "Liquid Holdup and Dispersion in Trickle Bed Reactors", submitted to the AIChE Journal (1976).

60. Scotti, L. J., "Char Oil Energy Development," Interim Report No. 2, R & D Report No. 73, U.S. Department of Interior, Office of Coal Research (1974).

61. Smith, A. J., G. Myers, Jr., and W. C. Slaner, Jr., Mikrochimica Acta (Wien), 217(1972).

62. Sokolnikoff, I. S. and R. M. Redheffer, Mathematics of Physics and Modern Engineering, M Graw-Hill, New York (1966).

63. Sooter, M. C., Ph.D. Thesis, Oklahoma State University, (1974).

64. _____, Summary Report of Coal Liquid Catalyst Work Performed at School of Chemical Engineering, OSU to Pittsburg and Midway Coal Mining Company (February 1975).

65. Tung, S. E. and E. McIninch, J. Catal., 3, 229(1964).

66. Van Deemter, J. J., Third European Symposium on Chemical Reaction Engineering, 215(1964).

67. Van Zoonen, D. and C. T. Douwes, Journal of Petroleum, 49, 383 (1963).

68. Voorhoeve, R. J. H. and J. C. M. Stuiver, J. Catal., 23, 243 (1971).

69. Wan, K. T., M.S. Thesis, Oklahoma State University (1973).

APPENDIX A

CORRECTION OF DISTILLATION VAPOR TEMPERATURE DATA

ASTM D1160 Distillations were performed on eight selected samples in this study. Unfortunately, the distillations were done in such a manner that the vapor temperatures obtained in these studies were all too low. The principal cause of this error was the low heating rate of the distillation flask. This allowed the vapor reflux line to drop below the column thermalcouple which measured vapor temperature. As a result the vapor temperatures were generally not accurate. Also recorded during these runs were pot temperatures. The pot temperature was measured by a mercury thermometer in a thermal well on the distillation flask. Since pressure control was accurate, the pot temperature data obtained should also be accurate. With this in mind, an effort was made to determine a relationship between the pot temperature and the vapor temperature. In order to do this distillations of raw anthracene oil were made at higher pot powerstat settings. The vapor temperatures in these studies were recorded continuously on a chart recorder. The results of these runs are shown in Figure 22. In order to insure that the samples of this study also agreed with this figure, a distillation of BCW 2 was made at the higher powerstat settings. This data is also shown in Figure 22. As can be seen, the distillation data obtained from this sample agrees with the data obtained from raw anthracene oil

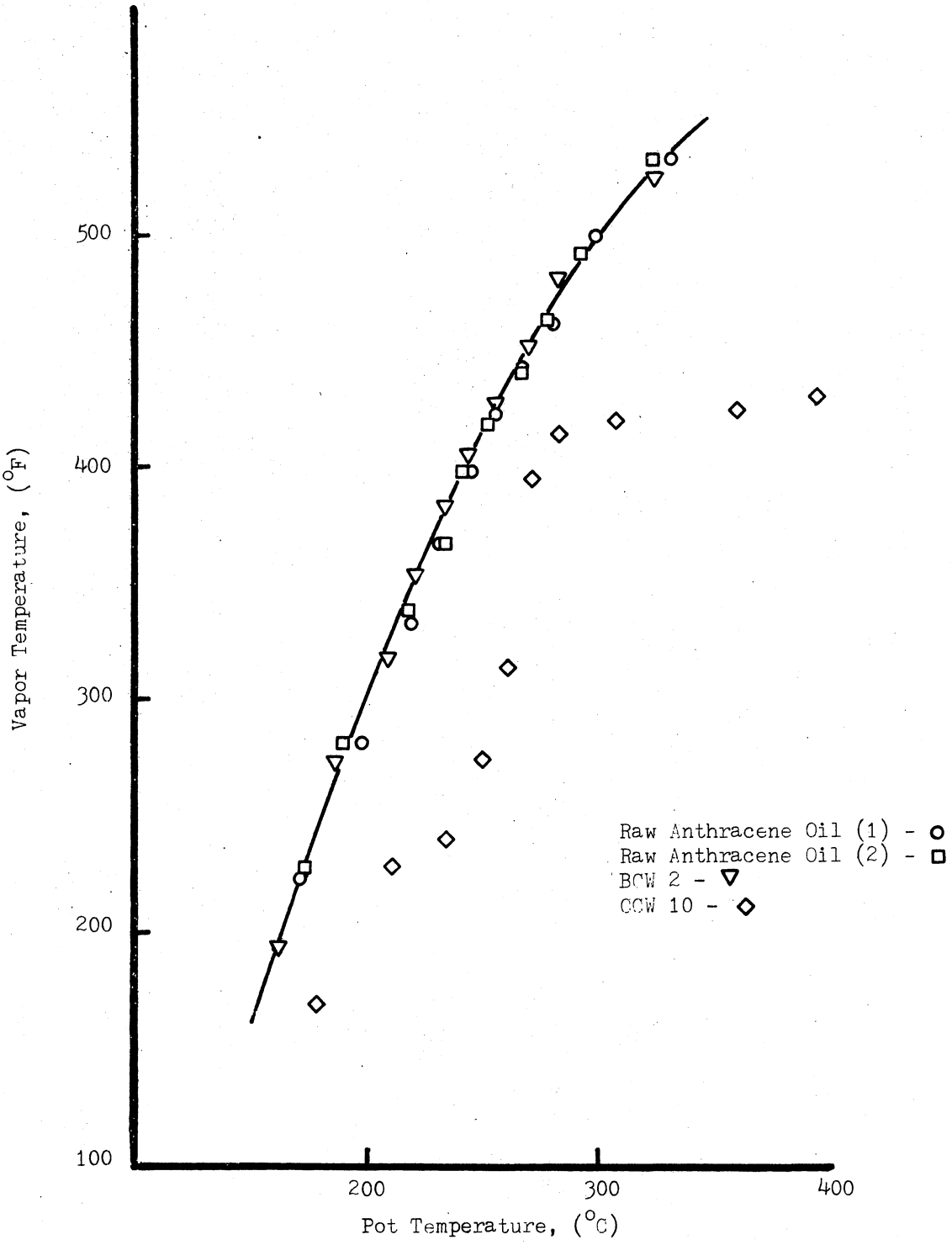

Figure 22. The Effect of Heating Rate on Vapor Temperature

distillations. Also shown in Figure 22 is the original data from the distillation of sample CCW 10. This shows that the vapor temperatures obtained in the original distillations were erratic and low.

The data presented in Figure 22 suggests a definite relationship exists between the pot temperature and the vapor temperature. In order to find an analytical expression to describe this curve a least square curve fit was made with a second order polynomial. A computer program was then developed to correct the experimental temperature of the original runs. This correlation resulted in a vapor temperature which was on the average 15°F too high. This was caused by the rate of heating effect on the pot temperature. As was stated earlier, BCW 2 and the raw anthracene oil series were performed at a higher pot heat flux. The higher rate of heating did not allow the pot temperature to come to the same degree of equilibrium as when heated at a slower rate. Therefore, the vapor temperatures based on the original higher pot temperatures are on the average 15°F too high. With this in mind, the following correlation was proposed:

$$T_v = (-416.087 + 4.626\ T_p - .005275\ T_p^2) - 15$$

where T_v = vapor temperature, °F

T_p = pot temperature, °C.

Here the first part corresponds to the relation obtained from the least square curve fit and the second part is the result of the correction for different heating rates.

In order to check the validity of this correlation the results of the BCW 2 distillation was compared to the corrected results BCW 10. As can be seen in Appendix B, the condition and composition of these samples are very similar. Therefore, these samples should have a

similar vapor temperature versus percent volume distilled curves. These are shown in Figure 23. As can be seen, the maximum difference between the corrected curve and the experimental curve is $\pm$ 10°F. Since the repeatability specified in the ASTM D1160 description is $\pm$ 10°F at 50 mm of Hg, one can conclude that the correlation resulted in a satisfactory correction of the original pot temperature to vapor temperature.

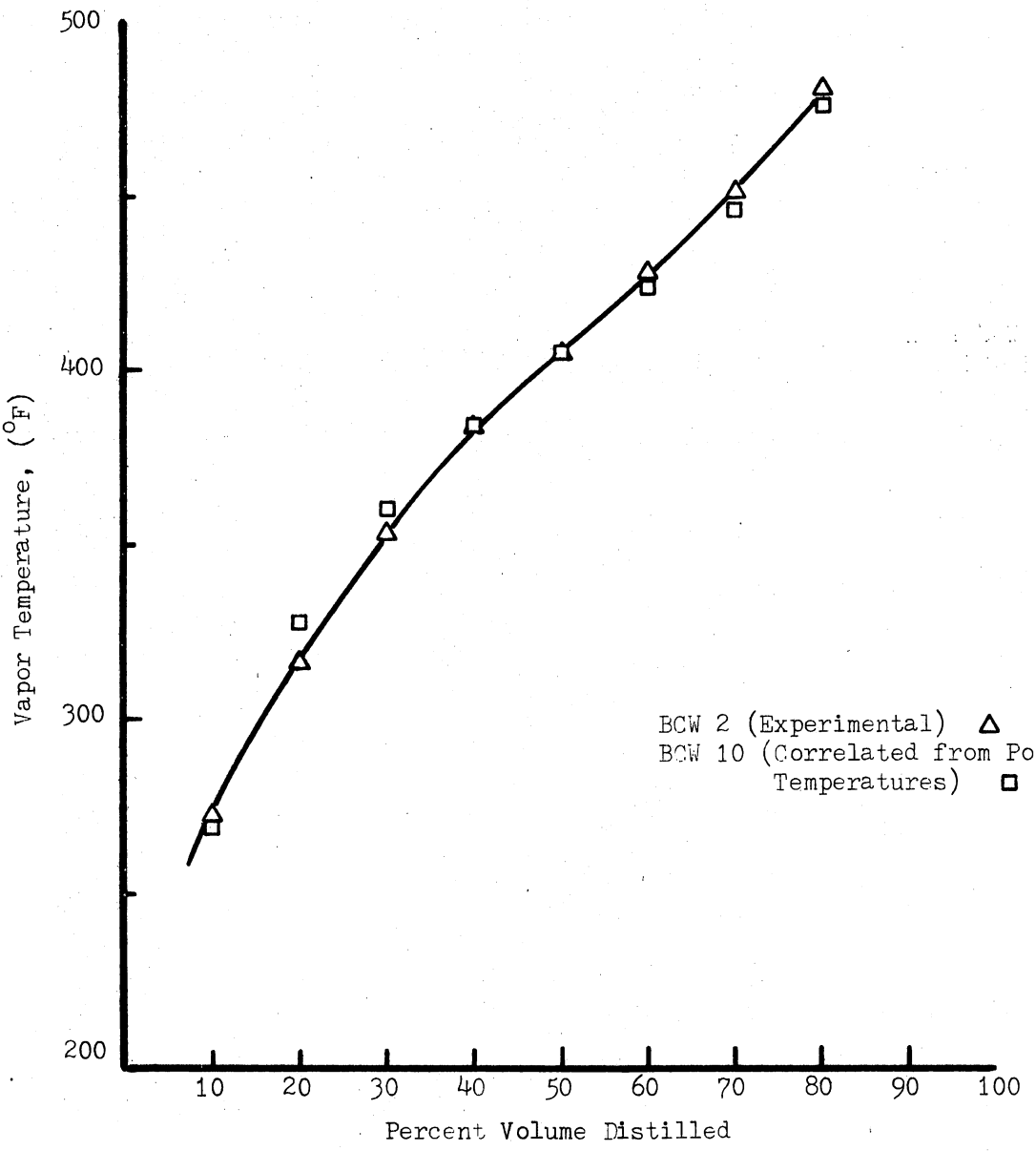

Figure 23. A Comparison of Experimental and Correlated Vapor Temperature

APPENDIX B

EXPERIMENTAL DATA

The conditions and the data obtained from runs ACW, BCW and CCW are listed. Note runs ACW and BCW differ only by the fact that BCW was presulfided. Also, run CCW was made at the same conditions but a treat gas of nitrogen was used instead of hydrogen.

TABLE XV

RESULTS WITH KETJEN 007-1.5E SUPPORT
(7.6 mm x 1.7 mm EXTRUDATE)
ACW UNSULFIDED, RAW ANTHRACENE
OIL FEEDSTOCK, HYDROGEN
GAS PRESENT

Sample Number	Temp[a] (°F)	Pressure (psig)	Space Time[b] (Volume hrly)	Hydrogen (SCF/BBL)	Hours[c] on oil	%S[d]	%S[e] Removal	%N[d]	%N[e] Removal	%H[d]
Feed						0.47		1.06		5.57
ACW 1	750	1500	1.84	1500	12	0.241	49	0.841	20[f]	
ACW 2	750	1500	1.84	1500	24	0.253	46	0.794	24	-
ACW 3	750	1500	1.84	1500	36	0.290	38	0.807	23	-
ACW 4	750	1500	1.84	1500	48	0.276	41	0.809	23	-
ACW 5	750	1500	0.92	1500	53	0.349	26	0.834	21	-
ACW 6	750	1500	0.92	1500	55	0.319	32	0.816	22	6.08
ACW 7	750	1500	0.46	1500	58.5	0.373	21	0.871	17	-
ACW 8	750	1500	0.46	1500	59.5	0.403	14	0.857	18	5.93
ACW 9	750	1500	1.84	1500	69.5	0.259	45	0.794	24	6.39
ACW 10	750	1500	1.84	1500	73.5	0.256	46	0.761	28	-

a. Nominal Reactor Temperature.

b. This is a volume hourly space time (volume of catalyst/volume of oil per hour).

c. Total hours which the catalyst has been contacted with oil at reaction conditions.

d. Percent of sulfur, nitrogen or hydrogen in liquid product.

e. % Removal = (fraction in feed less fraction in product)/(fraction in feed).

f. Helium filled nitrogen analysis capsule for all samples.

TABLE XVI

RESULTS WITH KETJEN 007-1.5E SUPPORT
(7.6 mm x 1.7 mm EXTRUDATE)
BCW PRESULFIDED, RAW
ANTHRACENE OIL FEEDSTOCK,
HYDROGEN GAS PRESENT

Sample Number	Temp[a] (°F)	Pressure (psig)	Space Time[b] (Volume hrly)	Hydrogen (SCF/BBL)	Hours[c] on oil	%S[d]	%S[e] Removal	%N[d]	%N[e] Removal	%H[d]
Feed										
BCW 1	750	1500	1.84	1500	16	0.258	45	0.778	26	-
BCW 2	750	1500	1.84	1500	28	0.242	48	0.749	29	-
BCW 3	750	1500	1.84	1500	40	0.247	47	0.759	28	-
BCW 4	750	1500	1.84	1500	52	0.229	51	0.769	27	-
BCW 5	750	1500	0.92	1500	56	0.306	35	0.778	26	-
BCW 6	750	1500	0.92	1500	59	0.321	32	0.835	20	-
BCW 7	750	1500	0.46	1500	61.5	0.381	19	0.862	18	-
BCW 8	750	1500	0.46	1500	62.5	0.394	16	0.878	16	-
BCW 9	750	1500	1.84	1500	72.5	0.261	44	0.762	27	-
BCW 10	750	1500	1.84	1500	76.5	0.256	46	0.756	28	-

a. Nominal Reactor Temperature.

b. This is a volume hourly space time (volume of catalyst/volume of oil per hour).

c. Total hours which the catalyst has been contacted with oil at reaction conditions.

d. Percent of sulfur, nitrogen or hydrogen in liquid product.

e. % Removal = (fraction in feed less fraction in product)/(fraction in feed).

f. Helium filled nitrogen analysis capsule for all samples.

TABLE XVII

RESULTS WITH KETJEN 007-1.5E SUPPORT
(7.6 mm x 1.7 mm EXTRUDATE)
RAW ANTHRACENE OIL FEEDSTOCK
NO HYDROGEN GAS PRESENT

Sample Number	Temp[a] (°F)	Pressure (psig)	Space Time[b] (Volume hrly)	Nitrogen (SCF/BBL)	Hours[c] on oil	%S[d]	%S Removal	%N[d]	%N[e] Removal	%H[d]
Feed						0.47		1.06		5.57
CCW 1	750	1500	1.84	1500	12	0.464	1.27	0.993	6.32	-
CCW 2	750	1500	1.84	1500	24	0.487	-	0.993	6.32	-
CCW 3	750	1500	1.84	1500	36	0.487	-	0.996	6.03	-
CCW 4	750	1500	0.92	1500	48	0.500	-	1.002	5.47	-
CCW 5	750	1500	0.92	1500	53	0.495	-	1.006	5.09	5.63
CCW 6	750	1500	0.92	1500	55	0.5205	-	1.004	5.28	-
CCW 7	750	1500	0.46	1500	56.5	0.4945	-	1.013	4.43	-
CCW 8	750	1500	0.46	1500	57.5	0.4985	-	1.006	5.09	5.66
CCW 9	750	1500	1.84	1500	68.5	0.485	-	1.004	5.28	-
CCW 10	750	1500	1.84	1500	72.5	0.4805	-	1.018	3.96	5.63

a. Nominal Reactor Temperature.

b. This is a volume hourly space time (volume of catalyst/volume of oil per hour).

c. Total hours which the catalyst has been contacted with oil at reaction conditions.

d. Percent of sulfur or nitrogen in liquid product.

e. % Removal = (fraction in feed less fraction in product)/(fraction in feed).

APPENDIX C

ASTM D1160 DISTILLATION AT OKLAHOMA STATE UNIVERSITY

Introduction

The following is a detailed procedure for ASTM D1160 Vacuum Distillation.

Procedure

1. Turn on the water heater on the tank behind the unit.
2. Connect the recorder to the temperature read out device. (Connect positive to positive and negative to negative.)
3. Set the recorder controls to a slow chart drive speed. Turn off the recorder.
4. Load the cold trap with acetone and dry ice.
5. Assemble the distillation unit without the sample in the flask. Lower the safety shield and be sure you are wearing goggles.
6. Turn on the vacuum pump and powerstat. Set the powerstat at 30 and open the valve to bypass the manostat.
7. Observe the cold trap. If acetone begins to accumulate, do not lower the pressure below the point at which the acetone in the cold trap starts to bump.
8. Turn off the vacuum pump, repressurize the system with nitrogen and drain the cold trap.

9. Again turn on the vacuum pump with no sample present and observe the cold trap. If no acetone appears, draw the system down to the lowest possible pressure. If acetone is still present, repeat Steps 7, 8 and 9.
10. Repressurize system with nitrogen gas. Load the distillation flask with the sample and four (4) boiling chips. Reassemble the system.
11. On the manostat, turn adjustment screw fully counterclockwise.
12. Activate vacuum pump and reduce the pressure to 20 mm of Hg. Turn off the vacuum pump and lead test the system by observing the system pressure on the manometer. It should remain steady.
13. Repressurize the system with nitrogen. (This maintains a non-combustible atmosphere.)
14. Turn on vacuum pump and reduce the pressure to 20 mm of Hg.
15. Close the manostat bypass valve and then repressurize with nitrogen to a pressure greater than 50 mm of Hg (~70 mm of Hg).
16. Note the final pressure of the system and adjust to 50 mm of Hg with adjustment screw on the manostat.
17. Lower the face shield and be sure you have your goggles on.
18. Turn on the powerstat, the hot cooling water and the cold cooling water. The initial setting of powerstat is determined by operator (recommend 90 or higher).
19. Turn on the recorder, recording the temperature at this point on the recorder output.
20. Watch for the vapor reflux line in the distillation flask and also be careful to avoid extensive bumping. (Small amounts of

bumping are acceptable as long as it does not cause carry over of the pot sample in distillate or touch the thermalcouple.)

21. Record the temperature of first drop on recorder output and in logbook.
22. Collect 10% of total sample volume in each test tube. Record the vapor and pot temperatures when test tube is changed.
23. Powerstat settings should be increased to give a smooth distillation curve. Be sure to avoid scallops in the curve.
24. Continue to increase the powerstat settings to maintain a smooth curve. On the last test tube, carefully watch the recorder output. It will begin to level off and drop as thermal cracking begins to occur. At this point shut theunit down, under no circumstances exceed 750°F (~ 400°C) pot temperature.
25. Shut down. Turn off the vacuum pump and the powerstat. Repressurize slowly with nitrogen.
26. Turn off recorder drive.
27. Isolate the manometer and bleed off the nitrogen through manometer - vacuum pump exhaust line.
28. Allow to cool for 20-30 minutes. Raise the safety shield.
29. Collect a bottom sample and other samples.
30. Clean up. Clean up is best accomplished by vacuum distillation of a small amount (20-30 ml) of raw anthracene oil, followed by atmospheric distillation of acetone.
31. De-energize all equipment.

APPENDIX D

ESTIMATE OF STANDARD DEVIATION OF THE NITROGEN AND HYDROGEN DATA

In this section, the results of 32 nitrogen analyses of raw anthracene oil and 5 hydrogen analyses are presented. These results were used to calculate the standard deviation. An unbiased estimate of the standard deviation was obtained from sample variance. The following equations were used (62).

$$S^2 = \frac{1}{n} \sum (x_i - \bar{x})^2$$

where S^2 - sample variance

n - number of independent observations

x_i - independent observations of variable x

$\bar{x}$ - mean of the x_i

$$\sigma^2 = \frac{n}{n - 1} S^2$$

where σ^2 unbiased estimate of the variable

σ - unbiased estimate of the standard deviation

NITROGEN

Weight Percent Nitrogen	$x - \bar{x}$	$(x - \bar{x})^2$	$\sum(x - \bar{x})^2$
1.046	-.009	8.1×10^{-5}	
1.082	.027	7.29×10^{-4}	8.1×10^{-4}
1.048	-.007	4.9×10^{-5}	8.59×10^{-4}
1.039	-.016	2.56×10^{-4}	1.115×10^{-3}
1.034	-.021	4.41×10^{-4}	1.556×10^{-3}
1.034	-.021	4.41×10^{-4}	1.997×10^{-3}
1.084	.029	8.41×10^{-4}	2.838×10^{-3}
1.043	-.012	1.44×10^{-4}	2.982×10^{-3}
1.025	-.03	9×10^{-4}	3.882×10^{-3}
1.022	-.033	1.089×10^{-3}	4.971×10^{-3}
1.049	-.006	3.6×10^{-5}	5.007×10^{-3}
1.049	-.006	3.6×10^{-5}	5.043×10^{-3}
1.065	.01	1×10^{-4}	5.143×10^{-3}
1.073	.018	3.24×10^{-4}	5.467×10^{-3}
1.082	.027	7.29×10^{-4}	6.196×10^{-3}
1.095	.04	1.6×10^{-3}	7.796×10^{-3}
1.083	.028	7.84×10^{-4}	8.53×10^{-3}
1.027	-.028	7.84×10^{-4}	9.364×10^{-3}
1.010	-.045	2.025×10^{-3}	0.11389
1.071	.016	2.56×10^{-4}	.011645
1.079	.024	5.76×10^{-4}	.012221
1.06	.005	2.5×10^{-5}	.012246
1.06	.005	2.5×10^{-5}	.012271
1.057	.002	4×10^{-6}	.012275
1.059	.004	1.6×10^{-5}	.012291
1.060	.005	2.5×10^{-5}	.012316
1.043	-.012	1.44×10^{-4}	.01246
1.052	-.003	9×10^{-6}	.012469
1.064	.009	8.1×10^{-5}	.01255
1.045	.01	1.0×10^{-4}	.01265
1.056	.001	1×10^{-6}	.012651
1.064	.009	8.1×10^{-5}	.012732

$$\sum x_N = 33.76$$

Number of samples run = 32

$$\bar{x}_N = 1.055$$

$$\sigma^2 = \frac{\sum[(x_i - \bar{x})^2]}{n - 1} = \frac{.012732}{31} = 4.10 \times 10^{-4}$$

$$\sigma = \pm .020248 \sim \pm .020 \text{ wt\% Nitrogen} \sim \pm 1.9\% \text{ (Absolute)}$$

HYDROGEN

Weight Percent Hydrogen	$x - \bar{x}$	$(x - \bar{x})^2$	$\sum (x - \bar{x})^2$
5.54	-.034	1.156×10^{-3}	-
5.69	.116	.0134	.014612
5.571	.003	9×10^{-6}	.014621
5.656	-.082	.006724	.021345
5.413	-.161	.025921	.047266

$$\sum x_H = 27.87$$

Number of samples run = 5

$$\bar{x}_H = 5.574$$

$$\sum (x - \bar{x})^2 = .047264$$

$$\sigma^2 = .011816$$

$$\sigma = \pm .10870 \text{ wt\% Hydrogen}$$

$$= 1.95\% \text{ (Absolute)}$$

APPENDIX E

SAMPLE CALCULATIONS FOR SULFUR, NITROGEN AND HYDROGEN ANALYSES

Sulfur Analysis

A sample of known sulfur content is analyzed to determine the furnace factor (F). This factor accounts for error due to incomplete conversion of sulfur to SO_2.

$$\text{Furnace Factor (F)} = \frac{(\text{Sample wt.}) \times (\text{known wt\% S})}{(\text{Volume Titrated} - \text{Blank})}$$

For Example,

Known Wt% S = 0.43%

Sample Wt. = 0.0345 gms

Blank = 0.034

Volume Titrated = 0.098

$$F = \frac{(0.0345)(0.43)}{(0.098 - 0.034)} = 0.183$$

The furnace factor is used to calculate the weight percent sulfur of unknown samples.

$$\text{Wt\% S} = F\frac{(\text{Volume Titrated} - \text{Blank})}{\text{Sample Weight}}$$

For example,

$$F = 0.183$$

$$\text{Blank} = 0.034$$

$$\text{Sample Wt.} = 0.0325 \text{ gms}$$

$$\text{Volume Titrated} = 0.074$$

$$\text{Wt\% S} = \frac{0.183(0.074 - 0.034)}{0.0325} = 0.23 \text{ Wt\% S}$$

Nitrogen Analysis

Like sulfur, a sample of known nitrogen content is analyzed to determine a calibration factor K_N. This factor accounts for incomplete combustion and trap efficiencies.

$$\text{Calibration Factor}(K_N) = \frac{(\text{Read} - \text{Zero} - \text{Blank})\ 100}{(\text{Sample Wt}) \times (\text{Known Wt\% N})}$$

For example,

$$\text{Read} = 2784.$$

$$\text{Zero} = 66.$$

$$\text{Blank} = 30.$$

$$\text{Sample Wt.} = 3084.\mu g$$

$$\text{Wt\% N} = 10.42\%$$

$$K_N = \frac{(2784. - 60. - 30.)100.}{(3084.)(10.42)} = 8.36$$

Similarly, weight percent nitrogen of unknown samples are calculated.

$$\text{Wt\% N} = \frac{(\text{Read} - \text{Zero} - \text{Blank})100}{K_N(\text{Sample Wt})}$$

For example,

$$K_N = 8.36$$

$$\text{Sample Wt.} = 8724.\mu g$$

$$\text{Read} = 850.$$

$$\text{Zero} = 66.$$

$$\text{Blank} = 3.$$

$$\text{Wt\% N} = \frac{(850. - 66. - 30.)100.}{(8.34)(8724.)} = 1.03\%$$

Hydrogen Analysis

First, the calibration factor K_H for hydrogen is found by ana analyzing a sample of known hydrogen content.

$$\text{Calibration Factor } (K_H) = \frac{(\text{Read} - \text{Zero} - \text{Blank})100}{(\text{Sample Wt})(\text{Known Wt\% H})}$$

For example,

$$\text{Read} = 15{,}616.$$

$$\text{Zero} = 100.$$

$$\text{Blank} = 40.$$

$$\text{Sample Wt} = 3084.\mu g$$

$$\text{Wt\% H} = 6.68\%$$

$$K_H = \frac{(15{,}616. - 100. - 40.)100.}{(3084)(6.68)} = 75.1$$

This factor is then used to find the wt% hydrogen in unknown samples

$$\text{Wt\% H} = \frac{(\text{Read} - \text{Zero} - \text{Blank})100}{K_H(\text{Sample Wt.})}$$

For example,

$$K_H = 75.1$$

$$\text{Sample Wt} = 2{,}875\ \mu g$$

$$\text{Read} = 13{,}482$$

$$\text{Zero} = 100$$

$$\text{Blank} = 40$$

$$\text{Wt\% H} = \frac{(13{,}482 - 100 - 66)100}{75.1(2{,}875)} = 6.167\%$$

VITA

JAN WILLIAMS WELLS

Candidate for the Degree of

Master of Science

Thesis: AN EVALUATION OF THE ABILITY OF GAMMA ALUMINA TO REMOVE SULFUR AND NITROGEN FROM A COAL DERIVED LIQUID BOTH IN THE PRESENCE AND ABSENCE OF HYDROGEN TREAT GAS

Major Field: Chemical Engineering

Biographical:

Personal Data: Born Guthrie, Oklahoma, September 15, 1948 to Eugene Lincoln and V. Pauline Wells.

Education: Graduated from Ponca City High School, Ponca City, Oklahoma, in 1966. Received a Bachelor of Science Degree in Chemical Engineering from Oklahoma State University, Stillwater, Oklahoma, in May of 1971. Completed requirements for Master of Science in Chemical Engineering at Oklahoma State University in May, 1977.

Professional Experience: Reservoir Engineer for Atlantic Richfield Company, Dallas, Texas, Summer 1968. Technical Services Engineer for Exxon, Baton Rouge, Louisiana, Summer 1970. Research Assistant for School of Chemical Engineering, Oklahoma State University, December, 1975 to December, 1976.

Membership in Scholarly or Professional Societies: Sigma Tau, Engineering Honor Society; Omega Chi Epsilon, Chemical Engineering Honor Society; Phi Kappa Phi Scholastic Honor Society; American Institute of Chemical Engineers.

Military Service: Served as an officer in U. S. Navy from August, 1971 to December, 1975. Taught Heat Transfer, Fluid Flow and Physics at U. S. Naval Nuclear Power School, NTC Baubridge, Maryland.